EVALUATION OF STRESS INTENSITY FACTORS IN ORTHOTROPIC PLATES USING SPECIAL CRACK-TIP FINITE ELEMENT

A Thesis Submitted
In Partial Fulfilment of the Requirements
for the Degree of

MASTER OF TECHNOLOGY

by
BISWAJIT SEN

to the

DEPARTMENT OF AERONAUTICAL ENGINEERING
INDIAN INSTITUTE OF TECHNOLOGY, KANPUR
JULY , 1985

To Deep

CONTENTS

CERTIFICATE

This is to certify that the work 'Evaluation of stress intensity factors in orthotropic plates using special crack-tip finite element' has been carried out under my supervision and has not been submitted elsewhere for a degree.

(D. YADAV)
Assistant Professor
Department of Aeronautical Engineering
Indian Institute of Technology, Kanpur.

ACKNOWLEDGEMENT

I am deeply indebted to Dr. D. Yadav for his guidance, encouragement, inspiration and for many more occasions when he helped me out of a number of difficult situations throughout the tenure of this work.

I am grateful to Dr. N.G. R. Iyengar for his guidance during the early stage of this work and specially during the problem-selection-phase.

I sincerely thank Mr. M.K. Patra for some valuable advices he gave me on different occasions.

Thanks are due to everybody in my department who really gave me a very warm and friendly environment to carry out my work and specially to Mr. S.J. Gupta for his undoubtedly sincere effort for excellent typing of the manuscript.

B. SEN

ABSTRACT

Stress intensity factors in opening and sliding mode have been computed, with a finite element scheme using special crack tip element of large size and consequently a coarse mesh for thin orthotropic rectangular plates. Theoretically exact stress function has been used in the special crack tip element with a good number of terms in the series. The compatibility of displacement across the special element boundary has been satisfied in a least square sense.

Results have been verified in isotropic case using the same scheme. The maximum error with the theoretical value is only 4%. Energy release rate has been computed successfully in a case where direct computation of stress intensity factors are not possible. Evaluation of stress intensity factors have been done in primarily three different cases. They are a thin plate with a (1) central crack, (2) symmetric notches on both sides and (3) a notch in one side, where the loading is uniform tensile stress. Besides this case (3) has been dealt with under uniform shear stress and also a combination of uniform tensile and shear stress.

A really good convergence of the computed values of stress intensity factors with the increase in number of degrees of freedom in the special crack tip element has been observed in all the cases. The linearness of the relation of applied

stress and computed stress intensity factor values has been verified. Dependence of computed values of stress intensity factors on poisson's ratio has been studied in all three cases which unlike the isotropic case is unique in an orthotropic elastic field.

SYMBOLS

a_e	Elemental displacement vector
a_i	Displacement vector for ith node
$a_1 \ldots a_{4n}$	Unknown degrees of freedom
K_I	Stress intensity factor in mode I.
K_{II}	Stress intensity factor in mode II
K_{III}	Stress intensity factor in mode III
B	Strain shape function matrix
E	Modulus of elasticity
E_p	Percentage error with respect to K_I & K_{II} values corresponding to N = 16.
E_1	Modulus of elasticity in principal material direction 1.
E_2	Modulus of elasticity in principal material direction 2.
F	Nodal force vector
G	Energy release rate
G_{12}	Modulus of shear rigidity in 1-2 direction
K	Global stiffness matrix in isotropic case
$\bar{K}$	Global stiffness matrix in orthotropic case
K_e	Element stifness matrix in isotropic case
$\bar{K}_e$	Element stifness matrix in orthotropic case
L	Transformation matrix
N	Number of degrees of freedom excluding rigid body translation and rotation u_o, v_o & w in special crack tip element.
r	Radial distance from the origine
r_c	Radius of the special crack tip element

Q	Modified elasticity matrix
T	Geometric transformation matrix
U	Displacement in X-direction
u_i	Nodal displacement of the ith node in X-direction
V	Displacement in Y-direction
v_i	Nodal displacement of the ith node in Y-direction
w	Rotational displacement
V_s	Strain energy
Z_1	Complex argument
Z_2	Complex argument
α	Real part of the root of the characteristic equation
β	Imaginary part of the root of the characteristic equation.
φ	Stress function
λ	The vector containing unknown degrees of freedom ($a_1 \ldots\ldots a_{4n}$, u_o, v_o, w)
π	Total potential of a structure
μ	Root of the characteristic equation
ν	Poisson's ratio
ν_{12}	Poisson's ratio in principal material direction 1-2
σ	Normal stress
σ_x	Stress in X-direction
σ_y	Stress in Y-direction
σ_I	Applied normal stress 30 degree inclined to Y-direction
τ_{xy}	Shear stress in X-Y direction

Note : Other symbols used in this work have been clarified in places where-ever they are used.

LIST OF TABLES

LIST OF FIGURES

CHAPTER - 1

INTRODUCTION

The rapid cultivation and development of fracture mechanics has been taking place owing to the fact that crack is the root cause of structural failure in many cases. A majority of large scale failures in such diverse structures as storage tanks, pressure vessels, pipelines, bridges, turbine generator rotors, ships, aircrafts, rocket motors etc., have been invariably traced to the presence of a crack originating from a site of stress concentration. The famous accidents in the year of 1954 involving 'Comet" jet aircrafts on schedule flights were traced to fatigue cracks at the corners of the windows, due to stress concentration in the fuselage. Accounts can be given on many other structural disasters whose root cause lie in development of cracks.

1.1 Fracture mechanics and stress intensity factor

The stress and strain patterns change abruptly, when a crack is introduced in a solid body, in the regions near the crack tip. This phenomenon gradually diminishes as one moves further and further away from the crack tip. In such a cracked body, when external loads are applied, the stresses increase rapidly in the vicinity of the crack tip and become unbounded when one reaches the crack tip. Linear fracture mechaniesis based on the premise that the stress-state in the vicinity of the crack tip can be characterized by stress

intensity factors. There are distinctly three different modes of fracture and they are : (1) opening mode, (2) sliding mode and (3) tearing mode as illustrated in Fig. 1(a). A general fracture can be any possible combination of these different modes of fracture. Conventionally, the stress intensity factors in these three modes are represented as K_I, K_{II} and K_{III} respectively.

The relations of stress and displacement components with the stress intensity factor may be illustrated as follows. Consider a simplified case of a crack in a uniform tensile field, see Fig. 1(b). Here σ_x, σ_y and τ_{xy} in the vicinity of crack tip can be expressed by the following expressions.[1]

$$\sigma_x = \frac{K_I}{(2\pi r)^{\frac{1}{2}}} \cos(\theta/2)\,(1 - \sin(\theta/2).\sin(3\theta/3)) \quad (1.1)$$

$$\sigma_y = \frac{K_I}{(2\pi r)^{\frac{1}{2}}} \cdot \cos(\theta/2)\,(1 + \sin(\theta/2).\sin(3\theta/2)) \quad (1.2)$$

$$\tau_{xy} = \frac{K_I}{(2\pi r)^{\frac{1}{2}}} \sin(\theta/2) \cdot \cos(\theta/2).\,.\cos(3\theta/2).. \quad (1.3)$$

The two displacement components u & v along x and y axes can be written by the following expressions.[1]

$$u = \frac{K_I}{4G} (r/2\pi)^{\frac{1}{2}} (2k-1)\cos(\theta/2) - \cos(3\theta/2) \quad (1.4)$$

$$v = \frac{K_I}{4G} (r/2\pi)^{\frac{1}{2}} (2k+1)\sin(\theta/2) - \sin(3\theta/2) \quad (1.5)$$

where $k = (3-4\nu)$ for plane strain and $k=(3-\nu)/(1+\nu)$ for plane stress.

K_I i.e. the stress intensity factor in Mode I fracture is only dependent on the geometry of the cracked body and magnitude and configuration of the applied loading. There is another important parameter used in fracture mechanics called the energy release rate, denoted as 'G'[2]. When a crack is extended by a small length of 'da' there is some work done by the external loads which is equal to the amount of energy released'd π' from the body. Therefore $G = \frac{d\pi}{da}$. To predict whether a crack will propagate in a body under a set of external load we need to know a critical value of G i.e. critical energy release rate 'G_c' or a critical value of stress intensity factor which is otherwise called 'fracture toughness' and noted as K_c. K_c and G_c are dependent on material properties.[3] When the stress intensity factor or energy release rate, which are only dependent on loading configuration and geometry of the cracked body, surpasses the critical values K_c and G_c respectively a stable or unstable crack propagation will take place. If the crack propagation is unstable it leads to failure inevitably. Therefore, when a cracked structural member is under service condition one should be careful about either the energy release rate or the stress intensity factor does not exceed the respective critical value . Energy release rate and stress intensity factors are related by the following relations.[2,3]

For Mode I fracture in plain stress : $G_I = \frac{K_I^2}{E}$ (1.6)

For Mode I fracture in plain strain : $G_I = \frac{K_I^2 (1-\nu)^2)}{E}$ (1.7)

For Mode II fracture in plain stress: $G_{II} = \frac{K_{II}^2}{E}$ (1.8)

For Mode II fracture in plain strain: $G_{II} = \frac{K_{II}^2 (1-\nu)^2)}{E}$ (1.9)

1.2 Evaluation of Stress Intensity Factor

1.2.1 Types of Evaluation Methods

Analytical attempts for elastic stress analysis of cracked bodies were first made as early as in the year of 1913. It has developed considerably in the last two decades. Numerous contributions have been made in the development of analytical and numerical techniques. As it stands today, the complex variable techniques can handle a variety of crack shapes while finite element methods have attained an impressive position for application to problems with complicated geometry. Recently people have started using experimental techniques for the determination of stress intensity factors. Experimental methods are intended as alternatives to analytical techniques for practical complex configurations. But as a matter of fact the rapid progress of two-dimensional analysis with complex variable and finite element methods are at every stage pushing the experimental methods into unattractive

positions. However, even today three dimensional analyses are analytically difficult and computationally so unwieldy and expensive that for three dimensional problems, experimental methods are still preferred to analytical and numerical techniques. Amongst the experimental methods both two and three dimensional photoelastic techniques are widely used and their choice is based on their simplicity.

1.2.2 Anisotropic elastic field

With exception to some of the recent advancements, specially in aerospace engineering, the conventional structural materials are all metals or its alloys. As a matter of consequence, almost all the developments in fracture mechanics have dealt with the isotropic elastic fields. It is worth mentioning here that till early seventies there has not been any considerable development made in anisotropic field so far as the linear fracture mechanics is concerned. It is only since mid-seventy that people have started realising the hidden potential of fibre composite materials specially in the fields where weight reduction is one of the most important criteria of structural design. Currently almost every aerospace company is developing different products made of fibre composites and trying to successfully use them in aircrafts to substitute conventional structural materials. It is presently in the experimental stage and companies like 'General Dynamics' and

Mc Donnell Douglas are using fibre composites in horizontal and vertical stabilisers, for some portions in the fuselage as well as engines. Currently with various conventional metal alloys, thrust to weight ratio of 5 to 1 has been achieved. Reinforced plastics may lead to thrust to weight ratio as high as 16 to 1. Ultimately with advanced graphite fibre composite thrust to weight ratio as high as 40 to 1 appear possible.[20] However, the road to this goal can be perilous as the failure behaviour of fibre-composites are not as well known as that of metals or metal alloys. Inspite of the past developments of fracture mechanics in isotropic field, the study of cracks in orthotropic or other anisotropic materials are of immense current importance to cater to the practical necessities. Today lot of work is being carried out all over the world to study the different failure phenomena in orthotropic or other anisotropic elastic fields to develop a profound theoretical background for failures in fibre composites.

1.3 Literature Survey

In early days of development of finite element methods, the crack problems have been dealt with conventional triangular and other higher order elements. It is known from the continuum analysis that a singularity in stresses of the order of $r^{-\frac{1}{2}}$ exists at the tip of the crack. For these problems,

very soon, the inability of conventional elements to represent these situations of large stress concentration or to represent the regions of large stress gradients is fast realized. Using conventional elements the stress distribution derived are in substantial error in the immediate vicinity of the crack. The stress intensity factors were determined only by extrapolating the stresses away from the crack tip with the known forms of near-crack tip stress field. Considering the rectangular plate with the central crack under pure tension the near tip stress-field is known of the form the equations[1] (1.1), (1.2) & (1.3).

The stresses derived from the conventional finite element analysis slightly away from crack tip were fitted with this distribution and K_I was determined. However, this method has not been found to yield accurate estimate of stress intensity factor. Then the realisation came that a different method of introducing crack tip singularity is necessary into the finite element methods. This lead to the development of methods of analysis wherein the region close to the crack tip is treated with special singular elements and the regions away from the crack tip are dealt with conventional finite elements. One of the significant development is the hybrid method where the displacement description in singular element is drawn from the continuum solutions, either full solution or sometime only the relevant part of the solutions representing the crack tip

elastic singularity. Extensive literature has appeared in the development of hybrid methods and significant part of it is listed in the ref. [4-13]. Besides hybrid method, the development of isoparametric elements leading to singularity of the order $r^{-\frac{1}{2}}$ at the crack tip has been another major breakthrough in this area. With the development of isoparametric elements it is felt that singular crack tip elements of hybrid type are not necessary.

Some special crack tip elements have been used by Byskov[4], and Tracey[5] which represent $(1/r)^{\frac{1}{2}}$ stress singularity for elastic analysis. But the element displacement functions, however, did not satisfy inter-element compatibility criteria. Pian and Tong[6] have developed stress hybrid model using the modified principle of minimum complementary energy for which the functional is $\pi_\sigma = \sum_m \int_{V_m} \frac{1}{2} S_{ijkl}\, \sigma_{ij}\, \sigma_{kl}\, dv - \int_{\delta V_m} T_i v_i\, ds +$

$$\int \bar{T}_i\, v_i\, ds \qquad \ldots \qquad (1.11)$$

σ_{ij} = stress tensor

S_{ijkl} = elastic compliance tensor

V_m = volume of the element

δV_m = boundary of the element

S = part of V_m on which tractions are specified

v_i = boundary displacements

$\bar{T}_i$ = boundary tractions.

The complimentary displacement hybrid model had been used by Atluri[7,8] using the functional :

$$\pi_D = \sum_m \int_{V_m} (E_{ijkl}.\epsilon_{ij}\epsilon_{kl} - \bar{F}_i u_1)dv + \int_{V_m} \bar{\bar{T}}_i (V_i - u_i)\, ds - \int_S T_i V_i\, ds \qquad \ldots \quad (1.12)$$

where

E_{ijkl} is stiffness tensor

$$\epsilon_{ij} = \tfrac{1}{2}\left(\partial u_i/\partial x_j + \partial u_j/\partial x_i\right) \qquad (1.13)$$

$\{u_i\}$ = interior displacements.

For singular elements, the displacements are assumed as

$$\{u_i\} = (U_R)\{\beta\} + (U_s)\begin{Bmatrix} K_I \\ K_{II} \end{Bmatrix} \qquad (1.14)$$

$$= (U_R)\{\beta\} + (U_s)\{K_s\}$$

in which (U_R) is simple polynomials and (U_s), are known as displacement functions for plane problems with crack, obtained from crack tip stress fields. The inter-element boundary displacement $\{V_i\}$ is assumed in terms of nodal displacements $\{q_i\}$ i.e.

$$\{V_i\} = (L_R)\{q_i\} \qquad (1.15)$$

where (L_R) is the transformation matrix. The inter element compatibility is thus assumed. On the element boundaries radiating from crack tip $(r)^{\frac{1}{2}}$ type displacement behaviour

is built in. For all elements around crack tip $\{K_s\}$ i.e. the stress intensity factor is same, and final equations are obtained in terms of nodal displacements q and the stress intensity factors $\{K_s\}$.

There have been a series of attempts around the same time in the development of hybrid elements. A hybrid method of analysis was developed at Indian Institute of Science by Rao, Raju and Krishna Murthy[9] for general problems of stress concentration. It is based on the development of large primary elements in the regions of stress concentration and stiffness of the primary elements are determined from an assumed displacement pattern provided by the continuum solutions. The stiffness matrix is finally derived from minimization of potential energy. The outside region was filled up by conventional elements. Alternative hybrid formulations around the same time has been done by Morley, Pian[6]. Another development is by Benzley[10] who undertook the development of a generalised quadrilateral finite element that includes a singular point at a corner. Interelement displacement continuity i.e. compatibility has been maintained so that convergence of the finite element is preserved. A global-local concept of finite element formulation is utilized to formulate the the complete set of stiffness relationships.

The superposition approach to finite element fracture analysis has been successfully applied by Yamamoto[11] and similar idea has also been used by Morley. The superimposition approach to finite element fracture analysis attempts to determine stress intensity factors through a linear combination of classical singularity solutions and a coarse finite-element grid. The concept involves first determining the classical solution for crack in a infinite elastic body as close to the problem of interest as possible. Now, the finite element method, because of its ability to model elastic bodies characterized by complicated displacement and force boundary conditions as well as complex geometries is called upon to provide the second solution. The results from the finite element solution and classical solution are superimposed to determine the final solution.

R.D. Henshell & K.G. Shaw[12] have made a remarkable contribution in this field by devising an isoparametric singular element. A standard eight noded isoparametric element in an X-Y space is transformed to a square in the ξ-η space with vertices at $(\pm 1, \pm 1)$. The midside nodes are shifted from their original position towards the crack tip at quarter point to exhibit a singularity of the order of $r^{-\frac{1}{2}}$. The considered interpolation along one edge say edge 1-2 (see Fig.1.(c)) with nodes at -1, 0 & +1 in the parameter plane. Then r is defined as $r = \frac{x - x_1}{x_2 - x_1}$, along the edge 1-2 r varies from

0 to 1, and the corner nodes are at r=0 & r=1 and midside node is at r=p. The interpolation functions are assumed as

$$r = a_1 + a_2 \xi + a_3 \xi^2 \tag{1.16}$$

and $$u = b_1 + b_2 \xi + b_3 \xi^2 \tag{1.17}$$

Then the relation between r and is obtained as :

$$= \frac{-1 + (1-8 + 8(1-2p)\, r + 16\, p^2)^{\frac{1}{2}}}{2(1-2p)} \tag{1.18}$$

$$\frac{d\xi}{dr} = 2\,(1-8p + 16\,p^2 + 8(1-2p)\, r)^{-\frac{1}{2}} \tag{1.19}$$

$\frac{d\xi}{dr}$ tends to infinity when $r = \frac{(1-4p)^2}{8(2p-1)}$. This singularity occurs at r=0 i.e. node 1, when $p=\frac{1}{4}$ i.e. when the mid side node is shifted to the quarter point. This yields $=-1+2(r)^{\frac{1}{2}}$ (1.20)

and $\frac{d}{dr} = (1/r)^{\frac{1}{2}}$. (1.21)

A number of special crack tip elements have been developed[4,5,10], where displacement method has been used. Also hybrid method has been used to develop singular elements[7,8,9]. These special crack tip elements contain a singularity in the strain field at the crack tip equal to theoretical singularity[12]. One disadvantage of these special crack tip elements[4,5] is that they lack the constant strain and the rigid body motion nodes. Therefore they do not pass the patch test[13] and necessary requirements of convergence[10] are not

present. R.S. Barsoum[14] & R.D. Henshell[12] both independently developed isoparametric crack tip elements incorporating $(1/r)^{\frac{1}{2}}$ singularity satisfying the convergence criteria. Both of them dealt with 8-noded element and shifting the midside nodes towards the crack tip at quarter points. R.S. Barsoum[15], a general curved element of arbitrary shape for both thick and thin shells is proposed for linear fracture analysis of a through crack in a shell or a plate. The element is derived from a degenerate 20-noded solid isoparametric element using reduced integration technique. The $(1/r)^{\frac{1}{2}}$ singularity is obtained by the same procedure proposed earlier for two and three dimensional problems[16,17], by placing midside nodes near the crack tip at quarterpoints. Several illustrated examples ranging from classical solutions to practical problems were given to assess the accuracy of solution attainable.

Some time later triangular and prismatic elements[18] were developed (quadratic and isoparametric). They were formed by collapsing one side and placing the mid side node at quarter point near the crack tip which show to embody $(1/r)^{\frac{1}{2}}$ singularity of elastic fracture mechanics and $(1/r)$ singularity for perfect plasticity. In this work a 8 noded isoparametric element is taken and one side of the element is collapsed at the crack tip, see Fig. 1(d) and mapped into a square (ξ, η) space. The transformations used are :

$$x = \sum_{i=1}^{8} Ni\,(\xi,\eta)\, x_i \tag{1.22}$$

and

$$y = \sum_{i=1}^{8} Ni\,(\xi,\eta)\, y_i \tag{1.23}$$

$$Ni(\xi,\eta) = (1+\xi\xi_i)(1+\eta\eta_i) - (1-\xi^2)(1+\eta\eta_i) -$$

$$-(1-\eta^2)(1+\xi\xi_i) + \xi_i^2\xi_i^2/4 + (1-\xi^2)(1+\eta\eta_i)$$

$$(1-\xi_i^2)\,\xi_i^2 + (1-\eta^2)(1+\xi\xi_i)(1-\eta_i^2)\,\xi_i^2/2 \tag{1.24}$$

where ξ_i, η_i are (± 1) for corner nodes & (0) for midside nodes. x_i, y_i are the nodal coordinates for the element. With this formulation it has been shown that the strains have the following singularities :

$$\frac{\partial u}{\partial x} = \frac{A_o}{\sqrt{r}} + \frac{b_o'}{r} + A_1 \tag{1.25}$$

where A_o, b_o' & A_1 are independent of r and are constants for $(\theta$ = constant).

Similarly,

$$\frac{\partial u}{\partial y} = \frac{B_o}{\sqrt{r}} + \frac{b_o''}{r} + B_1 \tag{1.26}$$

and

$$\frac{\partial v}{\partial x} = \frac{C_o}{\sqrt{r}} + \frac{d_o'}{r} + C_1 \tag{1.27}$$

Similarly,

$$\frac{\partial v}{\partial y} = \frac{D_o}{\sqrt{r}} + \frac{d''_o}{r} + D_1 \qquad (1.28)$$

where u & v are the two displacement components.

In the year of 1977 R. Jones and R.J. Callinan[19] presented a finite element method for determining stress intensity factors in a cracked elastic sheet. Special crack tip elements are placed around each crack tip. In the special elements the stress and displacements are derived from the exact stress function i.e. Airy's stress function while the continuity of displacements across the special element boundary is satisfied in a least square sense. Formulation and numerical investigation has been done in case of isotropic elastic field and a modified formulation has been proposed in orthotropic case but no numerical investigation has been done to verify the results.

1.4 Objectives of the present work

The present work concerns with the cracks in orthotropic plates. Attempt has been made for calculating stress intensity factors varying poisson's ratio for centrally located crack and symmetric side notches on both sides in orthotropic rectangular and thin plates under uniform tensile stress field. See Fig. 1(e) & 1(f). Another case of a single side

notch in rectangular and orthotropic plate has also been studied under pure tensile stress and shear stress and also a combination of tensile stress and shear stress. See Fig.1(g). Stress intensity factors have been found out for opening mode of fracture as well as sliding mode of fracture i.e. mode I and mode II as described in Fig. 1 (b). Use has been made of a special crack-tip element which is so placed around the crack tip and crack lies on the x-axis in the positive direction. In the special element the stresses and the displacements are derived from the exact stress function (Airy's stress function) while the continuity of displacements across the boundary of the special element and other general elements has been satisfied in a least square sense. Constant strain triangular elements have been used as general elements to discretize the rest of the structure, which substantially has reduced the domputational cost. The reasons which justify the use of the special crack tip element incorporated in this work are the following :

(1) The stress function used in the formulation of this special element is the actual stress function that exists in the vicinity of the crack tip which ensures good convergence and the error is very much negligible.

(2)This special element can be of any size or shape which gives the liberty to discretize the rest of the structure

as per convenience. A fairly coarse mesh can be used which in turn significantly increases the computational economy and reduces the effort required for data preparation.

This special element has not been used so far in orthotropic elastic field though this has been used in previous works and tested to find very attractive results in isotropic case. In the present work, the application of this special element has been extended to the orthotropic elastic field in three different cases as illustrated in Fig. 1(e), 1(f) and 1(g) and in all the three cases satisfactory convergence of stress intensity factors have been found. In chapter 2, equation (2.87) shows that when is equal to zero, the evaluation of stress intensity factor is impossible using the general procedure. To overcome the inherent limitation of this special element a scheme has been developed to use this special element to find out energy release rate to substitute for stress intensity factor whose evaluation is not possible as described above, with the direct method. This scheme has clearly been shown in section 3.2. The effect of applied external stress and poisson's ratio on stress intensity factors and energy release rates have been studied in all the three cases. To reduce the computational effort and cost advantage has been exploited of symmetry of loading and geometry of the plates wherever possible.

CHAPTER - 2

PROBLEM FORMULATION

The formulation consists of two basically different parts. One is the formulation of the special element which is placed around the crack tip and the other is the formulation of the constant strain triangles which fills up the rest of the structure.

2.1 Formulation of the constant strain triangles

2.1.1 Displacement functions

Fig. 2(a) shows a typical triangular element[1] considered with nodes i,j, m numbered in an anticlockwise order. The displacement of a node has two components :

$$a_i = \begin{Bmatrix} u_i \\ v_i \end{Bmatrix} \qquad \ldots \quad (2.1)$$

The six components of element displacements are listed as vector:

$$a^e = \begin{Bmatrix} a_i \\ a_j \\ a_m \end{Bmatrix} \qquad \ldots \quad (2.2)$$

The displacement within an element have to be uniquely defined by these six values. The simplest representation is clearly given by two linear polynomials

$$\left.\begin{aligned} u &= \alpha_1 + \alpha_2 x + \alpha_3 y \\ v &= \alpha_4 + \alpha_5 x + \alpha_6 y \end{aligned}\right\} \qquad \ldots \quad (2.3)$$

The six constants 'α' can be solved easily by solving the two sets of three simultaneous equations which will arise if the nodal coordinates are inserted and the displacements equated to the appropriate nodal displacements. Writing for example

$$\begin{aligned} u_i &= \alpha_1 + \alpha_2 x_i + \alpha_3 y_i \\ u_j &= \alpha_1 + \alpha_2 x_j + \alpha_3 y_j \\ u_m &= \alpha_1 + \alpha_2 x_m + \alpha_3 y_m \end{aligned} \qquad \ldots (2.4)$$

We can solve for α_1, α_2 and α_3 in terms of the nodal displacements u_i, u_j and u_m and obtained finally the horizontal displacement[1]

$$\begin{aligned} u = \frac{1}{2\Delta} & (a_i + b_i x + c_i y) \cdot \\ & u_i + (a_j + b_j x + c_j y) \\ & u_j + (a_m + b_m x + c_m y) \cdot u_m \end{aligned} \qquad \ldots (2.5)$$

in which

$$a_i = x_j y_m - x_m y_j \; ; \; b_i = y_j - y_m = y_{jm} \; ; \; c_i = x_m - x_j = x_{mj} \quad \ldots (2.6)$$

and Δ is the area of the triangle and

$$2\Delta = \det \begin{vmatrix} 1 & x_i & y_i \\ 1 & x_j & y_j \\ 1 & x_m & y_m \end{vmatrix} = 2 \text{ (area of the triangle ijm)} \qquad \ldots (2.7)$$

The equation for vertical displacement are ,

$$v = \frac{1}{2\Delta}(a_i+b_ix+c_i y)\, v_i+(a_j+b_jx+c_jy)\, v_j+(a_m+b_mx+c_my)v_m \quad \ldots \quad (2.8)$$

Now we can write in general way

$U = \begin{Bmatrix} u \\ v \end{Bmatrix} = N\, a^e = (\, I\, N_i,\ I\, N_j,\ I\, N_m\,)\, a^e$ where N is the shape function and I is a two by two identity matrix.

$N_i = (\, a_i + b_i\, x + c_i y)\, /2\Delta\,;$

$N_j = (a_j + b_j\, x + c_j\, y)/2\Delta$ and $N_m = (a_m+b_mx + c_my)/2\Delta$.. (2.9)

The chosen displacement function automatically guarantees continuity of displacements with adjacent elements because the displacements vary linearly along any side of the triangle and with identical displacement imposed at the nodes, the same displacement will clearly exist all along an interface.

2.1.2 Strain

The total strain at any point within the element can be defined by its three components which contribute to internal work.[1]

$$\epsilon = \begin{Bmatrix} \epsilon_x \\ \epsilon_y \\ \epsilon_{xy} \end{Bmatrix} = \begin{bmatrix} \partial/\partial x & 0 \\ 0 & \partial/\partial y \\ \partial/\partial y & \partial/\partial x \end{bmatrix} \begin{Bmatrix} u \\ v \end{Bmatrix} = L.\, U \quad \ldots \quad (2.10)$$

Substituting equation (2.8) we have

$$= B.a^e = (\, B_i \;\; B_j \;\; B_m\,) \begin{Bmatrix} a_i \\ a_j \\ a_m \end{Bmatrix} \quad \ldots \quad (2.11)$$

With a typical matrix B_i given by $B_i = LIN_i$

$$= \begin{bmatrix} \partial N_i/\partial x & 0 \\ 0 & \partial N_i/\partial y \\ \partial N_i/\partial y & \partial N_i/\partial x \end{bmatrix} = \frac{1}{2\Delta} \begin{bmatrix} b_i & 0 \\ 0 & c_i \\ c_i & b_i \end{bmatrix} \quad \ldots \quad (2.12)$$

In general $B = LN$ (2.13)

Therefore, the full B matrix look like :

$$B = \begin{bmatrix} \partial N_i/\partial x & 0 & \partial N_j/\partial x & 0 & \partial N_m/\partial x & 0 \\ 0 & \partial N_i/\partial y & 0 & \partial N_j/\partial y & 0 & \partial N_m/\partial y \\ \partial N_i/\partial y & \partial N_i/\partial x & \partial N_j/\partial y & \partial N_j/\partial x & \partial N_m/\partial y & \partial N_m/\partial x \end{bmatrix}$$

$\ldots$ (2.14)

so, (B) is a (6 x 3) matrix which is actually a strain shape function matrix.

2.1.3 Elasticity Matrix

When the elasticity matrix is evaluated in terms of principal material direction, it takes the shape given below[20]:

$$\begin{Bmatrix} \sigma_1 \\ \sigma_2 \\ \tau_{12} \end{Bmatrix} = \begin{bmatrix} Q_{11} & Q_{12} & 0 \\ Q_{12} & Q_{22} & 0 \\ 0 & 0 & Q_{66} \end{bmatrix} \begin{Bmatrix} \epsilon_1 \\ \epsilon_2 \\ \epsilon_{12} \end{Bmatrix} \quad \ldots \quad (2.15)$$

where $Q_{11} = \frac{E_1}{1-\nu_{12}\nu_{21}}$; $Q_{12} = \frac{12.\ E_2}{1-\nu_{12}\nu_{21}}$;

$$Q_{22} = \frac{E_2}{1-\nu_{12}\nu_{21}} \quad \text{and} \quad Q_{66} = G_{12} \qquad (2.16)$$

When we calculate the elasticity matrix with reference to any arbitrary pair of axes (x-y) which makes an angle 'θ' with the material principal axes, see Fig. 2(b), following is the elasticity matrix

$$(\bar{Q}) = (T)^{-1} (Q) (T)^{-T} \qquad \cdots (2.17)$$

where $(\bar{Q})$ is the modified elasticity matrix and (T) is the transformation matrix.

$$T = \begin{bmatrix} \cos^2\theta & \sin^2\theta & 2\sin\theta.\cos\theta \\ \sin^2\theta & \cos^2\theta & -2\sin\theta.\cos\theta \\ -\sin\theta.\cos\theta & \sin\theta.\cos\theta & (\cos^2\theta - \sin^2\theta) \end{bmatrix} \qquad \cdots (2.18)$$

Then the stress-strain relation in x-y co-ordinate system is

$$\begin{Bmatrix} \sigma_x \\ \sigma_y \\ \tau_{xy} \end{Bmatrix} = (\bar{Q}) \begin{Bmatrix} \epsilon_x \\ \epsilon_y \\ \epsilon_{xy} \end{Bmatrix} = \begin{bmatrix} \bar{Q}_{11} & \bar{Q}_{12} & \bar{Q}_{16} \\ \bar{Q}_{12} & \bar{Q}_{22} & \bar{Q}_{26} \\ \bar{Q}_{16} & \bar{Q}_{26} & \bar{Q}_{66} \end{bmatrix} \begin{Bmatrix} \epsilon_x \\ \epsilon_y \\ \epsilon_{xy} \end{Bmatrix} \cdots (2.19)$$

where

$$\bar{Q}_{11} = Q_{11} \cos^4\theta + 2(Q_{12} + 2Q_{66}) \sin^2\theta \cos^2\theta + Q_{22} \sin^4\theta$$

$$\bar{Q}_{12} = (Q_{11}+Q_{22}-4Q_{66}) \sin^2\theta \cos^2\theta + Q_{12} (\sin^4\theta + \cos^4\theta)$$

$$\bar{Q}_{22} = Q_{11} \sin^4\theta + 2(Q_{12} + 2Q_{66}) \sin^2\theta \cos^2\theta + Q_{22} \cos^4\theta$$

$$\bar{Q}_{16} = (Q_{11}-Q_{12} \quad -2\ Q_{66})\ \sin\theta.\cos^3\theta+(Q_{12}-Q_{22}+2Q_{66})\sin^3\theta.\cos\theta$$

$$\bar{Q}_{26} = (Q_{11}-Q_{12} \quad -2\ Q_{66})\ \sin^3\theta.\cos\theta+(Q_{12}-Q_{22}+2Q_{66})\sin\theta.\cos^3\theta$$

$$\bar{Q}_{66} = (Q_{11}+Q_{22} \quad -2Q_{12}-2Q_{66})\ \sin^2\theta.\cos^2+Q_{66}(\sin^4\theta+\cos^4\theta).$$

... (2.20)

2.1.4 Element Stiffness Matrix

The stiffness matrix of the element ijm is defined from the general relationship[1]

$$K^e_{ij} = \int (B_i)^T (\bar{Q})(B_i)\ .\ t\ dx\ dy \qquad \cdots (2.21)$$

where 't' is the thickness of the element. For constant strain elements B is independent of x and y i.e. the strain is constant throughout the domain of the element, so, the elements of the stiffness matrix take the following

$$K^e_{ij} = (B_i)^T\ (\bar{Q})(B_i)t.\Delta \qquad \cdots (2.22)$$

where is the area of the triangle

ijm i.e. $\Delta = \int_A dx\ dy$ ... (2.23)

2.2 Formulation of special crack tip element

2.2.1 General formulation in isotropic case

Consider a polygonal element with its centre at the crack tip see Fig.2(c), and let the element co-ordinate systems be placed with its origin at the centre. Then in polar co-ordinate system the stress function may be expressed as:[19]

$$= \sum_{n=1}^{N} (-1)^{n-1} \frac{r^{n+\frac{1}{2}}}{r_c^{n-\frac{1}{2}}} \left[d_{2n-1} \frac{2n-3}{2n+1} \cdot \cos\left(\frac{2n+1}{2}\right)\cdot\theta \right.$$

$$- \cos\left(\frac{2n-3}{2}\right)\theta + c_{2n-1} \sin\left(\frac{2n+1}{2}\right)\theta - \sin\left(\frac{2n-3}{2}\right)\theta$$

$$+ (-1)^{n} \left. d_{2n} \cos(n+1)\theta - \cos(n-1)\theta + c_{2n} \left(\frac{n-1}{n+1}\right). \right.$$

$$\left. \sin(n+1)\theta - \sin(n-1)\theta \right] \qquad (2.24)$$

which satisfies the requirement that the crack is stress free, i.e.

$$\sigma_\theta \ (\text{at } \theta = \pm\pi) = \frac{\partial^2 \varphi}{\partial r^2} \ (\text{at } \theta = \pm\pi) = 0; \qquad \ldots \qquad (2.25)$$

$$\text{and } \tau_{r\theta} \ (\text{at } \pm\pi) = \frac{1}{r^2} \frac{\partial \varphi}{\partial \theta} - \frac{1}{r} \frac{\partial^2 \varphi}{r \partial \theta} (\text{at } \theta = \pm\pi) = 0 \qquad (2.26)$$

Here r_c is the radius of the circumscribing circle, See Fig.2(c) the number of terms i.e. N, considered in the series expression for φ must be such that it gives accurate values for the stresses in the region $r < r_c$. For any given structure as r_c increases the value of N should be increased. Here, the

coefficients d_1, d_2, ... d_{2n}, c_1, c_2, ... c_{2n} are 4 X N number of degrees of freedom associated with the polygonal element. However, the element has an additional three degrees of freedom, those are, u_o, v_o and w for the rigid body translation in vertical and horizontal direction and the rigid body relation about the origin.

The strain energy of this polygonal element in plane stress case is given by the following expression [19]

$$V_s = \frac{h}{2E} \iint (\nabla^2 \varphi)^2 + 2(1+\nu) \left(\frac{1}{r^2}\frac{\partial \varphi}{\partial \theta} - \frac{1}{r}\frac{\partial^2 \varphi}{\partial r \partial \theta}\right)^2 - \frac{2}{r^2}\left(\frac{1}{r}\frac{}{r} + \frac{1}{r^2}\frac{2}{\theta^2}\right) r\, dr\, d\theta, \ldots \quad (2.27)$$

Here h is the thickness, is the poisson's ratio and E is the Young's modulus. The element stiffness matrix K^e for the polygonal element may as usual be obtained by substituting for in the strain energy expression and differentiating with respect to each of the element degree of freedom, i.e.,

$$\{F\} = \left\{\frac{\partial V_s}{\partial \lambda}\right\} \text{ or } (K^e)\{\lambda\} = \left\{\frac{\partial V_s}{\partial \lambda}\right\} \ldots \quad (2.28)$$

where $(\lambda)^T = (d_1, d_2 \ldots d_{2n}, c_1, c_2, \ldots c_{2n}, u_o, v_o, w)$ (2.29)

Here, $\{F\}$ is the force vector.

Now, any general term of the element stiffness matrix K^e_{ij} conceptually means the contribution in the force of the ith node due to the displacement at the jth node.[19]

Now,

$$K^e_{ij} = \frac{h}{2E} \iint \Big(2\nabla^2 \varphi_i \, \varphi_j + 2(1+\nu) \Big) \Big(2 \Big(\frac{1}{r^2} \frac{\partial \varphi_i}{\partial \theta} - \frac{1}{r} \frac{\partial^2 \varphi_i}{\partial r \partial \theta} \Big)$$

$$\Big(\frac{1}{r^2} \frac{\partial \varphi_j}{\partial \theta} - \frac{1}{r} \frac{\partial^2 \varphi_j}{\partial r \partial \theta} \Big) - \frac{\partial^2 \varphi_i}{\partial r^2} \nabla^2 \varphi_j \frac{\partial^2 \varphi_j}{r^2} \nabla^2 \varphi_i$$

$$+ 2 \frac{\partial^2 \varphi_i}{\partial r^2} \frac{\partial^2 \varphi_j}{\partial r^2} \Big) \Big) \; r \; dr \; d\theta \; \ldots\ldots \qquad (2.30)$$

where, $\nabla^2 \varphi_i = \frac{\partial^2 \varphi_i}{\partial r^2} + \frac{1}{r} \frac{\partial \varphi_i}{\partial r} + \frac{1}{r^2} \frac{\partial^2 \varphi_i}{\partial \theta^2}$ (2.31)

and for $i \leqslant 2N$

$$\varphi_i = (-1)^{\frac{i-1}{2}} \frac{r^{i/2+1}}{r_c^{i/2}} \Big(\frac{i-2}{i-2} \cos(i/2+1)\theta - \cos(i/2-1)\theta \Big)$$

for odd i ..(2.32)

and $\varphi_i = (-1)^{i/2} \frac{r^{i/2+1}}{r_c^{i/2}} (\cos (i/2+1)\theta - \cos(i/2-1)\theta)$ for even i

.., (2.33)

whilst for $2N \leqslant i < 4N$

$$i = (-1)^{\frac{i-1}{2}-N} \frac{r^{i/2-N+1}}{r_i^{i/2-N}} (\sin (i/2-N+1)\theta - \sin(i/2-N-1)\theta)$$

for odd i (2.34)

and $\varphi_i=(-1)^{i/2-N}\frac{r^{i/2-N+1}}{r_c^{i/2-N}}\left(\frac{i-2N-2}{i-2N+2}\right.\sin(i/2-N+1)\theta-\sin(i/2-N-1)\theta)$

for even i .. (2.35)

for $4N \leq i,j < 4N+3$, i.e., for rigid body motion K^e_{ij} is identically zero.

In practice to find out K^e_{ij} the integration is done numerically, and the shape of the element is largely governed by the ease of coupling the remainder of the structure to this special element. When the number of sides along the boundary of the special element is large then error in approximating this polygon by a circle is small. For example in case of 10,15 and 20 sided polygon the difference in area between these polygons and the corresponding circumscribing circle is 6.9, 3.0 and 1.6 percent respectively. Consequently when the number of sides is greater than say, 20 the numerical intigration may be approximated by integrating over the circumscribing circle and multiplying the result by the ratio of the area of the polygon to the area of the circle.

Because of the singularity at the crack tip Papaioannou[21] and Wilson[22] have found that when only a few terms in the series for are retained (e.g. N=1 or 2), so that r_c is by necessity very small, then a very fine mesh is required in the vicinity of the special element. This is natural enough since in this region the stresses are still changing very

rapidly. Consequently the mesh required for the entire structure is quite fine. As observed in [21] it is therefore necessary to have r_c quite large, in relation to the crack length, so as to escape this region of rapidly changing stress. This requires that more terms in the series expansion for be retained and the value of N be greater than that previously considered.

With the stress function as given in eqn. (2.24), the expression for the radial and tangential displacements $U(r,\theta)$ and $V(r,\theta)$ become[19] :

$$U(r,\theta) = \frac{1}{2\mu} \sum_{n=1}^{N} (-1)^n \left(\frac{r}{r_c}\right)^{n-\frac{1}{2}} \left(d_{2n-1} \frac{2n-3}{2} \cos\left(\frac{2n+1}{2}\right)\theta + (3.5-n-4\sigma) \cos\left(\frac{2n-3}{2}\right)\theta + c_{2n-1} \frac{2n+1}{2} \sin\left(\frac{2n+1}{2}\right)\theta + (3.5-n-4\sigma) \sin\left(\frac{2n-3}{2}\right)\theta + (-1)^{n+1} \left(\frac{r}{r_i}\right)^{n} \left(d_{2n} (n+1) \cos (n+1)\theta + (3-4\sigma-n) \cos (n-1)\theta + c_{2n} (n-1) \sin (n+1)\theta + (3-n-4\sigma) \sin (n-1)\theta\right) \quad \ldots \quad (2.36)$$

and

$$V(r,\theta) = \frac{1}{2} \sum_{n=1}^{N} (-1)^n \left(\frac{r}{r_i}\right)^{n-\frac{1}{2}} \left(c_{2n-1} \frac{2n+1}{2} \cos\left(\frac{2n+1}{2}\right)\theta - (2.5+n-4\sigma)\cos\left(\frac{2n-3}{2}\right)\theta + d_{2n-1} (2.5+n-4\sigma)\sin\left(\frac{2n-3}{2}\right)\theta -\right.$$

$$\frac{2n-3}{2} \sin\left(\frac{2n+1}{2}\right)\theta \Big) + (-1)^{n-1} \left(\frac{r}{r_i}\right)^{n} \left(d_{2n} \; (n+3-4\sigma)\right.$$

$$\sin(n-1)\theta - (n+1)\sin(n+1)\theta + c_{2n} \; (n-1)\cos(n+1)\theta - (n+3$$

$$\left. - 4\sigma)\cos(n-1)\theta \right) \qquad \ldots \qquad (2.37)$$

where, $\sigma = \nu$ for plane strain and $\sigma = \nu/(1+\nu)$ for plane stress. At the ith node, the cartesian displacements are u_i and v_i are related to $U(r,\theta)$ and $V(r,\theta)$ by the following formulae :

$$u_i = U(r_i,\theta_i)\cos\theta_i - V(r_i,\theta_i)\sin\theta_i + u_o - w_{yi} \qquad (2.38)$$

$$v_i = U(r_i,\theta_i)\sin\theta_i + V(r_i,\theta_i)\cos\theta_i + w_{xi} \qquad (2.39)$$

where r_i and θ_i are the polar co-ordinates of the ith node and x_i, y_i are the cartesian co-ordinates of the ith node.

Substitution of the expression for $U(r,\theta)$ and $V(r,\theta)$, i.e., eq. (2.36) and (2.37) into eqns. (2.38) and (2.39) results in a matrix equation of the form

$$L\,\lambda = \delta, \qquad (2.40)$$

where, $\delta^T = (u_1, v_1, u_2, v_2, \ldots\ldots u_m, v_m)$, m is the number of nodes in the special element boundary and L is a transformation matrix of dimension $2m \times (4N+3)$. Since it is conceivable that the special element may be coupled to the rest of the structure at more points than there are degrees of freedom use of least square technique is made to minimise discontinuity of the displacement across the boundary of the special element. This yields [18].

$$\lambda = (\ L^T .\ L)^{-1}\ L^T \delta \qquad \cdot \quad \ldots \qquad (2.41)$$

so that when the nodal displacements u_i and v_i are considered as the degrees of freedom then the element stiffness matrix becomes

$$\bar{K} = (\ (L^T\ L^{-1}\ L^T)^T\ K^e\ (L^T L)^{-1}\ L^T \quad .. \quad (2.42)$$

This formulation of the stiffness matrix is when over, it can be assembled to the global stiffness matrix.

2.2.2 Extension of the formulation in orthotropic elastic field .

$$\sigma_x = \frac{\partial^2 \varphi}{\partial y^2} \ ; \sigma_y = \frac{\partial^2 \varphi}{\partial x^2} \ ; \ \tau_{xy} = - \frac{\partial^2 \varphi}{\partial x\, \partial y} \quad \ldots \qquad (2.43)$$

where in this case the stress function satisfies the compatibility equation :

$$\frac{1}{E_2} \frac{\partial^4 \varphi}{\partial x^4} + \left(\frac{1}{G_{12}} - \frac{2\nu_{12}}{E_1}\right) \frac{\partial^4 \varphi}{\partial x^2 \partial y^2} + \frac{1}{E_1} \frac{\partial^4 \varphi}{\partial y^4} = 0 \quad \ldots \qquad (2.44)$$

In an isotropic case where $E_1 = E_2$; $\nu_{12} = \nu_{21} =$ and $G = \frac{E}{2(1+\ )}$, the compatibility equatio (2.44) reduces to biharmonic equation :

$$\nabla^4 \varphi = 0 \qquad \ldots\ldots \qquad (2.45)$$

which which the solution is given by equation (2.1). In the general case equation (2.44) can be factorized in the following form :

$$D_1 D_2 D_3 D_4 = 0 \quad \ldots \qquad (2.46)$$

where, for R=1,2, ...4

D_R designates the following operation :

$$D_R \equiv \frac{\partial}{\partial y} - \mu_R \frac{\partial}{\partial x} \quad \ldots \qquad (2.47)$$

As shown in[25] μ_R are the roots of the characteristic equation

$$\mu^4 + \left(\frac{E_1}{G_{12}} - 2\nu_{12}\right)\mu^2 + \frac{E_1}{E_2} = 0 \quad \ldots \qquad (2.48)$$

Clearly if $\mu = (\alpha + i\beta)$ is a solution to the characteristic equation (2.48) then so is $-\mu$, $\bar{\mu}$, $-\bar{\mu}$ where $\bar{\mu} = (\alpha - i\beta)$

And so denoting :

$$z_1 = x + \mu y \text{ and } z_2 = x + \mu y \quad \ldots \qquad (2.49)$$

then solution to the compatibility equation (2.44) may be written as

$$= 2\,\mathrm{Re}\left(\varphi_1(z_1) + \varphi_2(z_2)\right) \quad \ldots \qquad (2.50)$$

Where, φ_1 and φ_2 are the two arbitrary functions of complex arguments z_1 and z_2 respectively.

Let us now define two systems of polar co-ordinates (r_1, s_1) and (r_2, s_2) :

$$r_1 e^{is_1} = z_1 \quad \ldots \qquad (2.51)$$

$$r_2 e^{is_2} = z_2 \quad \ldots \qquad (2.52)$$

Then $r_1 = \left((x + \alpha y)^2 + (\beta y)^2\right)^{\frac{1}{2}} \quad \ldots \qquad (2.53)$

$$r_2 = \left((x - \alpha y)^2 + (\beta y)^2\right)^{\frac{1}{2}} \quad \ldots \qquad (2.54)$$

$$s_1 = a \tan \left(\frac{\beta y}{x + \alpha y} \right) \quad \ldots\ldots \quad (2.55)$$

$$s_2 = a \tan \left(\frac{-\beta y}{x - \alpha y} \right) \quad \ldots\ldots \quad (2.56)$$

With r_1, s_1, r_2, s_2 defined as above the stress function can be expressed in a generalized form :

$$= \sum_n \left(r_1^{n+1} \left(a_{4n-1} \cos (n+1) s_1 + a_{4n} \sin (n+1) s_1 \right) \right.$$

$$\left. + r_2^{n+1} \left(e_{4n+1} \cos (n+1) s_2 + e_{4n} \sin (n+1) s_2 \right) \right) \quad \ldots\ldots \quad (2.57)$$

In the limiting case when the elastic modulii tend to those of isotropic material, the stress function reduces to the same as given by M.L. Williams[24]. The stresses which are known to have the form :

$$\sigma_x = 2 \, \mathrm{Re} \left(\mu^2 \frac{d\varphi_1}{dz_1} + {}^2 \frac{d\varphi_2}{dz_2} \right) \quad \ldots\ldots \quad (2.58)$$

$$\sigma_y = 2 \, \mathrm{Re} \left(\frac{d\varphi_1}{dz_1} + \frac{d\varphi_2}{dz_2} \right) \quad \ldots\ldots \quad (2.59)$$

$$\tau_{xy} = -2 \mathrm{Re} \left(\mu \frac{d\varphi_1}{dz_1} - \frac{d\varphi_2}{dz_2} \right) \quad \ldots\ldots \quad (2.60)$$

now become the following :[19]

$$\sigma_y = \sum_n n(n+1) \left(r_1^{n-1} \left(a_{4n-1} \cos (n-1) s_1 + a_{4n} \sin (n-1) s_1 \right) \right.$$

$$\left. + r_2^{n-1} \left(e_{4n-1} \cos (n-1) s_2 + e_{4n} \sin (n-1) s_2 \right) \right) \quad (2.61)$$

$$\sigma_x = \sum_n n(n+1)\,(r_1^{n-1}\,(((\alpha^2-\beta^2)\,a_{4n-1}+2\alpha\beta\,a_{4n})\cos(n-1)\,s_1 + ((\alpha^2-\beta^2)\,a_{4n}-2\alpha\beta\,a_{4n-1})\sin(n-1)\,s_1+r_2^{n-1}\,((\alpha^2-\beta^2)\,e_{4n-1}+2\alpha\beta\,e_{4n})\cos(n-1)\,s_2+((\alpha^2-\beta^2)\,e_{4n}-2\alpha\beta\,e_{4n-1})\sin(n-1)\,s_2)) \quad \ldots \quad (2.62)$$

$$\tau_{xy} = -\sum_n n(n+1)\,(r_1^{n-1}(\cos(n-1)s_1\,(\alpha\,a_{4n-1}+\beta\,a_{4n})+\sin(n-1)\,s_1\,(\alpha\,a_{4n}-\beta a_{4n-1}))-r_2^{n-1}(\cos(n-1)\,s_2\,(\alpha\,e_{4n-1}+\beta\,e_{4n})+\sin(n-1)\,s_2(\alpha e_{4n}-\beta e_{4n-1}))) \quad \ldots \quad (2.63)$$

If the system of cartesian co-ordinates is placed with its origin at the crack tip, see Fig.2(d) where for simplicity of analysis the geometry of the crack is the reverse of that given in Fig. 2(c), then the stresses σ_y and τ_{xy} must vanish on $y = \pm 0$. Noting that for $y = +0$ we have $r_1 = r_2 = x$.... and $s_1 = 0$; $s_2 = 2\pi$ ..... And for $y = -0$ we have $s_1 = 2\pi$; $s_2 = 0$; $r_1 = r_2 = x$.

Then the requirement that $\sigma_y = 0$ yields

$$a_{4n-1} = -e_{4n-1}\cos 2\pi(n-1) \quad \ldots \quad (2.64)$$

and $$\sin 2\pi(n-1) = 0 \quad \ldots \quad (2.65)$$

From equation (2.64) it is clear that $n = \frac{1}{2}, 1, 3/2, 2, \ldots$etc.

$$e_{4n} = \cos 2\pi(n-1)\left(a_{4n} + \frac{2\alpha \cdot a_{4n-1}}{\beta}\right) \quad \ldots \quad (2.66)$$

Substituting the values of e_{4n-1} and e_{4n} in terms of a_{4n-1} and a_{4n} as given in the equations (2.64) and (2.66), we finally obtain[19] :

$$\varphi = \sum_{n=\frac{1}{2},1,\ldots} a_{4n-1}\,(r_1^{n+1}\cos(n+1)\,s_1+\cos 2(n-1)\,r_2^{n+1}$$
$$\left(\frac{2\alpha}{\beta}\sin(n+1)\,s_2-\cos(n+1)s_2\right))+a_{4n}$$
$$(r_1^{n+1}\sin(n+1,\,s_1+\cos 2\pi(n-1,\,r_2^{n+1}\sin_2$$
$$(n+1))\;\ldots\qquad\ldots\qquad(2.67)$$

$$\sigma_x = \sum_{n=\frac{1}{2},1,\ldots} n(n+1)\,(a_{4n-1}\,(r_1^{n-1}\,((\alpha^2-\beta^2)\cos(n-1)\,s_1-$$
$$2\alpha\beta\sin(n-1)\,s_1)-\cos 2\pi(n-1)\,r_2^{n-1}$$
$$(((\alpha^2-\beta^2)-4\alpha^2)\cos(n-1)\,s_2-(2(\alpha^2-\beta^2)\frac{\alpha}{\beta}-2\alpha\beta)$$
$$\sin(n-1)\,s_2))+a_{4n}\,(r_1^{n-1}\,(\sin(n-1)\,s_1\,(\alpha^2-\beta^2)$$
$$+2\,.\cos(n-1,\,s_1)+\cos 2\pi(n-1)\,r_2^{n-1}$$
$$(\sin(n-1)\,s_2\,(\alpha^2-\beta^2)+2\alpha\beta.\cos(n-1,s_2)))\qquad(2.68)$$

$$\sigma_y = \sum_{n=\frac{1}{2},1,\ldots} n(n+1)(a_{4n-1}\,(\cos(n-1)\,s_1\,r_1^{n-1}-\cos 2\pi(n-1)$$
$$r_2^{n-1}\,(\cos(n-1)\,s_2-\frac{2\alpha}{\beta}\sin(n-1)\,s_2))$$
$$+a_{4n}\,(r_1^{n-1}\sin(n-1)\,s_1+\cos 2\pi(n-1)\,r_2^{n-1}$$
$$\sin(n-1)\,s_2))\qquad\ldots\qquad(2.69)$$

$$\zeta_{xy} = \sum_{n=\frac{1}{2},1,\ldots} - n(n+1)\,(a_{4n-1}\,(r_1^{\,n-1}\,(\alpha\cos(n-1)s_1 - \beta\sin(n-1)s_1) - \cos 2\pi(n-1)\,r_2^{\,n-1}\,(\alpha\cos(n-1)s_2 + \sin(n-1)s_2(\frac{2\alpha^2}{\beta}+\beta))) + a_{4n}\,(r_1^{\,n-1}\,(\cos(n-1)s_1 + \sin(n-1)s_1) - r_2^{\,n-1}\cos 2(n-1)\,(\cos(n-1)s_2 + \sin(n-1)s_2)) \quad \ldots \quad (2.70)$$

Let

$$p = p_1 + i\,p_2 \text{ and } q = q_1 + i\,q_2 \quad \ldots \quad (2.72)$$

where

$$p_1 = \mathrm{Re}\left(\frac{\mu^2}{E_1} - \frac{\nu_{12}}{E_1}\right) = \left(\alpha^2\frac{\beta^2}{E_1}\right) - \frac{\nu_{12}}{E_1} = -\frac{1}{2G_{12}} \quad \ldots \quad (2.73)$$

$$p_2 = \mathrm{Im}\left(\frac{\mu^2}{E_1} - \frac{\nu_{12}}{E_1} = \frac{2\alpha\beta}{E_1}\right) \quad \ldots \quad (2.74)$$

$$q_1 = \mathrm{Re}\left(\frac{\mu^2}{E_1} - \frac{1}{\mu E_2}\right) = \frac{\alpha}{E_2(\alpha^2+\beta^2)} - \frac{\alpha\nu_{12}}{E_1} \quad \ldots \quad (2.75)$$

$$q_2 = -\mathrm{Im}\left(\frac{\mu^2}{E_1} - \frac{1}{E_2\mu}\right) = -\frac{\beta\nu_{12}}{E_1} - \frac{\beta}{E_2(\alpha^2+\beta^2)} \quad (2.76)$$

Then expressions for u and v become :

$$u = \sum_{n=\frac{1}{2},1,\ldots} (n+1)\,(a_{4n-1}\,(r_1^{\,n}\,(p_1\cos n s_1 - p_2\sin n s_1) - r_2^{\,n}\cos 2\pi(n-1)\,(\cos n s_2\,(p_1 - \frac{2\alpha}{\beta}p_2) - \sin n s_2\,(2p_1\frac{\alpha}{\beta} + p_2))) + a_{4n}\,(r_1^{\,n}(p_2\cos n s_1 + p_1\sin n s_1) + r_2^{\,n}\cos 2\pi(n-1)\,(p_2\cos n s_2 + p_1\sin n s_2))) + u_o - wy \quad \ldots \quad (2.77)$$

$$v = \sum_{n=\frac{1}{2},1,..} (n+1)\,(a_{4n-1}\,(r_1^n\,(q_1 \cos n s_1 - q_2 \sin n s_1) + r_2^n \cos 2\pi(n-1)\,(\cos n s_2 \cdot (q_1 - \frac{2\alpha}{\beta} q_2) - \sin n s_2 \cdot (2 q_1 \frac{\alpha}{\beta} + q_2))) + a_{4n}\,(r_1^n\,(q_2 \cos n s_1 + q_1 \sin n s_1) - r_2^n \cos 2\pi(n-1)\,(q_2 \cos n s_2 + q_1 \sin n s_2))) + v_o + wx \quad \ldots \quad (2.78)$$

where u_o, v_o and w are the three degrees of freedom for the rigid body motions as considered earlier also.

Element stiffness matrix

In this case the strain energy is given by the equation[19]

$$\bar{V}_s = \frac{h}{2} \iint \left(\frac{\sigma_x^2}{E_1} - \frac{2\nu_{12}}{E_1} \sigma_x \sigma_y + \frac{\sigma_y^2}{E_2} - \frac{\tau_{xy}^2}{G_{12}} \right) dy\,dx \quad (2.79)$$

This integration is done over the whole area of the special element. As before, the expressions for stresses are substituted in equation (2.79) and differentiating the total strain energy $\bar{V}_s$ with respect to each elemental degree of freedom. We can write

$$\bar{K}^e \cdot \bar{\lambda} = \frac{\partial \bar{V}_s}{\partial \bar{\lambda}} \quad \ldots \quad (2.80)$$

where $\bar{\lambda}^T = (a_1, a_2, a_3 \ldots a_{4n-1}, a_{4n}, u_o, v_o, w)$ .. (2.81)

Here bar is used for denoting parameters in case of orthotropic elastic field.

The stiffness matrix $\bar{K}_e$ may be computed as follows [19].

for i, j $\leq$ 4 N :

$$\bar{K}^e_{ij} = h\iint \left(\frac{\sigma_{xi}\,\sigma_{xj}}{E_1} - \frac{\nu_{12}}{E_1}\left(\sigma_{xi}\,\sigma_{yj} + \sigma_{xj}\,\sigma_{yi}\right) + \frac{\sigma_{yi}\,\sigma_{yj}}{E_2} + \frac{\tau_{xyi}\,\tau_{xyj}}{G_{12}}\right) dx\,dy \quad \ldots \quad (2.82)$$

while $\bar{K}^e_{ij} = 0$ for i, j > 4 N.

Here σ_{xi}, σ_{yi} and τ_{xyi} denote the coefficients of the ith terms of the series expansions of the stresses σ_x, σ_y and τ_{xy} as given by the equations (2.68), (2.69) and (2.70) respectively i.e., the coefficients of a_i for i=1, 4N. As discussed in the case of isotropic elastic field, it is desirable that the special element be connected to the rest of the structure at more points than there are degrees of freedom. And the discontinuity in displacement across the special element boundary is minimized in a least square sense. Substituting co-ordinates of the nodes in the equations (2.77) and (2.78) again results in a matrix equation of the form :

$$(\bar{L})\ \{\bar{\lambda}\} = \{\bar{\delta}\} \quad \ldots \quad (2.83)$$

where $$\bar{\delta}^T = (u_1, v_1, u_2, v_2, \ldots u_m, v_m) \quad (2.84)$$

is the nodal displacement vector where m is the number of nodal points on the boundary of the special element. $\bar{L}$ is a transformation matrix of dimension 2mx(4N+3). So the stiffness matrix

for the special element, when the nodal displacements are treated as the degrees of freedom, becomes[19] :

$$(\bar{K}) = (((\bar{L})^T (\bar{L}))^{-1} (\bar{L})^T) (\bar{K}^e) ((\bar{L})^T (\bar{L}))^{-1} (\bar{L})^T \qquad (2.85)$$

Then $(\bar{K})$ is assembled to the global stiffness matrix. Once the nodal displacements are solved $\bar{\ }$ can be evaluated by the relation :

$$\bar{\lambda} = (\bar{L}^T \bar{L})^{-1} \bar{L}^T \bar{\delta} \quad . \qquad \ldots \qquad (2.86)$$

The stress intensity factors K_I and K_{II} may be evaluated, once the vector $\bar{\lambda}$ is known using the formulae[19] :

$$K_I = \lim_{\substack{x \to 0 \\ y \to 0}} \sigma_y \, (2\pi (x^2+y^2))^{\frac{1}{2}}$$

$$= \tfrac{3}{4} \, (2\pi)^{\frac{1}{2}} \, \frac{2\alpha}{\beta} \, a_1 \qquad \ldots \qquad (2.87)$$

where a_1 is the first element of the vector $\bar{\lambda}$.

$$K_{II} = \lim_{\substack{x \to 0 \\ y \to 0}} \tau_{xy} \, (2\pi (x^2+y^2))^{\frac{1}{2}}$$

$$= \tfrac{3}{4} \, (\frac{2\alpha^2}{\beta} a_1 + 2\alpha a_2) \, . \, (2\pi)^{\frac{1}{2}} \ldots \qquad (2.88)$$

where a_2 is the second element of the vector $\bar{\lambda}$.

In calculating K_I and K_{II} use is made of the series expansions (2.69) and (2.70) for σ_y and τ_{xy} respectively.

CHAPTER - 3

NUMERICAL SCHEME

3.1 Programme description

The whole programme is basically an assemblage of twentyone sub programme segments meant for different specific operations. The main programme is the monitoring part which decides the actions and work flow line of the rest twenty programme segments or subprogrammes. There are eighteen subroutines and two functions as follow :

1. SMTRX	8. TROMB1	15. F04AAF
2. BMTRX	9. TROMB	16. SIF
3. ESM	10. SESM	17. STRESS
4. ASMBLE	11. MATINV	18. POLAR
5. SPCL	12. ASMBLS	19. F1
6. ELMTRX	13. DSMBLE	20. F
7. UMTRX	14. DSMBLS	

In addition to the control or monitor part the main programme consists of two more portions which calculate energy release rate and stresses in each element after the displacements at all the nodes are known if control options for their evaluation are given in the data as directed in the beginning of the programme listing (Appendix I). A brier account of purpose and function of each subprogramme is given below in order.

1. SMTRX:

This subroutine calculates the stiffness constants for the material to relate stress and strain at any point in the domain. It takes material constants like E_1, E_2, G_{12} and ν_{12} as input and after calculating stiffness constants as described by the equation(2.20)it passes these constants to the main programme and they are stored.

2. BMTRX :

It calculates (B) as given in equation(2.14)for each general element and passes it to 'ESM' to calculate element stiffness matrix.

3. ESM :

It calculates the stiffness matrix for each general element. It takes (B) of equation(2.14)and $(\bar{Q})$ of equation(2.20) as input and calculates each element of each element stiffness matrix according to the equation(2.23).

4. ASMBLE :

For each general element, once the element stiffness matrix is formed by 'ESM' it is passed to this subroutine. The function of this subroutine is to assemble each element stiffness matrix in the global or master stiffness matrix at relevant positions.

SPCL :

This is a control subroutine for evaluation of special element stiffness matrix by monitoring the subroutines which are

employed to perform this evaluation. Its function is to develop the element stiffness matrix for the special element around the crack tip. This calls directly three more subroutines to do that. These subroutines are : 'ELMTRX', 'UMTRX' and 'SESM'.

6. ELMTRX :

This subroutine develops the $\bar{L}$ matrix of the equation(2.83) when it is called to do that by SPCL. To do that it takes the help of equations (2.77) and (2.78) which describe the total displacement field in terms of nodal co-ordinates of the special element and the unknown constants i.e. $\{\bar{\lambda}\}$ of equation(2.83).

7. UMTRX :

This subroutine generates the elements of stiffness matrix ($\bar{K}^e$) using the equations (2.82). This subroutine has to perform a double integration over two dimensional space of a complicated function. This is done numerically, To do this it calls 'TROMB1'.

8. TROMB1 :

This does the outer integration of the equation (2.79) over the whole area of the special element. This subroutine integrates IB for the total range of x where $IB=\int F(x,y)\, dy$. The limit for y at any value ofx is a function determined by the shape of the element. This subroutine calls F1 to evaluate IB at every step of x. The integration is done by 'repeated interval-halving and Romberg integration' technique[27].

9. F1 :

This function calls another subroutine called 'TROMB' which performs the integration of F(x,y, with respect to y to evaluate IB.

10. TROMB :

This does the integration of F(x,y) with respect to y by 'repeated interval-halving and Romberg integration' technique[27].

11. F :

This is the function body which evaluates F(x,y) with input of x and y values.

12. SESM :

This subroutine is developed to perform a number of matrix operations like transposition, multiplication and inversion to evaluate $(\bar{K})$ of the equation (2.85). Except the inversion all other operations are done in this subroutine and for inversion it calls another subroutine called 'MATINV'. It is only here, that final element stiffness matrix $(\bar{K})$ for the special element is formed.

13. MATINV :

This subroutine has been developed for matrix inversion by partitioning[28].

14. ASMBLS :

Once the element stiffness matrix for the special element is formed this is passed to the subroutine 'ASMBLS' which assembles in in the global stiffness matrix in relevant positions.

15. DSMBLE :

This subroutine is needed only when the calculation of energy release rate is performed. To be precise what it does is just the opposite of 'ASMBLE'. This removes the particular contribution of any element stiffness matrix of any general element from the global stiffness matrix. When the stiffness matrix of an element undergoes some change, this routine is used to remove the previous element stiffness matrix from the global stiffness matrix and the new stiffness matrix for the element is evaluated by 'ESM' and assembled to the global stiffness matrix by 'ASMBLE'. This operation will be discussed later in this section only.

16. DSMBLS :

This is a subroutine whose function is identically same as 'DSMBLE' but this only deals with the element stiffness matrix of the special element.

17. FC4AAF :

This is a standard subroutine for simultaneous equation s olving in the NAG library. Use has been made of this subroutine to find out the displacement vector after the force vector and the global stiffness matrix have been formed of the equation

$$\{F\} = (K)\ \{R\} \qquad \ldots \qquad (3.1)$$

Here $\{F\}$ is the force vector. $\{R\}$ is the displacement vector i.e. the solution vector and (K) is the global stiffness matrix.

18. SIF :

Once the displacement vector is known this subroutine calculate the stiffness intensity factor by using the equations(2.86), (2.87) and (2.88) respectively. The equation (2.87) is used to find out stiffness intensity factor in mode I or the opening mode and (2.88) is used to calculate that in mode II or the sliding mode.

19. STRESS :

When some points in the special element are given with their coordinates in the data, this subroutine calculates the stresses at those points if the control option is given for that as described in the beginning of the programme listing in Appendix I. After the unknown coefficients in the equations(2.67), (2.68) and (2.69) are known, this subroutine makes the use of same equations to find out the stresses.

20. POLAR :

If the control option for this is given in the data as described in the programme listing, it converts all the stresses in polar coordinate in the output.

3.2 Scheme for energy release rate

It already has been mentioned in section 1.4 that from equation (2.87) it is clear that when is zero, the calculation of stiffness intensity factors using equation (2.87) is impossible. To overcome this drawback another scheme to determine the energy release rate has been introduced in this work. The technique that has been used here to evaluate energy release rate is very efficient and economic too. The details are presented in ref. (29,30). For the sake of completeness the method is briefly discussed below :

This method involves calculations based on the direct evaluation of changes in the potential energy content as the crack progresses. For instance, the potential energy could be found for two different positions of the crack tip. In Fig.2(c) it has been shown somewhat crudely, a finite element idealization of a structure including a crack. The energy is now evaluated for two different positions of the crack tip separated by Δa and approximately we obtain

$$\text{Energy release rate} = G = \frac{d\pi}{da} \quad \frac{\pi_1 - \pi_2}{\Delta a} \qquad \ldots \qquad (3.2)$$

Such approaches were first suggested by Dixon and Pook[31] and followed by others.[32-34].

The two separate solutions implicit in such method are uneconomic and the direct determination of 'G' from a single

solution would be preferable. However, with a simple modification suggested by Parks[29] and Hellen[30] it is possible to avoid such 'double work'.

To describe this method the system illustrated in Fig.2(c) will again be considered. Let K, a and f correspond to the stiffness matrix, displacement vector and the external load vector respectively with original position of the crack.Further let Δa and Δk be the changes in these quantities due to the extension of the crack by Δa. With original crack positions we have

$$Ka + f = 0 \quad \ldots \quad (3.3)$$

We can now write the change in potential energy due to the crack extension as

$$\Delta\pi = \tfrac{1}{2} (a+\Delta a)^T (K+\Delta K) (a+\Delta a) + (a+\Delta a)^T f - \tfrac{1}{2} a^T K a - a^T f \quad \ldots (3.4)$$

Neglecting the second order terms we get

$$\Delta\pi = \tfrac{1}{2} a^T \Delta K a \quad \ldots \quad (3.5)$$

Therefore, $G = \Delta\pi / (\Delta a . t)$ ... (3.6

where 't' is the thickness of the plate.

It is evident that to determine G only evaluation of 'a' by single solution is required. And to calculate ΔK the appropriate stiffness changes when the crack propagates by Δa, are to be calculated. This is done by recomputing the stiffness matrices and substituting the previous stiffness matrices in the global stiffness

matrix for those few elements only in the vicinity of the crack tip whose geometry gets altered by the crack extension including the special element ofcourse.

CHAPTER - 4

RESULT AND DISCUSSION

To verify the formulation of special element in orthotropic case as presented in section 2.2.2 alongwith the whole numerical scheme and the computer programme, the results obtained in this work are compared with those given in ref. 19. The values of stress intensity factor have been calculated in [19] using the special element in isotropic case as described in section 2.2.1. But in the present work the stress intensity factors have been calculated using the special element in orthotropic case with $E_1 = E_2$ and $\nu_{12} = \nu_{21} =$ to bring the isotropicity in the orthotropic formulation. The value of K_I that has been compared with that given in [19] in the case of a thin plate of dimension 254 mm x 508 mm. The uniform tensile stress of 689 kPa has been applied in Y-direction while the crack is 84.66 mm long. The comparison of values of K_I has been done in two cases. In the first case r_c has been taken to be 25.4 mm whereas in the second case r_c has been taken to be 16.9 mm, where r_c is the radius of the special polygonal element as shown in Fig. 4.9. The comparison of the values of K_I obtained in the present work and in [19] alongwith the theoretical value assuming infinitely long plate has been presented below :

r_c	Ref. 19 K_I(kPa.$M^{\frac{1}{2}}$)	Present work for N = 16 K_I (kPa. $M^{\frac{1}{2}}$)	Theoretical value K_I(kPa. $M^{\frac{1}{2}}$)
25.4	265.5	266.7	273.5
16.9	263.3	264.1	

There are five cases in all for which numerical investigation have been done. The convergence test has been performed in all these five cases. It has been successfully observed that the values of stress intensity factors are converging very fast with the increase of the number of degrees of freedom i.e. the number of elements in the vector λ in equation (2.83). When this number is increased from 14 to 16 the average change in the values of stress intensity factors are of the order of 0.06% which is really good enough for any practical engineering purpose.

This has been clearly mentioned in Chapter-1 (page 3) that the stress intensity factors do not depend on the material properties of the material concerned. They only depend on the geometry of the structure, crack geometry and the applied stress conditions. But this is true so far as the isotropic elastic field is concerned. In orthotropic elastic field it is true that the stress intensity factors do not depend on the absolute values of E_1, E_2 or even G_{12} but they depend

been performed in last two cases i.e. case-4 and case-5. had there been enough computational facilities. But as there is limited computational resources available the study of effect of poisson's ratio in case-4 and case-5 has been kept out of the scope of the present work. The material properties in all five cases are taken as follow :

$E_1 = 4.0 \times 10^8$ kPa ; $E_2 = 2.0 \times 10^8$ kPa ; $G_{12} = 1.5 \times 10^8$ kPa.

Now, all these five cases will be described and dealt with in an increasing order as follow :

CASE-1 In this case analysis has been performed for a central crack in a thin plate of dimension 160 mmx200 mm. The length of the crack is 40 mm and r_c=15 mm. To save the computational time and effort as well, the geometric and loading symmetry has been exploited. Only one quadrant i.e. one-fourth of the total structure has been considered as shown in Fig.4.9. It has eventually reduced the problem size to one-fourth of the original size.

The structure has been discretized in a fairly coarse mesh in the region far away from the crack-tip and the special element. Gradually the mesh is made finer and finer as it approached the special element as shown in Fig. 4.9. There are 88 elements in all including 87 general elements and one special element around the crack-tip. It has 60 nodes in total. In plain stress analysis there are only two degrees of freedom

per node u and v, so, the global stiffness matrix is of the size of 120 x 120 and each of the displacement vector and force vector contains 120 elements. A problem of this size with N = 14 and an integration scheme for the special element as described in section 3.1 with J_{max} =4 and N_{max}=4 as described in 'Repeated interval halving and Romberg integration'[27] takes little over 11 minutes of CPU time in DEC-1090 system, where N is the number of elements taken in vector λ of equation (2.83).

For this case convergence test has been performed and presented in Table 1. It can be seen from the table that N =14 gives a reasonably good convergence of E_p=0.065%. E_p has been calculated to show the percentage variation of the value of K_I for any value of N with respect to that for N =16.

The study of effect of applied stress on stress intensity factor K_I with different poisson's ratio values has been done for a range of 5000 kPa to 15000 kPa with a constant step increment of 1000 kPa in the applied stress. It has been presented in Table 9. It is seen that the value of K_I varies quite linearly with applied stress as shown in Fig. 4.1 to Fig. 4.5 which is of course theoretically expected. To save computer time this variation of applied tensile stress in Y-direction and calculation of corresponding K_I values has been done in the following manner :

Once the element stiffness matrices for all the elements including the crack-tip special element is done, they are effectively assembled to form the global stiffness matrix. When this stage of computation is once reached, a number of times the simultaneous equation solving is done with different load vectors $\{R\}$ and after the displacement vector is obtained each time, the stress intensity factor is calculated. This scheme, instead of having a run afresh each time for different applied stress waves lot of computational time and cost as well.

The study of effect of poisson's ratio on stress intensity factor K_I has been studied by varying the value of from 0.30 to 0.10 with a constant step reduction of 0.05. Thus 5 runs have been taken for $\nu_{12}=0.30$, $\nu_{12}=0.25$, $\nu_{12}=0.20$, $\nu_{12}=0.15$ and $\nu_{12}=0.10$. In this case for each value of a fresh run has been taken since when the value of changes all the element stiffness matrices undergo some change. The variation of K_I and a_1 (i.e. the first element of the vector) with respect to the value of ν_{12} is shown in Fig. 4.6 and relevant data is tabulated in Table 6. The Table 6 has been prepared for applied stress in Y-direction i.e. $\sigma_y=5000.0$ kPa. It is evident from Fig. 4.6 that a_1 decreases very slowly with the increase of the value of ν_{12} and K_I increases with a greater rate with respect to value of ν_{12} but this rate gradually dies down as the value of ν_{12} increases.

CASE-2 Here a thin plate with symmetric notches on both sides under uniform tensile stress in Y-direction is studied. The dimension of the plate is 160 mm x 200 mm. The length of each notch is 20 mm and r_c=15 mm. Here also exploiting the geometric and loading symmetry only one-fourth of the structure has been analysed. Only the first quadrant of the structure has been discretized for finite element model as shown in Fig. 4.10. The rest of the problem description in this case is identical to that in case-1.

In this case also a reasonably good convergence has been observed. This has been shown in Table 2. The percentage error in K_I value for N =14 is only 0.073% where E_p is calculated taking K_I value for N =16 as standard. In other words this is the value of percentage variation in K_I value for N =14 and N =16.

The effect of applied stress on stress intensity factor K_I with different poisson's ratio values has been studied the same way as in case-1. Fig. 4.1 to Fig. 4.5 and Table 10 are referred to in this connection.

The effect of poisson's ratio on stress intensity factor K_I has also been studied in an identical manner as in case-1. In this case a_1 increases very slowly with the increase of the value of poisson's ratio unlike that in case-1. as evident from Fig. 4.7 and Table 7. But K_I increases in the same fashion as that in case-1.

CASE-3 In this case a thin plate with a side notch on one side under uniform tensile stress in Y-direction has been taken. The plate is 80 mm wide and 140 mm long. The crack in this case is 15 mm long and r_c is also same as the crack length as shown in Fig. 4.11. Due to the asymmetry in the geometry of the structure and crack it is not possible in this case to reduce the problem. As a matter of consequence it is a much larger problem compared to those in Case-1 and Case-2. It has been so discretized for finite element idealisation that it has 104 nodes in all and 161 elements including 1 crack-tip special element. Here the special element has 18 nodes compared to 10 nodes in Case-1 and Case-2. The global stiffness matrix in this case is of the size 208x208 and both the displacement and external load vector are of the size 208x1. To execute this problem it takes a little more than 22 minutes of CPU time and a huge storage area to store arrays of very large size. For this reason to run this problem with a limited core area of 50 k here in DEC-1090 is very difficult owing to heavy page-fault during execution.

The convergence observed in this case is also very much satisfactory as presented in Table 3. The value of E_p for $N = 14$ is only 0.048% which is the least in all the five cases. Perhaps this is due to r_c is equal to the total crack length. This is seen in Table 3 that for any practical purpose $N = 14$ is really good enough.

The study of effect of applied stress on K_I has been performed in the same way as earlier described in Case-1 description. This study has been carried out with different values of poisson's ratio as in other cases and variation of K_I with respect to applied stress for ν_{12}=0.30 to ν_{12}=0.10 has been shown in Fig. 4.1 to Fig. 4.5 and the relevant results are tabulated in Table 11.

The effect of poisson's ratio on K_I has also been studied in an identical manner as done earlier in first two cases. Here the variation of K_I with respect to poisson's ratio resembles that in case-1 as evident from Fig. 4.8 and Table 11.

CASE-4 In this case a thin plate with a 15 mm long side notch has been analysed under uniform shear stress in positive X-direction. The plate is 80 mm wide and 140 mm long as in Case-3. In this case the finite element model is same as that in Case-3. (see Fig. 4.11). Only the loads those have been applied to achieve uniform shear stress are oriented in positive X-direction. In this case the fracture is in pure mode-II i.e. the sliding mode. Here K_{II} i.e. the stress intensity factor in sliding mode has been calculated for different applied stresses as done earlier in Case-1, Case-2 and Case-3. The effect of poisson's ratio on K_{II} could have been calculated as it has been done in all first three cases but the computational difficulty due to the shortage of storage in disk

and limited core area of 50 k as described earlier in Case-3 problem description, this has been kept out of the scope of the present work.

The variation of K_{II} with respect to applied shear stress has been studied and shown for only =0.15 in Fig.4.2. The relevant results of this study has been presented in Table 12. It is seen in Fig. 4.2a that K_{II} variation is exactly linear with respect to applied shear stress for different values of poisson's ratio, as it is expected to be.

CASE-5 This case is an extension of Case-4. The problem description in this case is same as that in Case-4 but the loading conditions here are different.Here the applied loads are 30° inclined to the vertical loads applied in Case-3 as shown in finite element model in Fig. 4.11. The vertical components of the applied loads in this case simulates a uniform tensile stress field and on the other hand the horizontal components i.e. along the positive X-direction of the applied loads simulate a uniform shear stress field. As a result the crack in this case is a combination of two modes of fracture i.e. opening mode and sliding mode. The stress intensity factors in both the modes i.e. K_I & K_{II} have been found out separately.

In this case the variation of K_I and K_{II} have been studied with respect to the applied stress σ_I normal to

a plane which is 30 degree inclined to the X-axis (See Fig. 4.11). Fig. 4.2a shows this variation which is perfectly linear as expected. All the relevant results are presented in Table 13.

The study of effect of poisson's ratio on stress intensity factors has been kept out of the scope of the present work owing to the same reason as mentioned in problem description of Case-3.

SPECIAL CASE The section 3.2 deals with the calculation of energy release rate. This case deals with one such case where the evaluation of stress intensity factors by the direct method is not possible. A thin plate made of 3MxP251S fibre glass/epoxy has been considered. The required data for its material properties has been taken from [20] as follows :
$E_1 = 8.0 \times 10^6$ psi ; $E_2 = 2.7 \times 10^6$ psi ; $G_{12} = 1.3 \times 10^6$ psi and $\nu_{12} = 0.25$.
In this case the characteristic equation (2.48) of Chapter 2 has such roots whose real parts i.e. α do not exist.
The calculation of energy release rate for a plate with a central crack of this material has been found out. The dimension and crack geometry are same as those in Case-1. The convergence of energy release rate G with the increase in number of terms of the vector λ of equation (2.83) has been observed and results are presented in Table 14.

CHAPTER - 5

CONCLUSIONS

5.1 The results of analysis can be summed up as follows :

1. The special crack tip element can be successfully used in orthotropic elastic field and this can be incorporated in any standard finite element programme for plane stress problems.

2. Since this element has no constrains on its size or shape, the discretization of the rest of the structure is quite flexible.

3. The convergence of stress intensity factors is reasonably good. It is felt that 14 or 16 no. of terms in the vector λ i.e. so many number of degrees of freedom excluding u_o, v_o and w i.e. the rigid body transitional and rotational degrees of freedom give very good results.

4. Energy release rate can also be evaluated if necessary using the same special crack tip element with the scheme described in section 3.2.

5. In orthotropic case the stress intensity factors depend on some ratios of material properties and poisson's ratio.

5.2 Suggestions for extension of the work

Present work can be extended in number of directions to study more about cracks in orthotropic plates. Here only the

effect of poisson's ratio on computed values of stress intensity factors have been studied. The dependence on other material property ratios like $\frac{E_1}{E_2}$ and $\frac{E_1}{G_{12}}$ can be studied to explore the possibility that some range of these ratios might exist that may be considered to be relatively safe in a sense that stress intensity factors in particular modes for those range are quite low. This is of practical importance since the material properties of fibre composites can be tailored likewise to get those ratios in the preferred ranges. An effective optimization of the material properties in this light will certainly lead to more economic and safer material design.

The plates analysed in the present work are all specially orthotropic, i.e. the material principal directions coincide with the reference axes of the special crack tip element. An extension of the work would be to modify for the general orthotropic case. The general elements used here can be used in the extended case also. In this work, the plates analysed are all laminae, which can be extended to all sort of laminates like symmetric, skew-symmetric etc.

A three-dimensional special crack-tip element can also be developed with the same concept of using theoretically exact stress function and restoring the compatibility of displacements across the special element boundaries in a least square sense.

CASE -1

CONVERGENCE TABLE FOR K_I

No. OF TERMS TAKEN N	STRESS INTENSITY FACTOR FOR $\nu_{12}=0.30$ K_I (KPa $M^{\frac{1}{2}}$)	PERCENTAGE ERROR E_p
6	2227.88	12.10%
8	2436.73	3.86%
10	2501.61	01.30%
12	2519.86	0.58%
14	2532.89	0.065%
16	2534.56	0.00%

TABLE : 1

CASE -2

CONVERGENCE TABLE FOR K_I

No. OF TERMS TAKEN N	STRESS INTENSITY FACTOR FOR $\nu_{12}=0.30$ K_I (KPa.$M^{\frac{1}{2}}$)	PERCENTAGE ERROR E_p
6	2724.71	13.41%
8	2962.28	5.86%
10	3060.77	2.73%
12	3133.15	0.43%
14	3144.38	0.073%
16	3146.68	0.00%

TABLE : 2

CASE-3

CONVERGENCE TABLE FOR K_I

No. OF TERMS TAKEN N	STRESS INTENSITY FACTOR FOR $\nu = 0.30$ K_I (KPa.$M^{\frac{1}{2}}$)	PERCENTAGE ERROR E_p
6	1886.75	10.23%
8	2008.44	4.44%
10	2067.08	1.65%
12	2091.46	0.49%
14	2100.75	0.048%
16	2101.76	0.00%

TABLE : 3

CASE-4

CONVERGENCE TABLE FOR K_{II}

No. OF TERMS TAKEN N	STRESS INTENSITY FACTOR FOR $\nu = 0.15$ K_{II} (KPa.$M^{\frac{1}{2}}$)	PERCENTAGE ERROR E_p
6	892.74	13.71%
8	986.56	4.63%
10	1022.15	1.19%
12	1030.74	0.36%
14	1033.91	0.053%
16	1034.46	0.00%

TABLE : 4

CASE -5

CONVERGENCE TABLE FOR K_I & K_{II}

NO. OF TERMS TAKEN N	STRESS INTENSITY FACTOR (MODE-1) FOR $\nu_{12}=0.15$ K_I(KPa.$M^{\frac{1}{2}}$)	PERCENTAGE ERROR E_p	STRESS INTENSITY FACTOR (MODE-2) FOR $=0.15$ K_{II}(K Pa.$M^{\frac{1}{2}}$)	PERCENTAGE ERROR E_p
6	616.94	14.01%	461.16	10.84%
8	678.99	5.36%	494.83	4.33%
10	701.81	2.18%	506.58	2.06%
12	713.50	0.55%	514.75	0.48%
14	716.94	0.071%	516.91	0.062%
16	717.45	0.00%	517.23	0.00%

TABLE : 5

EFFECT OF POISSON'S RATIO IN CASE-1

POISSON'S RATIO (ν_{12})	$\alpha = Re[\mu]$ $\beta = Im[\mu]$	FIRST COEFFICIENT OF VECTOR a_1	STRESS INTENSITY FACTOR (MODE-I) K_I (KPa $M^{\frac{1}{2}}$)
=0.30	= 0.43642 = 1.10624	1708.70	2534.56
=0.25	= 0.40643 = 1.11742	1733.85	2371.17
=0.20	= 0.37481 = 1.12857	1767.10	2206.61
=0.15	= 0.33971 = 1.13964	1803.35	2021.17
=0.10	= 0.30073 = 1.15055	1849.37	1817.51

TABLE : 6

EFFECT OF POISSON'S RATIO IN CASE-2

POISSON'S RATIO (ν_{12})	$\alpha = Re[\mu]$ $\beta = Im[\mu]$	FIRST COEFFICIENT OF VECTOR a_1	STRESS INTENSITY FACTOR (MODE-I) K_I (I. Pa.$M^{\frac{1}{2}}$)
0.30	= 0.43642 = 1.10624	2121.37	3146.68
0.25	= 0.40643 = 1.11742	2050.50	2804.21
0.20	= 0.37481 = 1.12857	1981.71	2474.60
0.15	= 0.33971 = 1.13964	1916.98	2148.52
0.10	= 0.30073 = 1.15055	1856.93	1824.94

TABLE : 7

EFFECT OF POISSON'S RATIO IN CASE-3

POISSON'S RATIO (ν_{12})	= Re [μ] = Im [μ]	FIRST COEFFICIENT OF VECTOR a_1	STRESS INTENSITY FACTOR (MODE-I), K_I (KPa.M$^{\frac{1}{2}}$)
0.30	= 0.43642 = 1.10624	1416.99	2101.76
0.25	= 0.40645 = 1.11742	1514.80	2071.48
0.20	= 0.37481 = 1.12857	1607.99	2007.88
0.15	= 0.33971 = 1.13964	1695.28	1900.05
0.10	= 0.30073 = 1.15055	1791.29	1760.43

TABLE : 8

EFFECT OF APPLIED STRESS IN CASE-1

STRESS APPLIED IN Y-DIRECTION σ_y(KPa)	STRESS INTENSITY FACTOR (MODE-I) FOR $\nu = 0.30$ K_I(KPa.$M^{\frac{1}{2}}$)	STRESS INTENSITY FACTOR (MODE-1) FOR $\nu = 0.25$ K_I(KPa.$M^{\frac{1}{2}}$)	STRESS INTENSITY FACTOR (MODE-1) FOR $\nu = 0.20$ K_I(KPa.$M^{\frac{1}{2}}$)
5000.0	2534.56	2371.16	2206.61
6000.0	3041.50	2845.41	2648.01
7000.0	3548.42	3319.68	3089.35
8000.0	4055.31	3793.91	3530.63
9000.0	4562.28	4268.18	3971.95
10000.0	5069.23	4742.42	4413.32
11000.0	5576.11	5216.66	4854.64
12000.0	6083.10	5690.78	5295.96
13000.0	6589.96	6165.17	5737.28
14000.0	7096.83	6639.36	6178.61
15000.0	7603.68	7113.48	6619.93

TABLE : 9

EFFECT OF APPLIED STRESS IN CASE-1

STRESS APPLIED IN Y-DIRECTION σ_y(KPa.)	STRESS INTENSITY FACTOR (MODE-I) FOR $\nu_{12} = 0.15$ K_I(KPa.$M^{\frac{1}{2}}$)	STRESS INTENSITY FACTOR (MODE-I) FOR $\nu_{12} = 0.10$ K_I(KPa.$M^{\frac{1}{2}}$)
5000.0	2021.16	1817.51
6000.0	2425.43	2181.10
7000.0	2829.71	2544.57
8000.0	3233.96	2908.12
9000.0	3638.18	3271.61
10000.0	4042.43	3635.13
11000.0	4446.65	3998.61
12000.0	4850.83	4362.12
13000.0	5255.15	4725.66
14000.0	5659.35	5089.21
15000.0	6063.59	5452.77

TABLE :9(contd.)

EFFECT OF APPLIED STRESS IN CASE-2

STRESS APPLIED IN Y-DIRECTION σ_y(KPa)	STRESS INTENSITY FACTOR (MODE-I) FOR ν_{12}=0.30 K_I (KPa.$M^{\frac{1}{2}}$)	STRESS INTENSITY FACTOR (MODE-I) FOR ν_{12}=0.25 K_I(KPa.$M^{\frac{1}{2}}$)	STRESS INTENSITY FACTOR (MODE-I) FOR ν_{12}=0.20 K_I(KPa.$M^{\frac{1}{2}}$)
5000.0	3146.68	2804.21	2474.60
6000.0	3776.01	3365.08	2969.62
7000.0	4405.44	3925.95	3464.54
8000.0	5034.74	4486.81	3959.36
9000.0	5664.12	5047.67	4454.28
10000.0	6293.46	5608.42	4949.31
11000.0	6922.78	6169.34	5444.22
12000.0	7552.13	6730.20	5939.04
13000.0	8181.39	7291.07	6434.07
14000.0	8810.80	7851.88	6928.88
15000.0	9440.08	8412.73	7423.88

TABLE : 10

STRESS APPLIED IN Y-DIRECTION σ_y(KPa)	STRESS INTENSITY FACTOR (MODE-I) FOR ν_{12} = 0.15 K_I(KPa.M$^{\frac{1}{2}}$)	STRESS INTENSITY FACTOR (MODE-I) FOR ν_{12} = 0.10 K_I(KPa.M$^{\frac{1}{2}}$)
5000.0	2148.52	1824.94
6000.0	2578.27	2189.98
7000.0	3007.98	2555.01
8000.0	3437.71	2920.11
9000.0	3867.36	3284.96
10000.0	4297.14	3649.94
11000.0	4726.77	4014.94
12000.0	5156.45	4379.91
13000.0	5586.25	4744.94
14000.0	6015.94	5109.93
15000.0	6445.67	5474.82

TABLE : 10 (CONTD.)

EFFECT OF APPLIED STRESS IN CASE-3

STRESS APPLIED IN Y-DIRECTION σ_y(KPa)	STRESS INTENSITY FACTOR (MODE-I) FOR ν_{12}=0.30 K_I(KPa.$M^{\frac{1}{2}}$)	STRESS INTENSITY FACTOR (MODE-I) FOR ν_{12}= 0.25 K_I(KPa.$M^{\frac{1}{2}}$)	STRESS INTENSITY FACTOR (MODE-I) FOR ν_{12}=0.20 K_I(KPa.$M^{\frac{1}{2}}$)
5000.0	2101.76	2071.49	2007.88
6000.0	2522.21	2485.85	2409.56
7000.0	2942.49	2900.08	2811.13
8000.0	3362.90	3314.48	3212.61
9000.0	3783.21	3728.74	3614.20
10000.0	4203.62	4142.99	4015.76
11000.0	4623.94	4557.36	4417.43
12000.0	5044.32	4971.67	4818.96
13000.0	5464.67	5385.87	5220.58
14000.0	5884.93	5800.27	5622.06
15000.0	6305.42	6214.56	6023.74

TABLE : 11

EFFECT OF APPLIED STRESS ON K_{II} IN CASE-4

STRESS APPLIED IN X-DIRECTION σ_x(KPa)	STRESS INTENSITY FACTOR (MODE-II) FOR ν_{12}=0.15 K_{II}(KPa.$M^{\frac{1}{2}}$)	STRESS APPLIED IN X-DIRECTION σ_x (KPa)	STRESS INTENSITY FACTOR (MODE-II) FOR ν_{12}=0.15 K_{II}(KPa.$M^{\frac{1}{2}}$)
5000.0	1034.46	11000.0	2275.61
6000.0	1241.30	12000.0	2482.84
7000.0	1448.14	13000.0	2689.66
8000.0	1655.24	14000.0	2896.38
9000.0	1862.13	15000.0	3103.55
10000.0	2068.94	-	-

TABLE : 12

EFFECT OF APPLIED STRESS ON K_I & K_{II} IN CASE-5

STRESS APPLIED 30 DEGREE INCLINED TO Y-AXIS σ_I(KPa)	STRESS INTENSITY FACTOR (MODE-I) FOR ν_{12}=0.15 K_I (KPa.$M^{\frac{1}{2}}$)	STRESS INTENSITY FACTOR (MODE-II) FOR ν_{12}=0.15 K_{II}(KPa.$M^{\frac{1}{2}}$)
5000.0	717.45	517.23
6000.0	860.96	620.68
7000.0	1004.51	724.21
8000.0	1147.86	827.63
9000.0	1291.47	931.07
10000.0	1434.97	1034.56
11000.0	1578.44	1137.98
12000.0	1721.93	1241.38
13000.0	1865.37	1344.85
14000.0	2008.91	1448.29
15000.0	2152.35	1551.72

TABLE : 13

SPECIAL CASE

CONVERGENCE TABLE FOR G

NO. OF TERMS TAKEN N	ENERGY RELEASE RATE G (N/M)	PERCENTAGE ERROR E_p
6	0.9538	9.81%
8	0.9021	3.86%
10	0.8803	1.35%
12	0.8699	0.16%
14	0.8693	0.08%
16	0.8686	0.00%

TABLE : 14

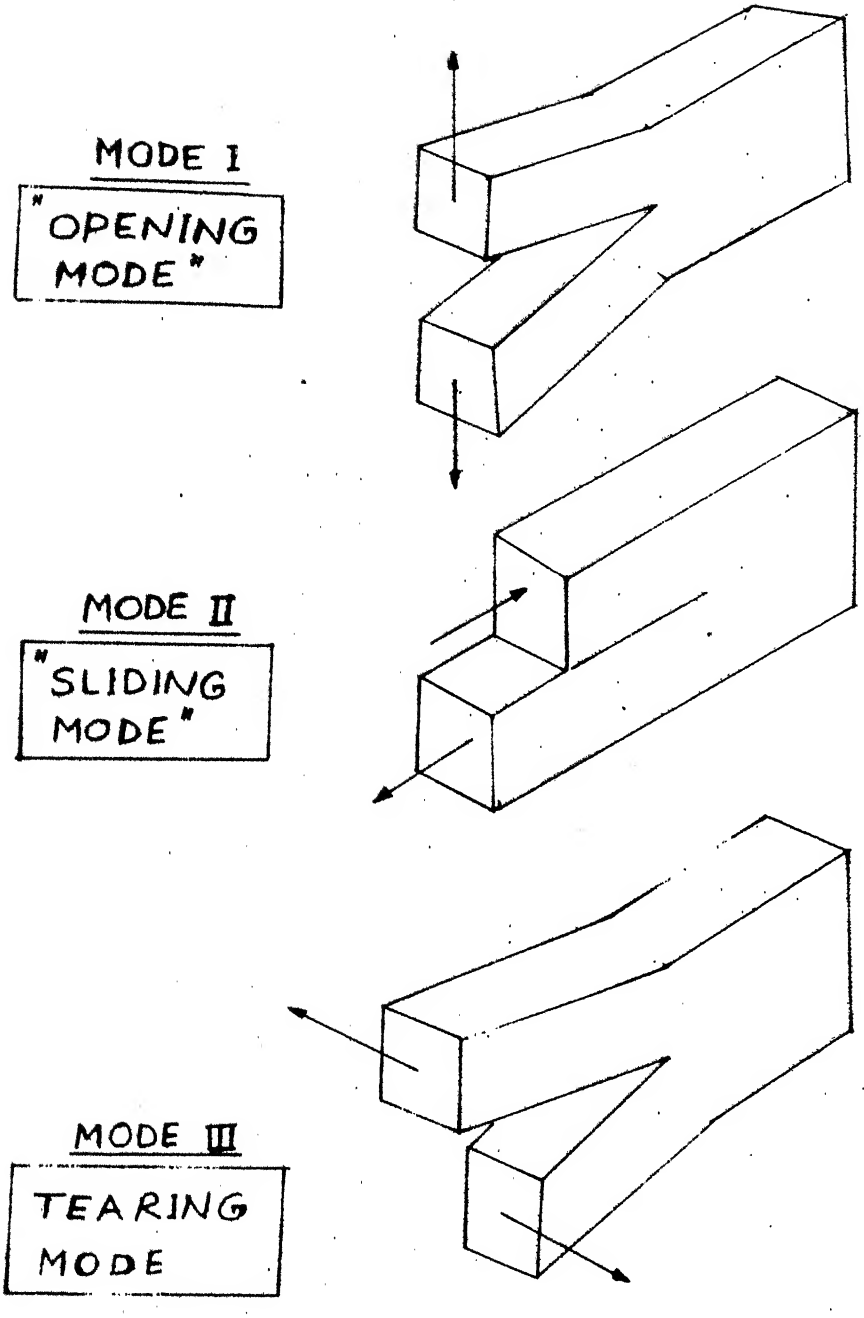

FIG. 1(a)

DIFFERENT MODES OF FRACTURE

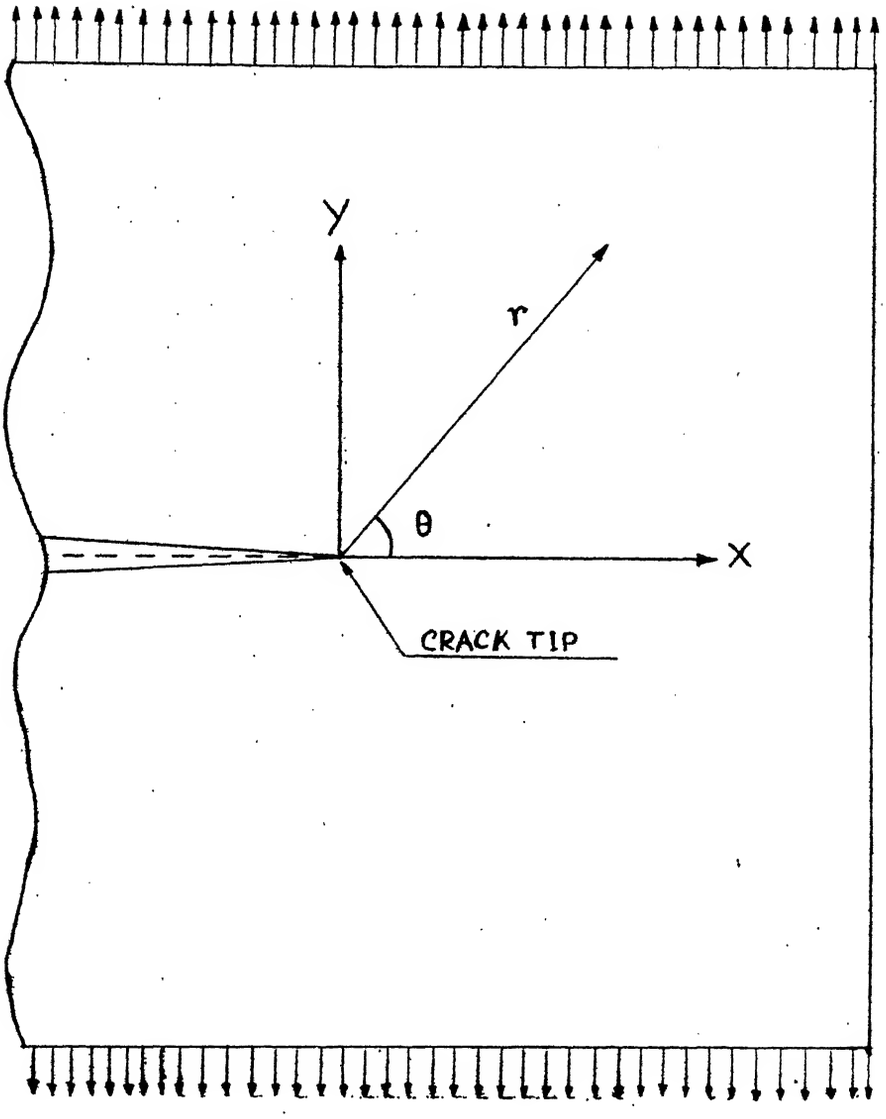

FIG. 1 (b).

CRACK UNDER UNIFORM TENSILE STRESS

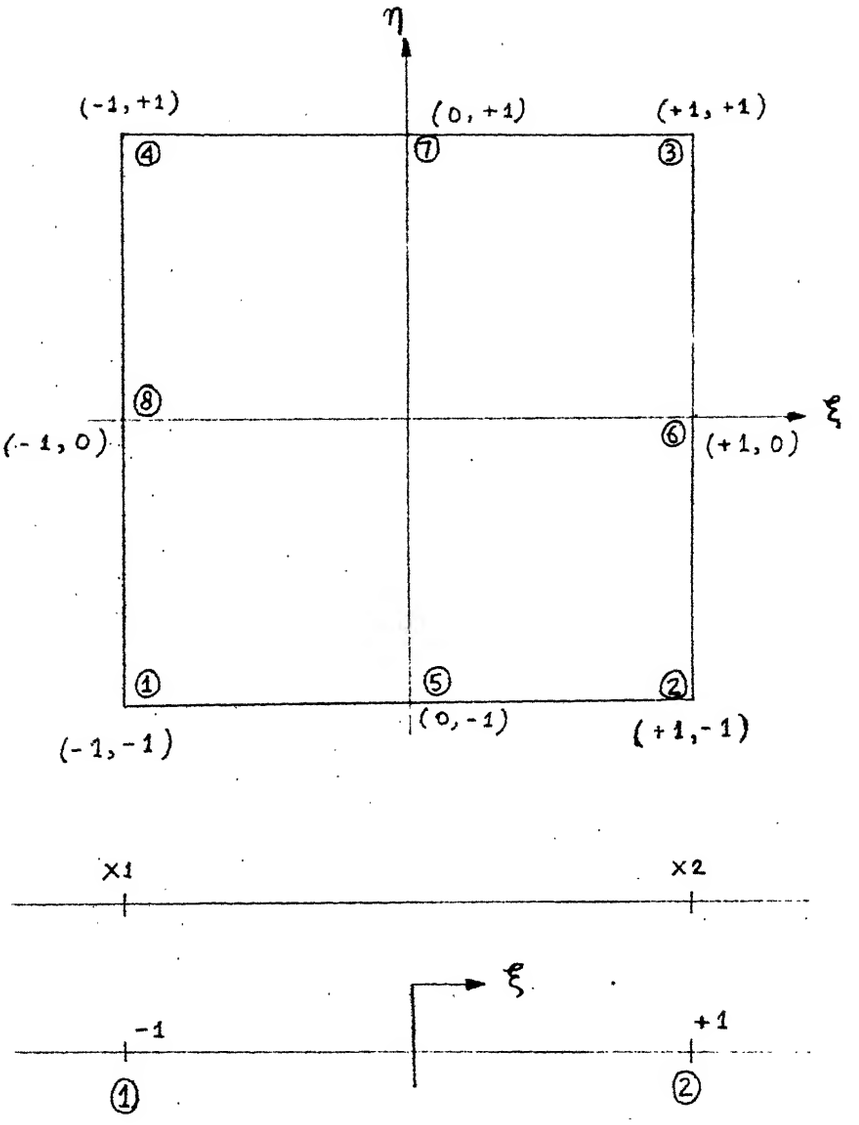

FIG 1 (c).

CRACK TIP ELEMENT OF REFERENCE 12

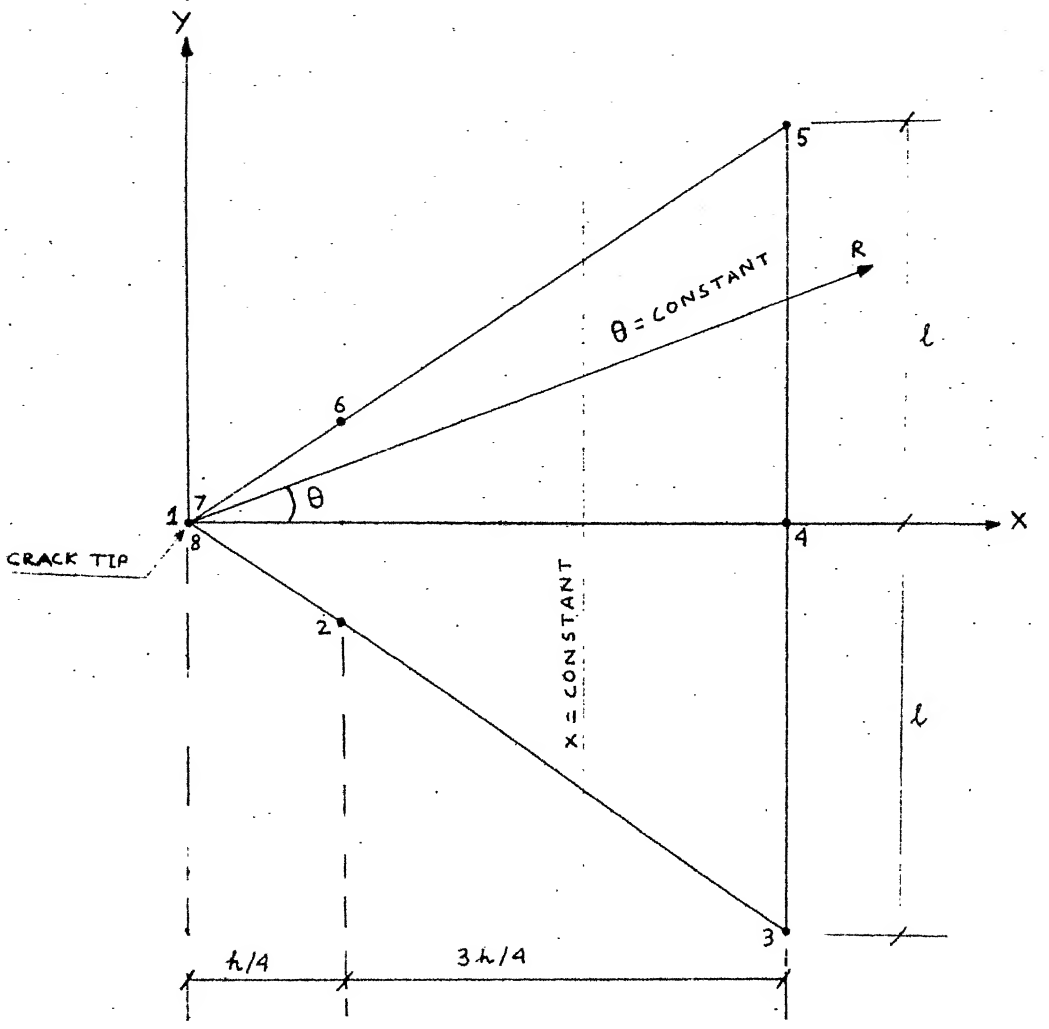

TRIANGULAR QUADRATIC ELEMENT.

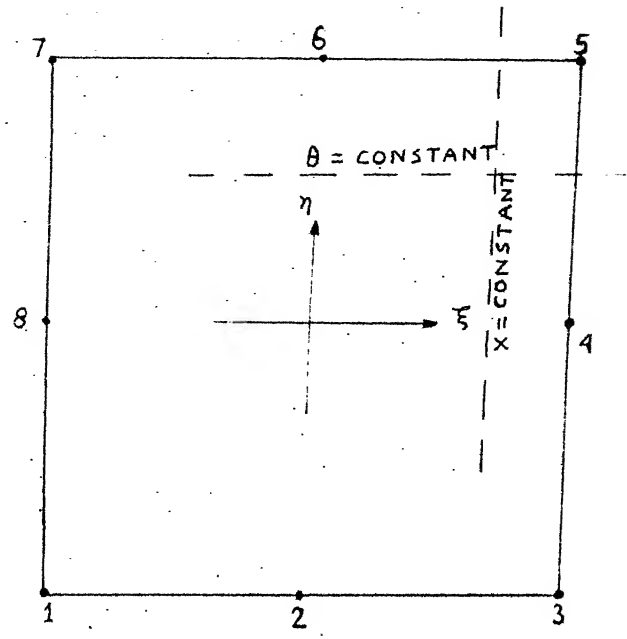

PARENT ELEMENT.

FIG 1(d).

CRACK TIP ELEMENT OF REFERENCE 14

A PLATE WITH CENTRAL CRACK

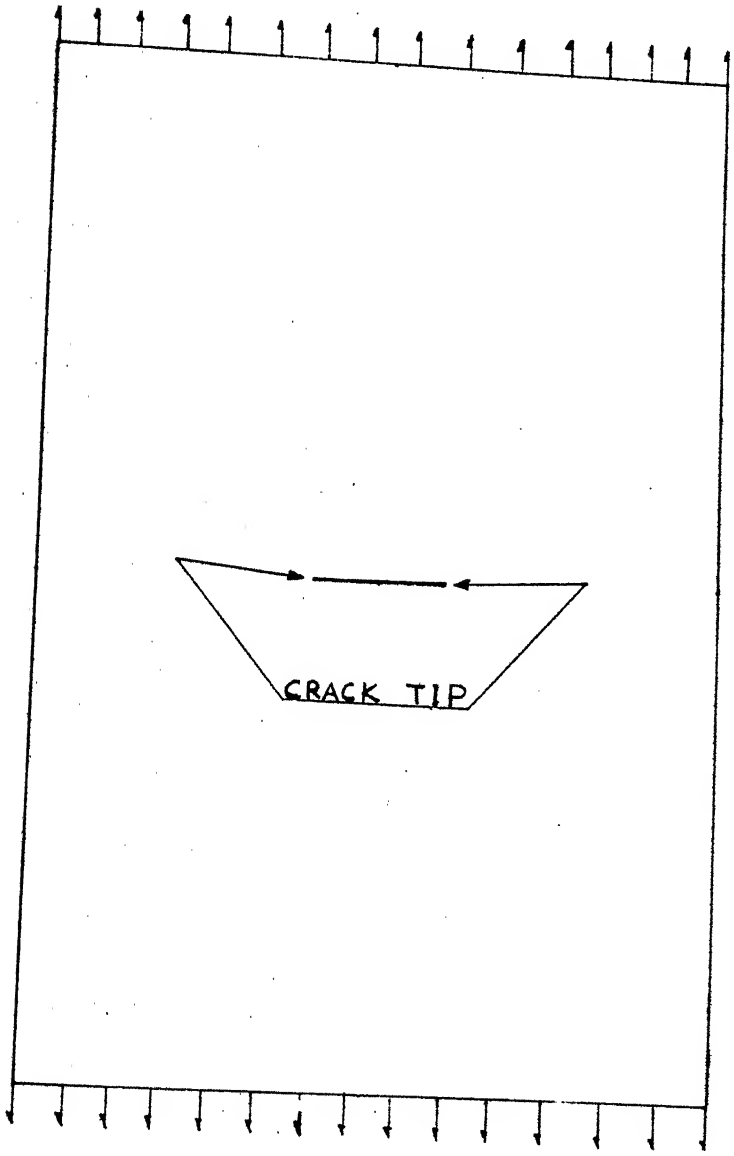

FIG. 1(e)

A PLATE WITH SIDE-NOTCHES ON BOTH SIDES

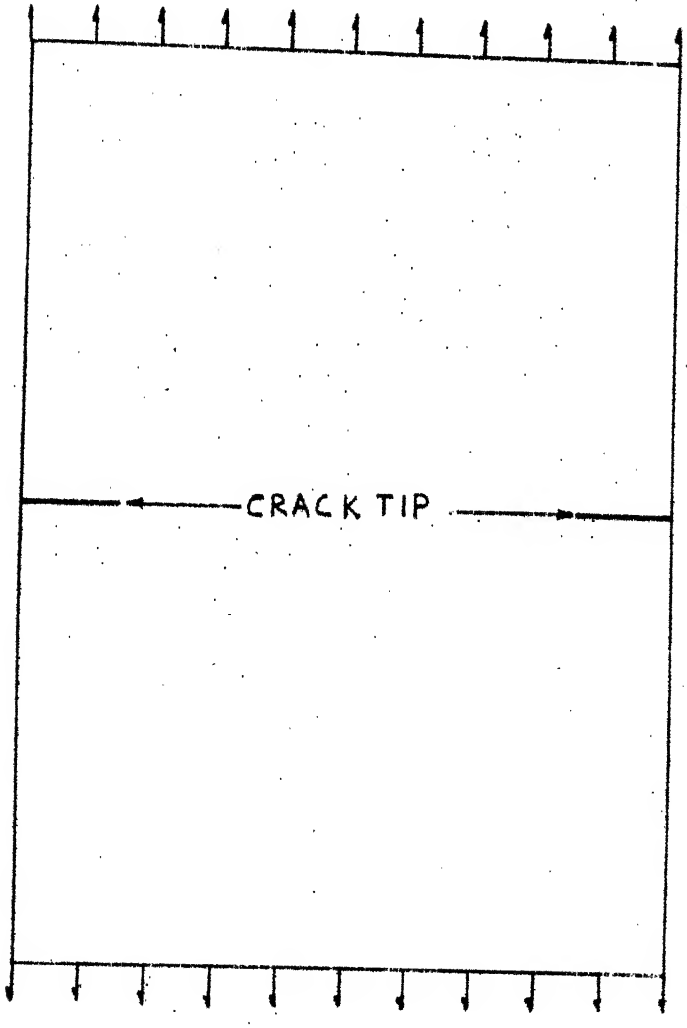

FIG. 1(f)

A PLATE WITH A SIDE-NOTCH

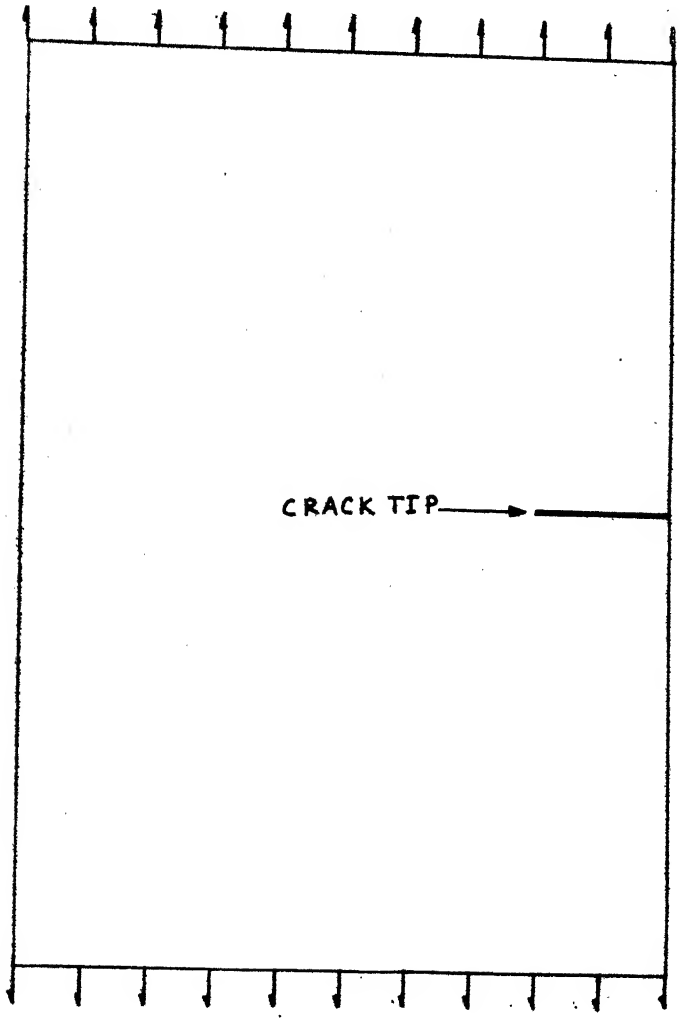

FIG. 1(8)

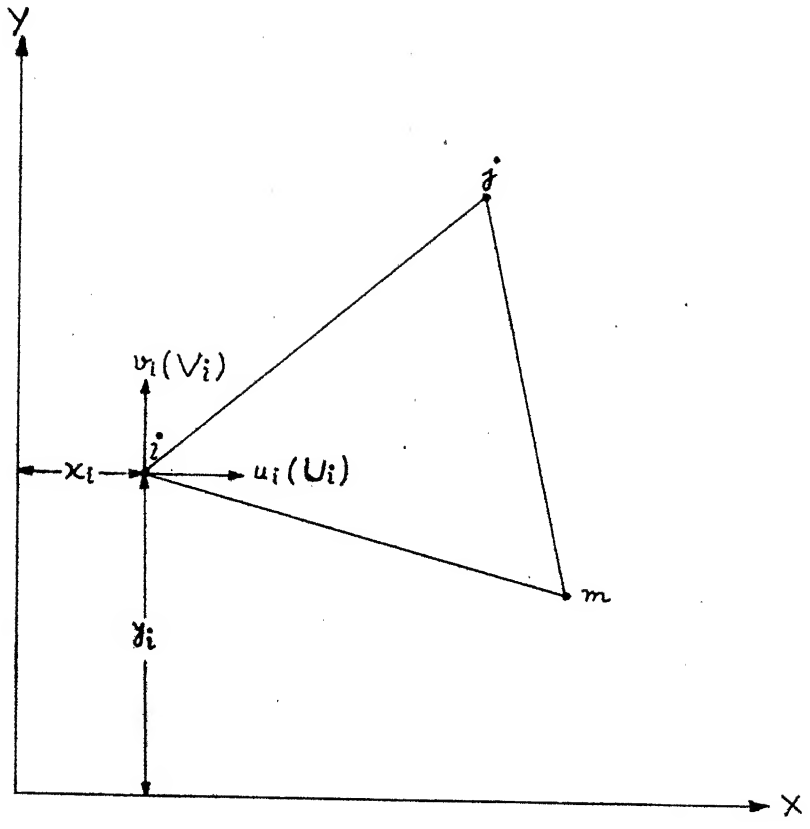

AN ELEMENT IN PLANE STRESS

FIG 2 (a).

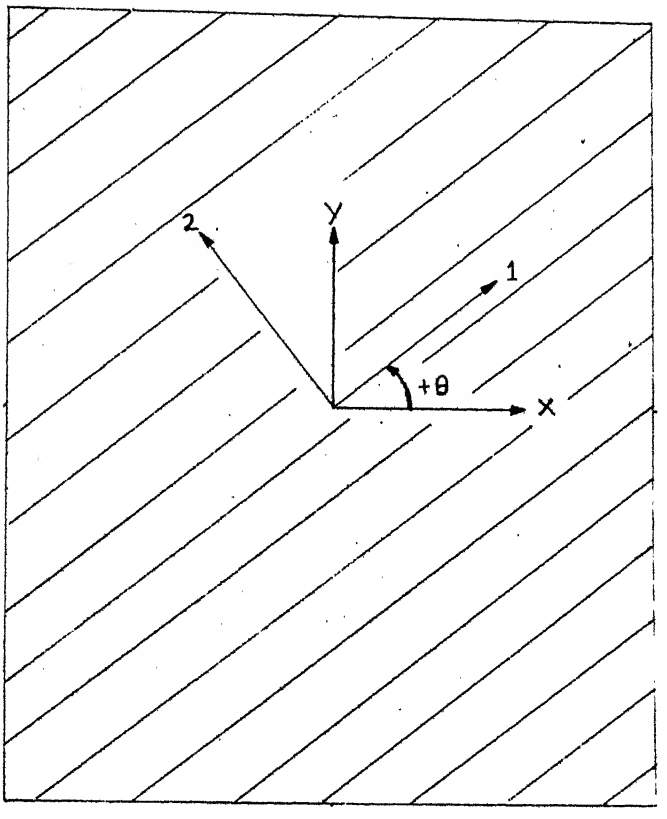

FIG 2 (b).

PRINCIPAL DIRECTIONS OF COMPOSITE MATERIAL LAMINA

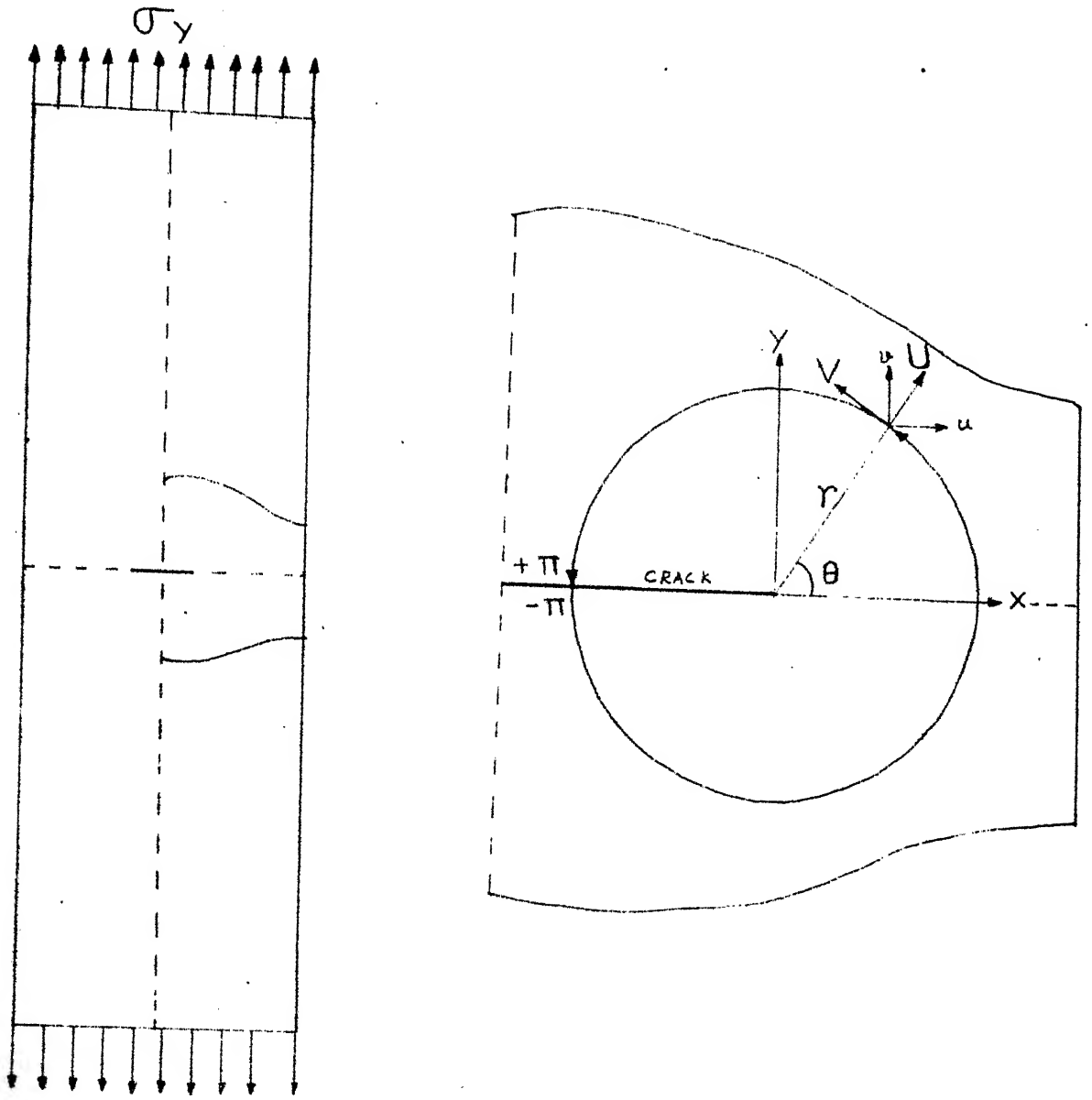

FIG 2(c).

CRACK GEOMETRY

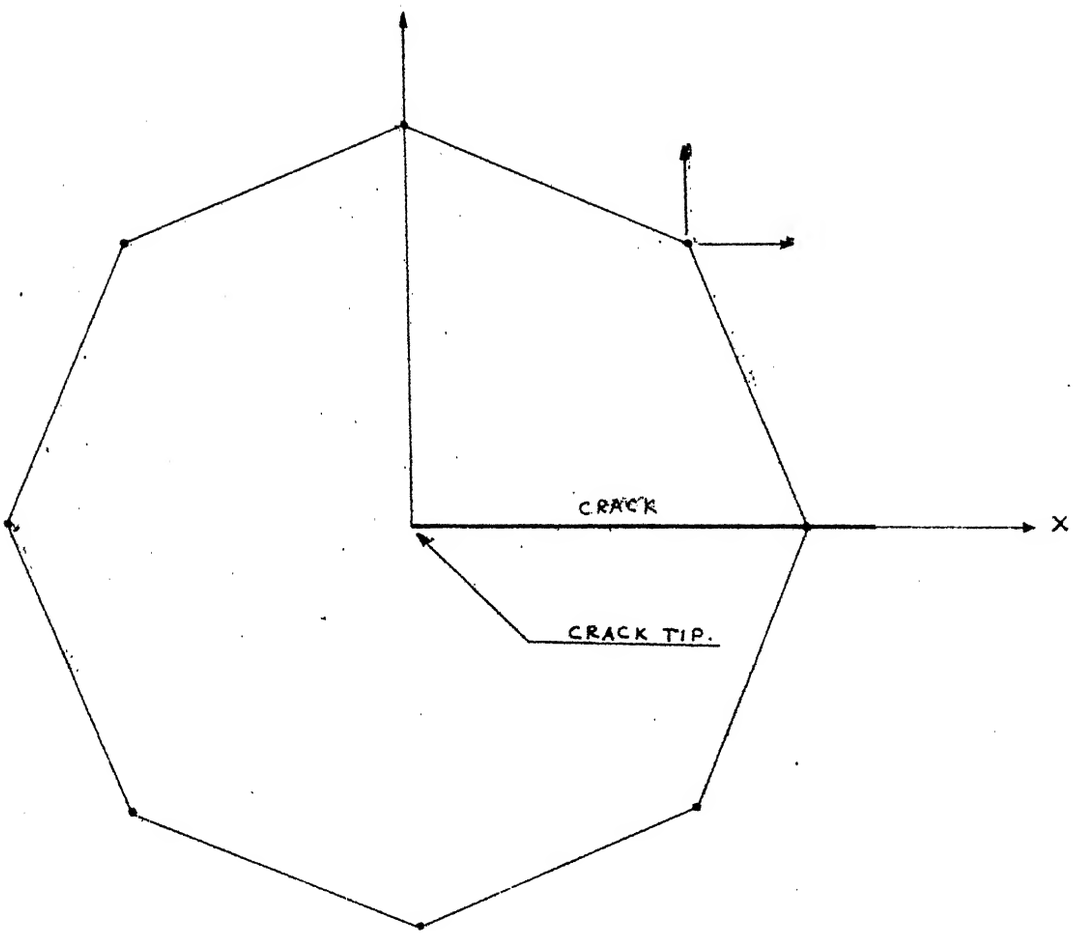

POLYGONAL ELEMENT FOR
CRACK IN ORTHOTROPIC LAMINA.

FIG 2(d).

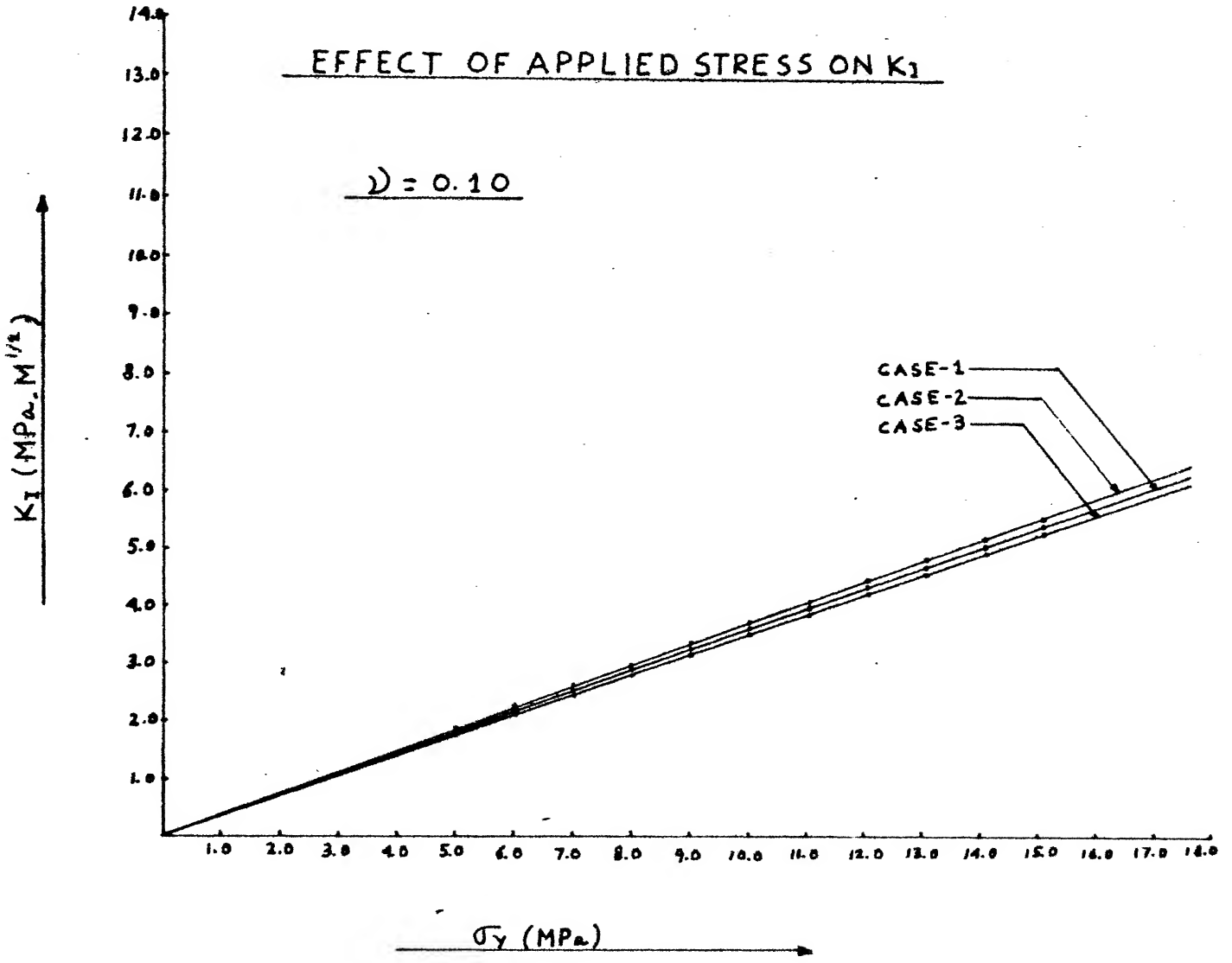
EFFECT OF APPLIED STRESS ON K_I
$\nu = 0.10$
CASE-1
CASE-2
CASE-3
K_I (MPa $\sqrt{m}$)
σ_y (MPa)
14.0
13.0
12.0
11.0
10.0
9.0
8.0
7.0
6.0
5.0
4.0
3.0
2.0
1.0
1.0 2.0 3.0 4.0 5.0 6.0 7.0 8.0 9.0 10.0 11.0 12.0 13.0 14.0 15.0 16.0 17.0 18.0

FIG. 4.1

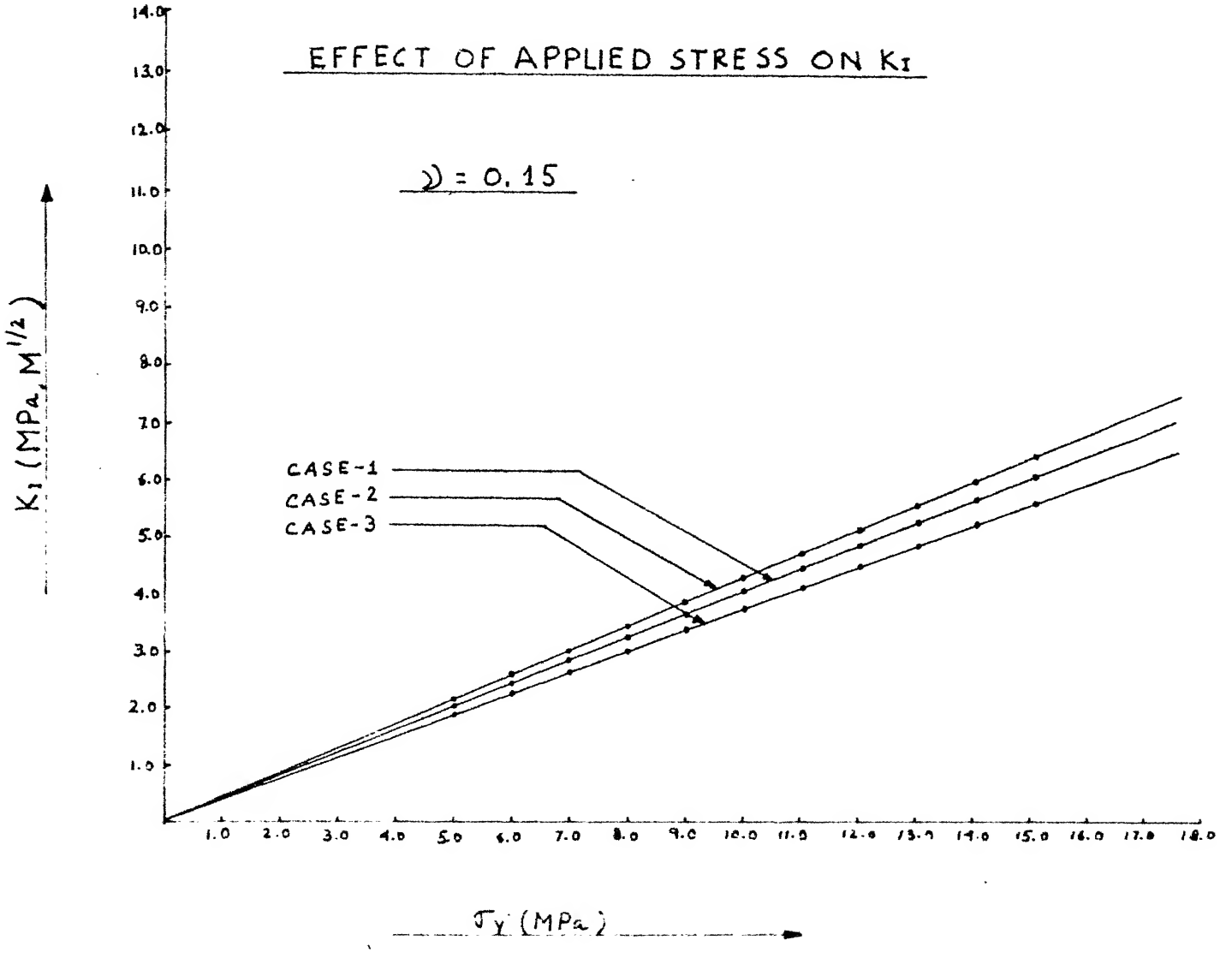
EFFECT OF APPLIED STRESS ON K_I
$\nu = 0.15$
K_I (MPa, $M^{1/2}$)
CASE-1
CASE-2
CASE-3
14.0
13.0
12.0
11.0
10.0
9.0
8.0
7.0
6.0
5.0
4.0
3.0
2.0
1.0
1.0 2.0 3.0 4.0 5.0 6.0 7.0 8.0 9.0 10.0 11.0 12.0 13.0 14.0 15.0 16.0 17.0 18.0
σ_Y (MPa)

FIG. 4.2

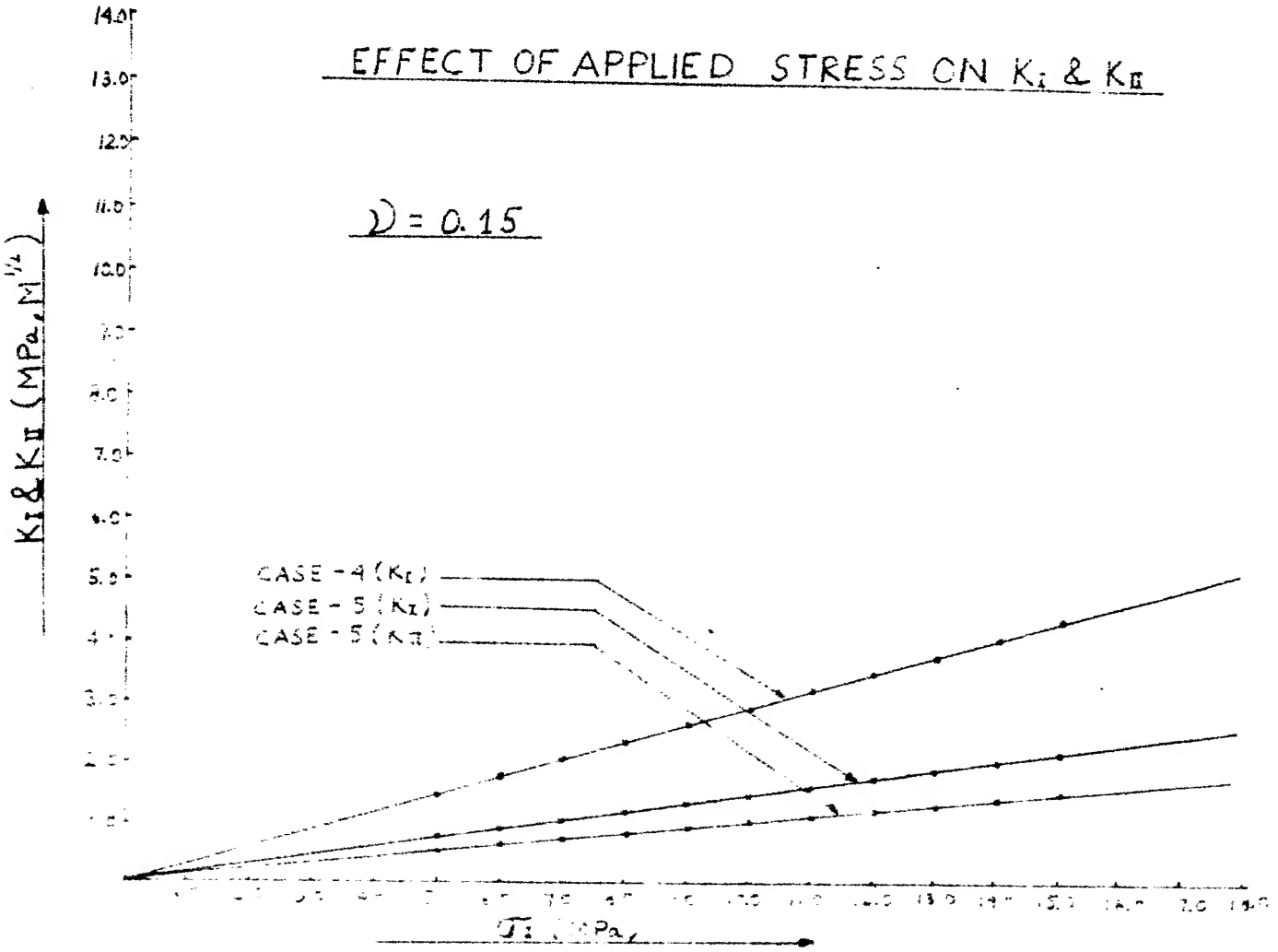
EFFECT OF APPLIED STRESS ON K_I & K_{II}
$\nu = 0.15$
K_I & K_{II} (MPa $M^{1/2}$)
14.0
13.0
12.0
11.0
10.0
7.0
5.0
CASE - 4 (K_I)
CASE - 5 (K_I)
CASE - 5 (K_{II})

FIG. 4.2 (a)

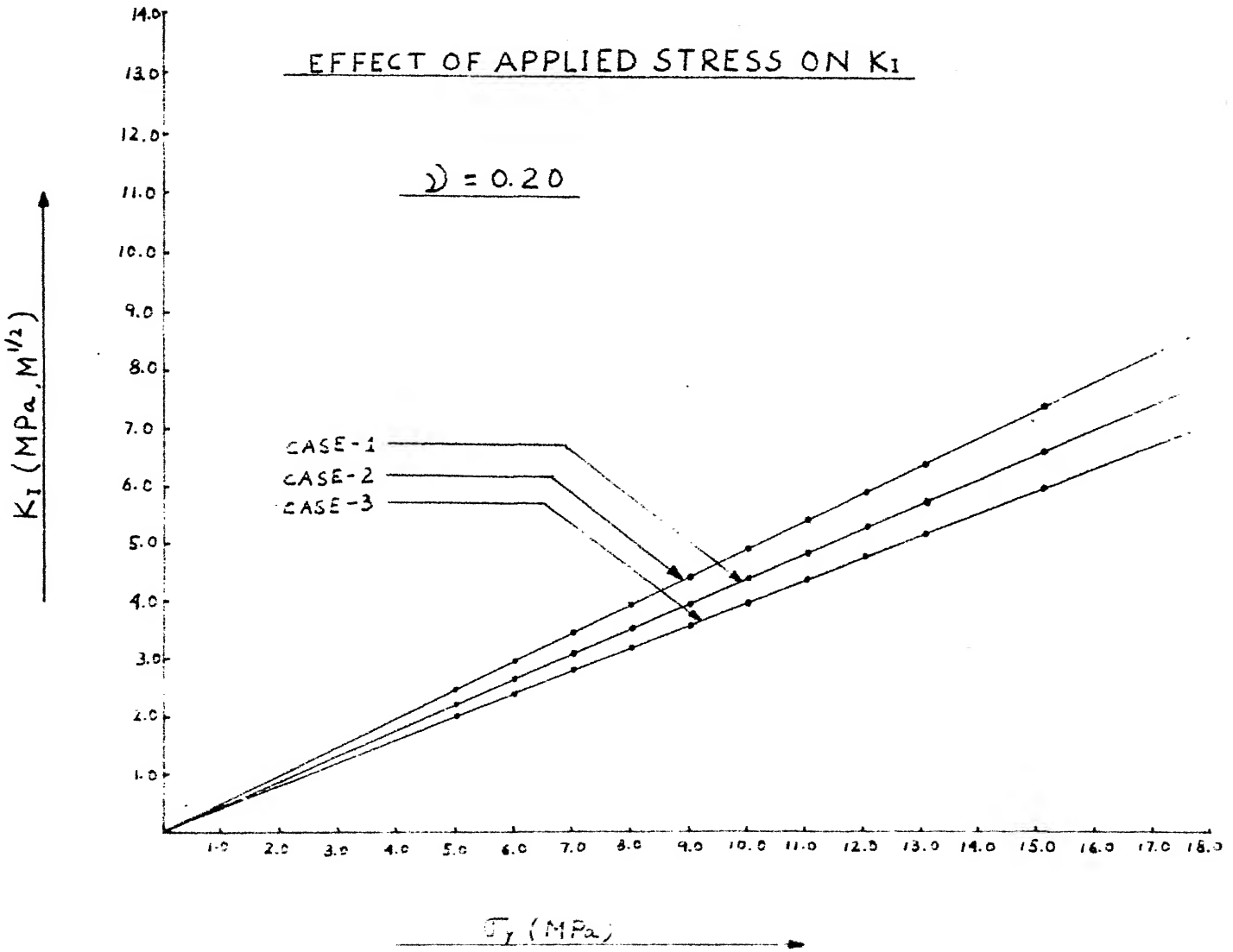
EFFECT OF APPLIED STRESS ON K1
ν = 0.20
CASE-1
CASE-2
CASE-3
K1 (MPa √M)
σy (MPa)
14.0
13.0
12.0
11.0
10.0
9.0
8.0
7.0
6.0
5.0
4.0
3.0
2.0
1.0
1.0 2.0 3.0 4.0 5.0 6.0 7.0 8.0 9.0 10.0 11.0 12.0 13.0 14.0 15.0 16.0 17.0 18.0

Fig. 4.3

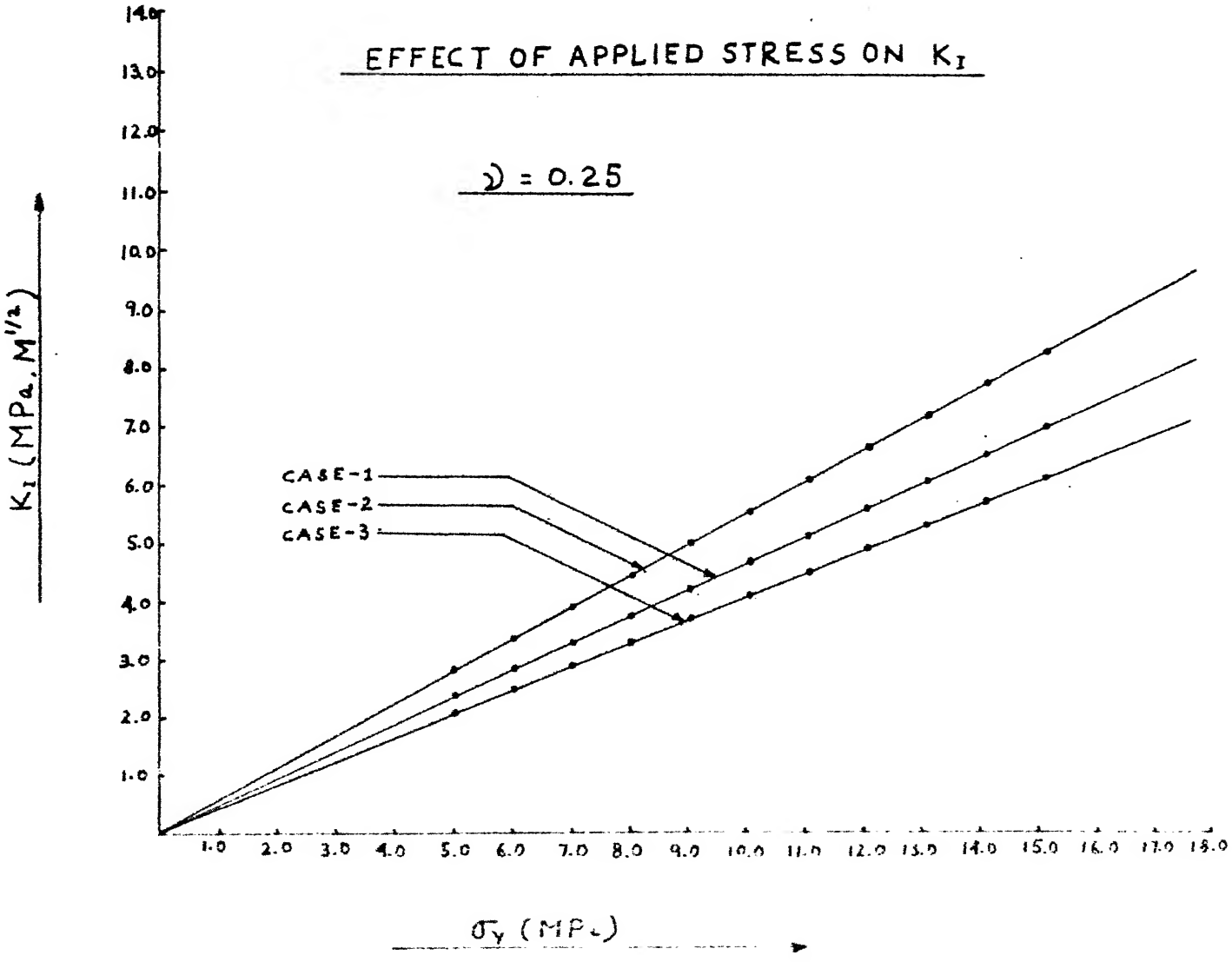
EFFECT OF APPLIED STRESS ON K_I
$\nu = 0.25$
K_I (MPa. $M^{1/2}$)
CASE-1
CASE-2
CASE-3
14.0
13.0
12.0
11.0
10.0
9.0
8.0
7.0
6.0
5.0
4.0
3.0
2.0
1.0
1.0 2.0 3.0 4.0 5.0 6.0 7.0 8.0 9.0 10.0 11.0 12.0 13.0 14.0 15.0 16.0 17.0 18.0
σ_Y (MPa)

FIG.44

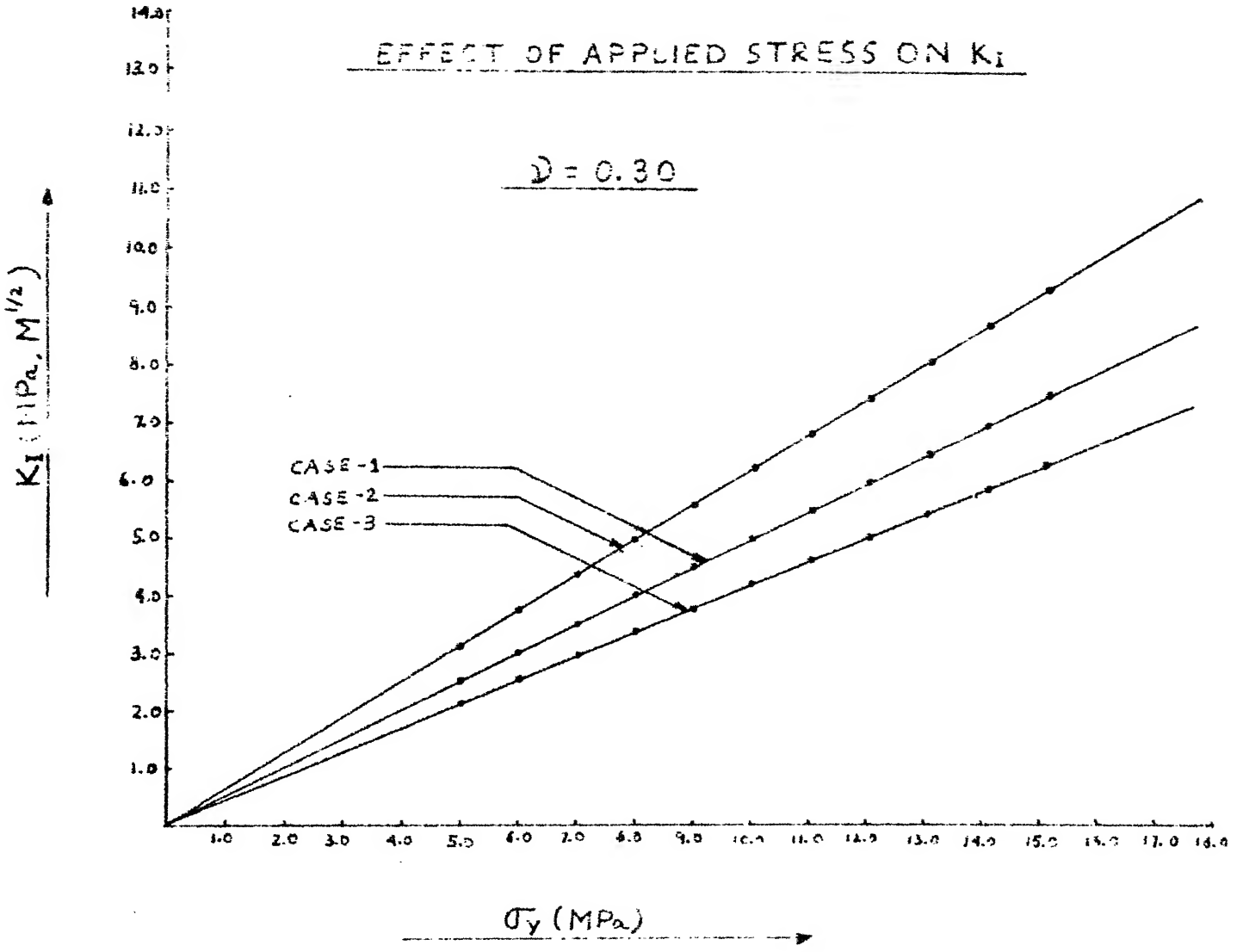
EFFECT OF APPLIED STRESS ON K_I
$\nu = 0.30$
K_I (MPa, $M^{1/2}$)
CASE -1
CASE -2
CASE -3
σ_y (MPa)

FIG. 4.5

ν Vs K_I IN CASE-1 WITH DIFFERENT σ_y

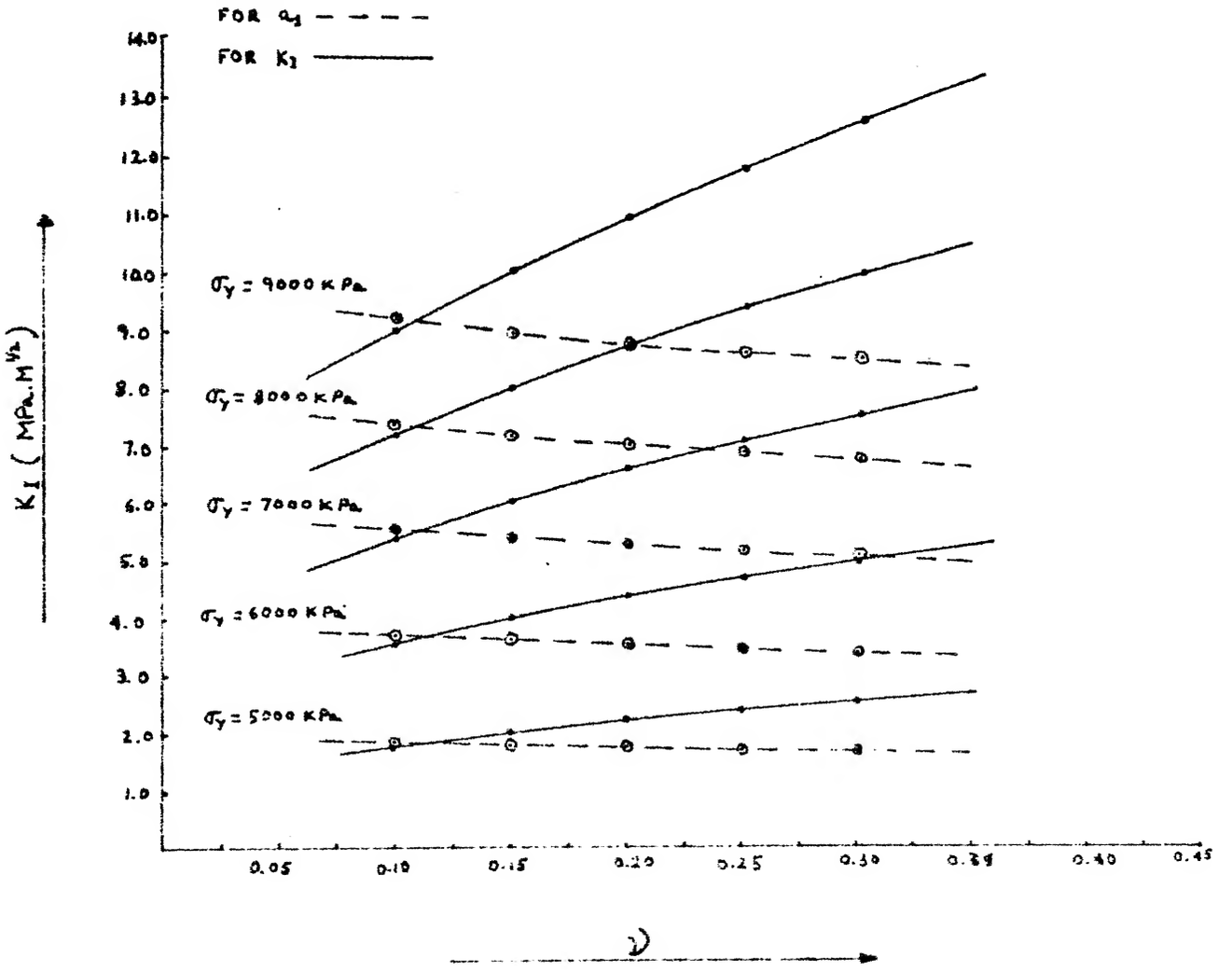

FIG. 4.6

Δ Vs K_I IN CASE-2 WITH DIFFERENT σ_y

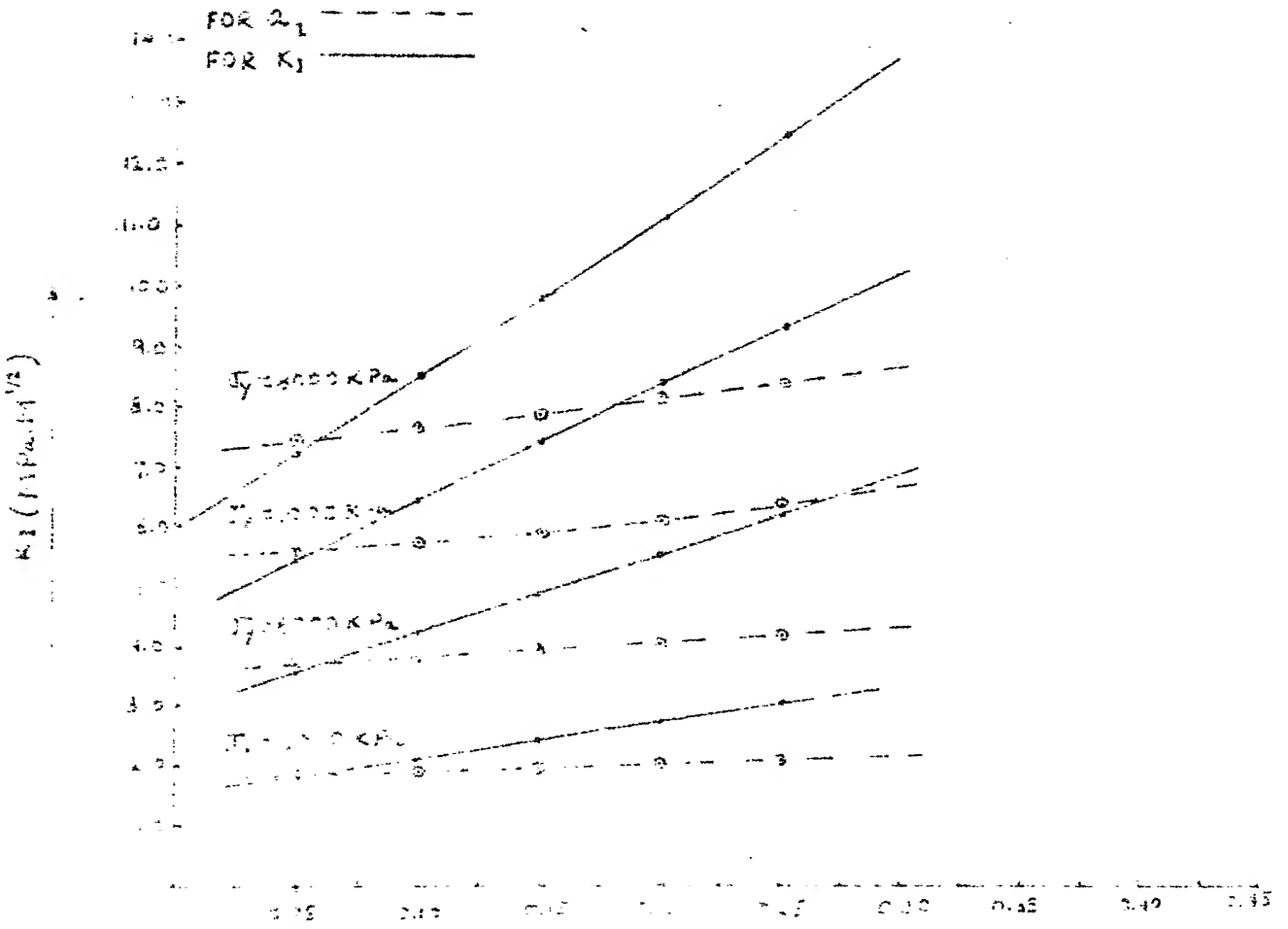

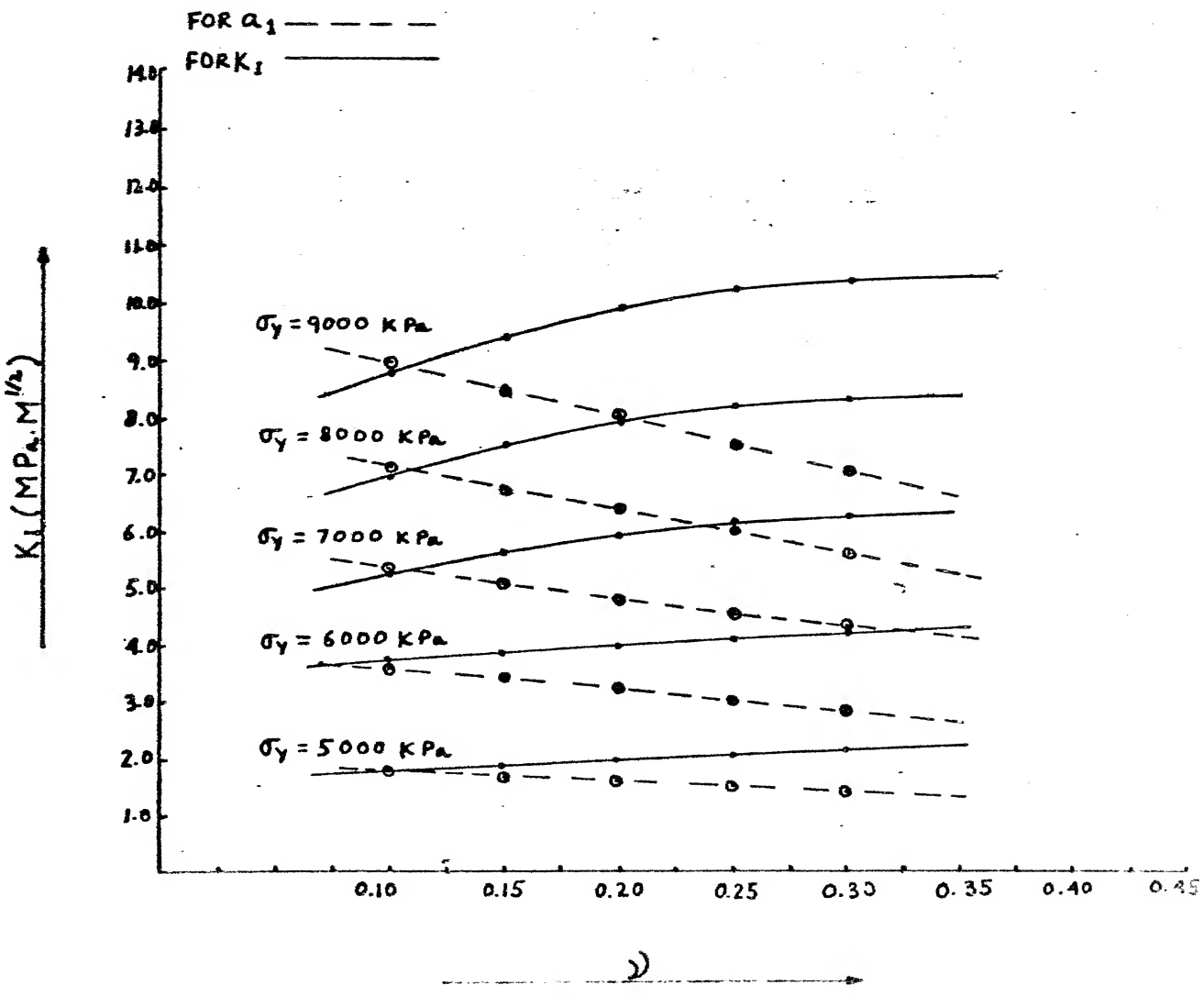
λ) Vs K1 IN CASE -3 WITH DIFFERENT σy
FOR a1 — — — —
FORK1 ——————
K1 (MPa.M^1/2)
σy = 9000 KPa
σy = 8000 KPa
σy = 7000 KPa
σy = 6000 KPa
σy = 5000 KPa
13.0
12.0
11.0
10.0
9.0
8.0
7.0
6.0
5.0
4.0
3.0
2.0
1.0
0.10
0.15
0.20
0.25
0.30
0.35
0.40
0.45
λ

FIG. 4.8

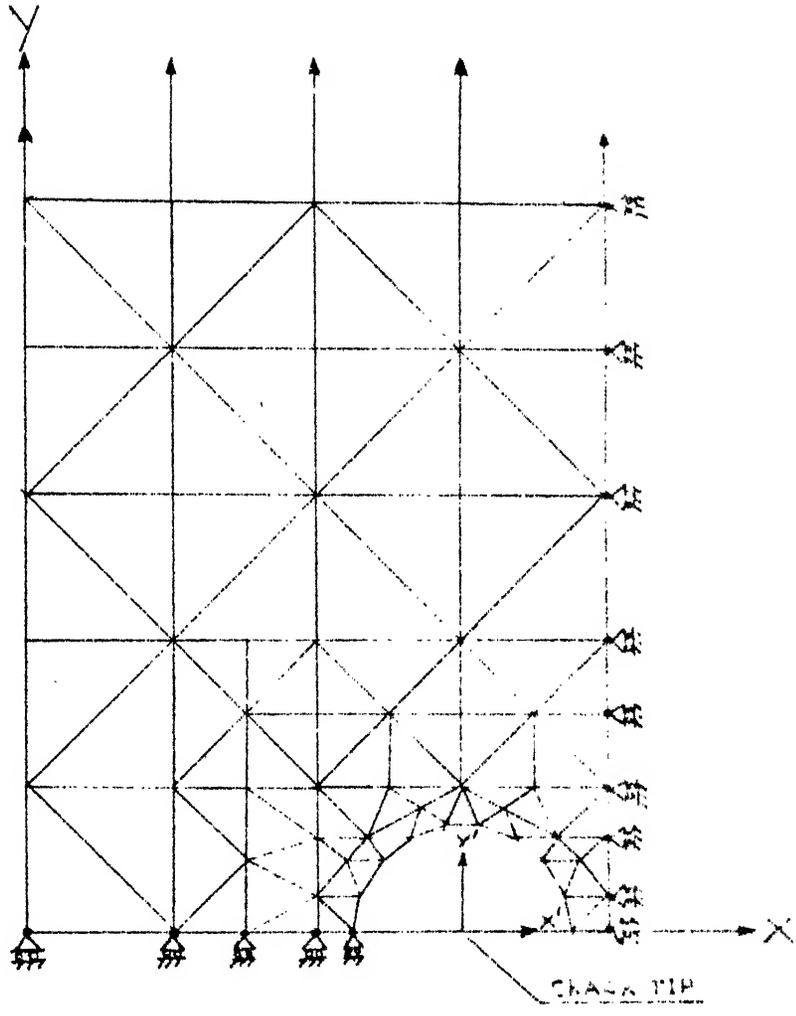

FIG. 4.9

F.E.M. MODEL IN CASE - 1.

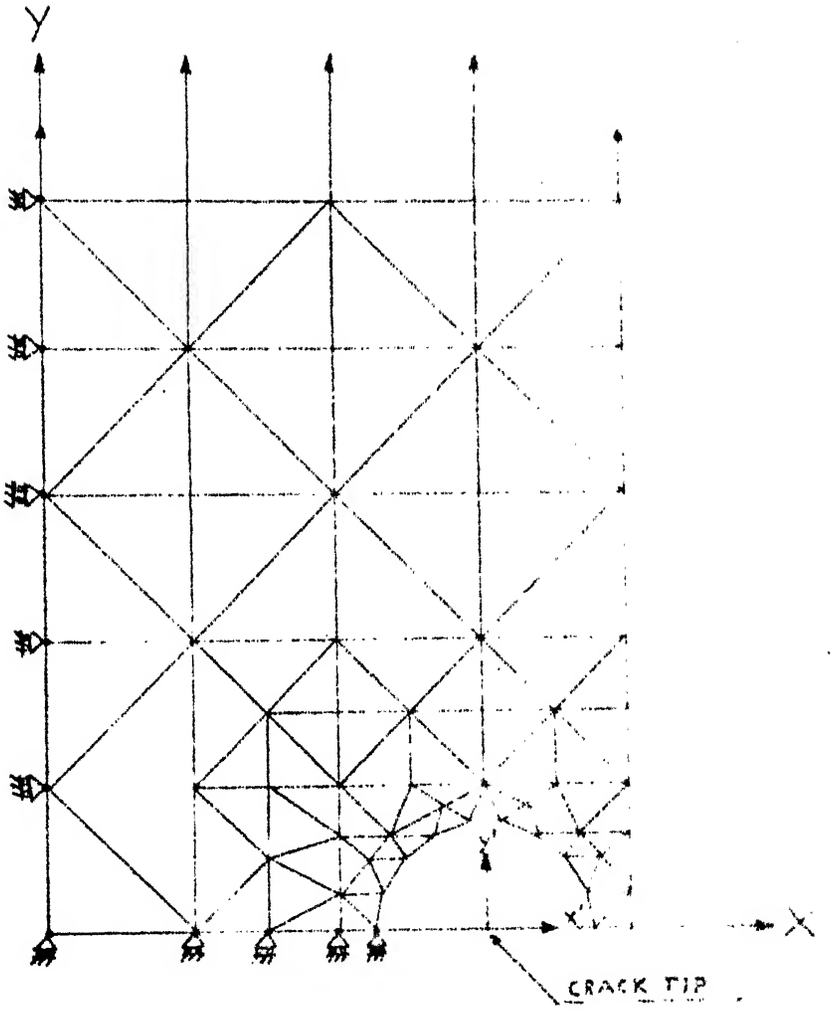

FIG. 4.10

F.E.M. MODEL IN CASE-2.

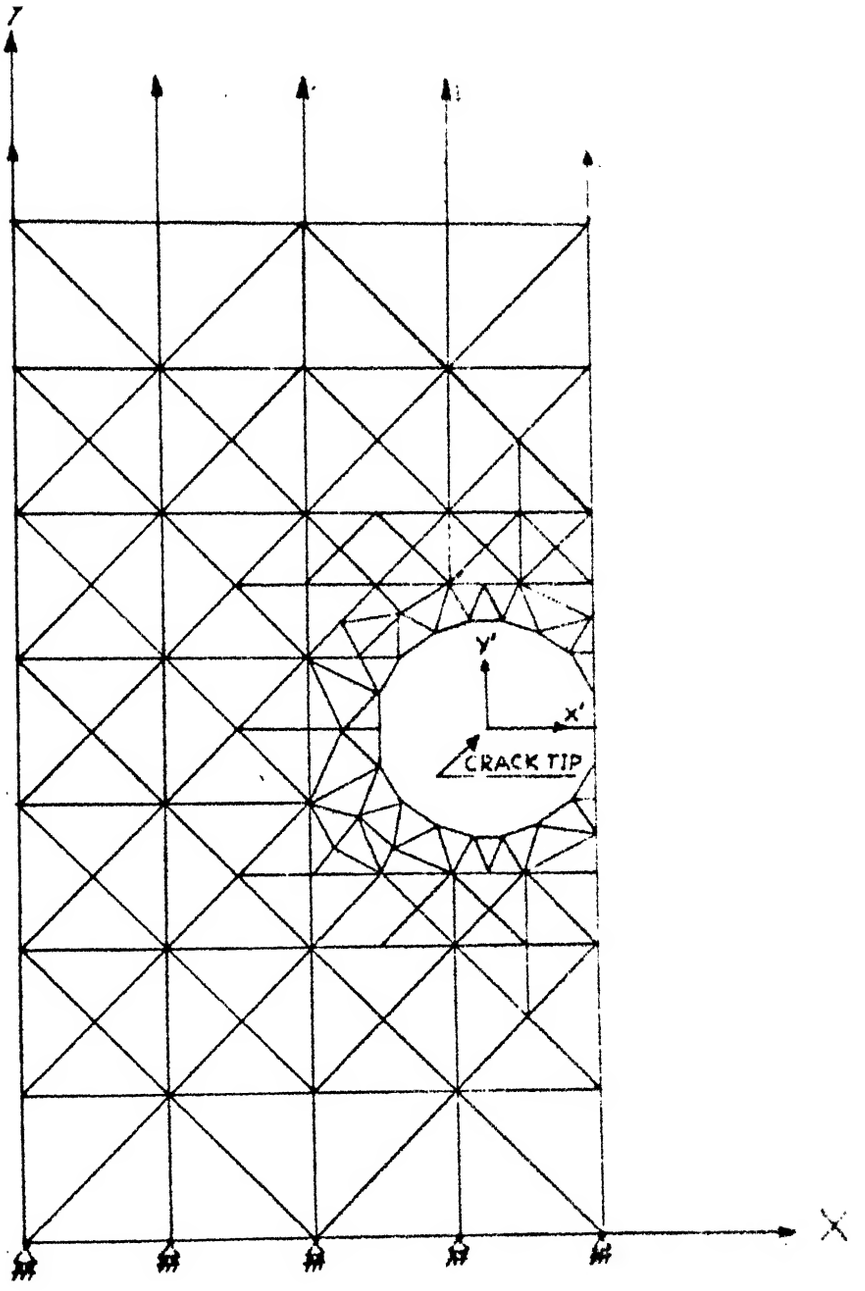

FIG. 4.11

F.E.M. MODEL IN CASE-3.

REFERENCES

1. Zienkiewicz, O.C., The finite element method : third edition, Tata McGraw-Hill Publishing Company Limited, 1977.

2. Griffiths, A.A., The phenomena of flow and rupture in solids, Phil. Roy. Soc., Lond., A 221, 98-163, 1920.

3. Ramamurthy, T.S., Fracture mechanics and application to design, Department of Aerospace Engineering, Indian Institute of Science, Bangalore, Vol. 1 and Vol. 2.

4. Byskov, E., The calculation of stress intensity factors using finite element method with crack-tip element, International Journal of Fracture Mechanics, Vol.6, 159-167, 1970.

5. Tracey, D.M., Finite element for crack-tip elastic stress intensity factor, Engineering Fracture Mechanics, Vol. 3, 255-265, 1971.

6. Pian, H.H., Tong, P., Luke, C., Elastic crack analysis by a finite element hybrid method, Proc. Third Air Conf. on matrix methods in structural mechanics, Dayton, Ohio,1971.

7. Atluri, S.N., Kobayashi, A.S., Nakagaki, M., The complimentary displacement hybrid model, J. AIAA, Vol. 13, No.6, 734-755, 1975.

8. Atluri, S.N., Kobayashi, A.S., Nakagaki, M., American Aeronautics and Astronautics Paper No. 74-390, Presented at the AIAA/ASME/AAE 15th Structures, Structural Dynamics and Materials Conf., Las Vegas, 1974.

9. Rao, A.K., Raju, I.S., Murthy, A.V.K., A hybrid method of analysis for general problems of stress concentration, International Journal for Numerical Methods in Engineering, Vol. 3, 389-404, 1971.

10. Benzley, S.E., Representation of singularities with isotropic finite elements, International Journal for Numerical Methods in Engineering, Vol. 8, No.3, 537-545, 1974.

11. Yamamoto, Y., Tokuda, N., Sumi, Y., Theory and practice in finite element structural analysis, Yamamoto, Y. and Gallagher R., Eds., University of Tokyo Press, 1973.

12. Henshell, R.D., Crack-tip elements are unnecessary, International Journal for Numerical Methods in Engineering, Vol. 10, 495-507, 1975.

13. Irons, B.M., Razzaque, A., 'Experiments with patch test for convergence, Proc. Conf. Math. Foundations of FEM with applications to partial differential equations, Academic Press, 557-558, 1972.

14. Barsoum, R.S., On the use of isotropic finite elements in linear fracture mechanics, International Journal for Numerical Methods in Engineering, Vol.10, 25-37, 1976.

15. Barsoum, R.S., A degenerate solid element for linear fracture analysis of plate bending and general shells, International Journal for Numerical Methods in Engineering, Vol. 10, 551-566, 1976.

16. Barsoum, R.S., Application of quadratic isoparametric finite elements in linear fracture mechanics, International Journal for Numerical Methods in Engineering, Reports on Current Research, Dec. 1974.

17. Barsoum, R.S., Further application of quadratic isoparametric finite elements in linear fracture mechanics, International Journal for Numerical Methods in Engineering,Vol.9, Part-II, 1975.

18. Barsoum, R.S., Triangular quarter point elements as elastic and perfectly plastic crack-tip elements, International Journal for Numerical Methods in Engineering,Vol.11,No.1, 85-98, 1977.

19. Jones, R., Callinan, R.J., On the special crack-tip elements in cracked elastic sheets, International Journal of Fracture, Vol. 13, 51-64, 1977.

20. Jones, R.M., Mechanics of composite materials, McGraw-Hill Kogakusha Limited, 1975.

21. Pappaioanou, S.G., Hilton, P.D., Lucas, R.A., A finite element method for calculating stress intensity factors and its application to composites, Engineering Fracture Mechanics, Vol. 6, 807-823, 1979.

22. Wilson, W.K., Crack-tip finite element for plane elasticity, Technical Report. Westinghouse Research Labs., 71-1E7-FMPWR-P2, June, 1971.

23. Lekhinitskii, S.G., Anisotropic Plates, Gordon and Breach Publishers, 1968.

24. Williams, M.L., On the stress distribution at the base of a stationary crack, Journal of Applied Mechanics, Vol.24, 109-114, 1957.

25. Blackburn, W.S., Calculation of stress intensity factors at the crack-tips using special finite elements, The Mathematics of Finite Elements and Applications, Academic Press, Lond., 1973.

26. Sneddon, I.N., Lowengrub, M., Crack problems in the classical theory of elasticity, John Wiley and Sons, Inc., 1969.

27. Carnahan, B., Luther, H.A., Wilkes, J.O., Applied Numerical Methods, John Wiley and Sons Inc., 1969.

28. McCormick, J.M., Salvadori, M.G., Numerical Methods in Fortran, Prentice Hall of India Pvt. Ltd., 1979.

29. Parks, D.M., A stiffness derivative finite element technique for determination of elastic crack-tip stress intensity factors, International Journal of Fracture, Vol.10, 487-502, 1979.

30. Hellen, T.K., On the methods of virtual crack extensions, International Journal for Numerical Methods in Engineering, Vol. 9, No. 1, 187-208, 1975.

31. Dixon, J.R., Pook, L.P., Stress intensity factors calculated generally by the finite element technique, Nature, 224, 166-178, 1969.

32. Dixon, J.R., Strannigan, J.S., Determination of energy release rates and stress intensity factors by the finite element method, Journal of Strain Analysis, Vol. 7, 125-131, 1972.

33. Mowbray, D.F., A note on the finite element method in linear fracture mechanics, Engineering Fracture Mechanics, Vol. 2, 173-176, 1970.

34. Watwood, V.B., Finite element method for prediction of crack behaviour, Nuclear Engineering Design, Vol. 2, No.2, 323-332, 1970.

```
00100  C                              APPENDIX
00200  C      ************************************************
00300  C      FINITE ELEMENT PROGRAM FOR STRESS INTESITY FACTOR AND
00400  C      RELEASE RATE EVALUATION AND STRESS ANALYSIS USING CRAC
00500  C      SPECIAL ELEMENT
00600  C      ************************************************
00700  C      MODE=1:FINDS STIFNESS INTENSITY FACTOR ONLY
00800  C      MODE=2:FINDS STIFNESS INTENSITY FACTOR AND DOES STRESS
00900  C      MODE=3:FINDS ENERGY RELEASE RATE ONLY
01000  C      MODE=4:FINDS ENERGY RELEASE RATE AND DOES STRESS ANALY
01100  C      IMODE=1:STRESS OUTPUT IS GIVEN IN (R-THETA) CO-ORDINAT
01200  C      IMODE=2:STRESS OUTPUT IS GIVEN IN (X-Y) CO-ORDINATE
01300  C      ISTRS=1:FINDS STRESSES INSIDE SPECIAL ELEMENT AT GIVEN
01400  C      ISTRS=0:OTHERWISE
01500  C      IDSP=1:DISPLACEMENT OUTPUT IS GIVEN (DISPLACEMENTS AT
01600  C      IDSP=0:OTHERWISE
01700          DIMENSION CORD(2,75),NODE(3,100),A(150,150),R(150),SN
01800          DIMENSION A11(150,150),R11(150),DELK(150,150),DELKR(1
01900          DIMENSION CORDS(2,75),NST(15),CST(2,15)
02000          DIMENSION B(3,6),BT(6,3),S(3,3),AE(6,6),WKSPCE(150)
02100          COMMON/A1/STM(25,25)
02200          COMMON/A3/NMAX,JMAX
02300          COMMON/A6/ALP,BET,EX,EY,GXY,RNUXY
02400          COMMON/A7/NODES(12,1)
02500          COMMON/A8/THCK
02600          COMMON/A12/C1(25)
02700          OPEN(UNIT=21,DEVICE='DSK',FILE='DATA11')
02800          OPEN(UNIT=22,DEVICE='DSK',FILE='OUT22')
```

```
02900           OPEN(UNIT=5,DEVICE='DSK')
03000           READ(21,*),MODE,IMODE,ISTRS,IDSP
03100           READ(21,*),NNODE,NEL,NLN,NR,EX,EY,GXY,THTA,RNUXY,THCK,
03200           READ(21,*),((CORD(I,J),I=1,2),J=1,NNODE)
03300           READ(21,*),((NODE(I,J),I=1,3),J=1,NEL-1)
03400           N=NNODE*2
03500           DO 33 I=1,2
03600           DO 33 J=1,NNODE
03700   33      CORD(I,J)=CORD(I,J)/100.0
03800           DO 34 I=1,2
03900           DO 34 J=1,NNODE
04000   34      CORDS(I,J)=0.0
04100           CALL SMTRX(EX,EY,RNUXY,GXY,THTA,S)
04200           DO 5 I=1,N
04300           DO 5 J=1,N
04400   C       TYPE *,I,J
04500   5       A(I,J)=0.0
04600           DO 10 IELL=1,NEL-1
04700           IEL=IELL
04800           CALL BMTRX(IEL,CORD,NODE,B,BT,AREA)
04900           CALL ESM(B,BT,S,AREA,AE,THCK)
05000           CALL ASMBLE(IEL,AE,NODE,A)
05100   C       TYPE *,IEL
05200   10      CONTINUE
05300           READ(21,*) NMAX,JMAX,ALP,BET
05400           READ(21,*) IFRN,IFRNP1,NNSM
05500           NS=NNODE-NNSM+1
05600           READ(21,*) (NODES(I,1),I=1,NNSM)
```

```
05700            READ(21,*) ((CORDS(I,J),I=1,2),J=NS,NNODE)
05800            DO 35 I=1,2
05900            DO 35 J=NS,NNODE
06000   35       CORDS(I,J)=CORDS(I,J)/100.0
06100            IELL=NEL;IEL=IELL
06200            CALL SPCL(IFRN,IFRNP1,NNSM,IEL,CORDS)
06300            CALL ASMBLS(NNSM,IEL,A,CORDS)
06400            DO 50 I=1,N
06500   50       R(I)=0.0
06600            DO 55 I=1,NLN
06700            READ(21,*),LNN,XL,YL
06800            R((LNN-1)*2+1)=XL
06900            R((LNN-1)*2+2)=YL
07000   55       CONTINUE
07100            DO 60 NN=1,NR
07200            READ(21,*),NI,J
07300            I=2*(NI-1)+J
07400            R(I)=0.0
07500            DO 65 JJ=1,N
07600            A(I,JJ)=0.0
07700            A(JJ,I)=0.0
07800   65       CONTINUE
07900            A(I,I)=1.0
08000   60       CONTINUE
08100            DO 44 K=1,N
08200   44       R11(K)=R(K)
08300            DO 46 I=1,N
08400            DO 46 J=1,N
```

```
08500   46      A11(I,J)=A(I,J)
08600           CALL F04AAF(A,150,R,150,N,1,R,150,WKSPCE,0)
08700           TYPE *,IFAIL
08800           IF(IDSP.EQ.0) GOTO 59
08900           DO 364 I=1,N,3
09000           J=I+1;K=J+1
09100   364     WRITE(22,345) I,R(I),J,R(J),K,R(K)
09200   345     FORMAT(5X,'R(',I3,')=',F12.5,5X,'R(',I3,')=',E12.5,5X,'R
09300           1')=',E12.5)
09400   59      IF(MODE-2) 69,69,79
09500   69      CALL SIF(R,NNSM,SIFAC,IFRNP1)
09600           WRITE(22,234) SIFAC
09700   234     FORMAT(5X,'STIFNESS INTENSITY FACTOR=',F12.6)
09800           TYPE *, SIFAC
09900           IF(MODE.EQ.2) GOTO 799
10000           GOTO 393
10100   79      READ(21,*),NEL1
10200           DO 22 IELL=NEL1,NEL-1
10300           IEL=IELL
10400           CALL BMTRX(IEL,CORD,NODE,B,BT,AREA)
10500           CALL ESM(B,BT,S,AREA,AE,THCK)
10600   22      CALL DSMBLE(IEL,AE,NODE,A)
10700           IELL=NEL;IEL=IELL
10800           CALL DSMBLS(NNSM,IEL,A,CORDS)
10900           DO 169 IJ=NS,NNODE
11000   169     CORD(1,IJ)=CORD(1,IJ)-DELFX
11100           DO 21 IELL=NEL1,NEL-1
11200           IEL=IELL
```

```
11300           CALL BMTRX(IEL,CORD,NODE,B,BT,AREA)
11400           CALL ESM(B,BT,S,AREA,AE,THCK)
11500           CALL ASMBLE(IEL,AE,NODE,A)
11600   21      CONTINUE
11700           DO 170 IJ=NS,NNODE
11800   170     CORDS(1,IJ)=CORDS(1,IJ)-DELEX
11900           CALL SPCL(IFRN,IFRNP1,NNSM,IEL,CORDS)
12000           CALL DSMBLS(NNSM,IEL,A,CORDS)
12100           DO 47 I=1,N
12200           DO 47 J=1,N
12300   47      DELK(I,J)=A11(I,J)-A(I,J)
12400           DO 49 I=1,N
12500           SUM=0.0
12600           DO 51 J=1,N
12700   51      SUM=SUM+DELK(I,J)*R11(J)
12800           DELKR(I)=SUM
12900   49      CONTINUE
13000           SUM=0.0
13100           DO 53 K=1,N
13200   53      SUM=SUM+R11(K)*DELKR(K)
13300           FKI=SUM/(2.0*THCK*DELEX)
13400           WRITE(22,121) FKI
13500   121     FORMAT(5X,'ENERGY RELEASE RATE=',E12.6)
13600           TYPE *, FKI
13700           IF(MODE.EQ.3) GOTO 393
13800   799     DO 701 IELL=1,NEL-1
13900           IEL=IELL
14000           CALL BMTRX(IEL,CORD,NODE,B,BT,AREA)
```

```
14100           DO 751 I=1,3
14200           SUM=0.0
14300           DO 801 M1=1,3
14400           DO 801 N1=1,3
14500           KK=2*(M1-1)+N1
14600           L=(NODE(M1,IEL)-1)*2+N1
14700   801     SUM=SUM+B(I,KK)*R(L)
14800           SN(I)=SUM
14900   751     CONTINUE
15000           DO 851 K=1,3
15100           SUM=0.0
15200           DO 901 J=1,3
15300   901     SUM=SUM+S(K,J)*SN(J)
15400           SS(K)=SUM
15500   851     CONTINUE
15600           IF(IMODE.EQ.1) GOTO 852
15700   C       WRITE(22,607) IEL,SS(1),IEL,SS(2),IEL,SS(3)
15800   C607    FORMAT(5X,'SIGMX(',I2,')=',E12.5,5X,'SIGMY(',I2,')=',E12.5
15900   C       1'TAOXY(',I2,F12.5)
16000           GOTO 701
16100   852     CALL POLAR(IEL,CORD,NODE,SS)
16200   701     CONTINUE
16300   393     IF(TSTRS-1) 394,395,395
16400   395     READ(21,*),NNST
16500           DO 814 KP=1,NNST
16600   814     READ(21,*),NST(KP),CST(1,KP),CST(2,KP)
16700           CALL STRESS(NST,CST,NNST)
16800   394     CLOSE(UNIT=21,DEVICE='DSK',FILE='DATA11')
```

```
16900           CLOSE(UNIT=22,DEVICE='DSK',FILE='OUT22')
17000           CLOSE(UNIT=5,DEVICE='DSK')
17100           STOP
17200           END
17300   C       ****************************************
17400           SUBROUTINE SMTRX(EX,EY,RNUXY,GXY,THTA,S)
17500   C       ****************************************
17600           DIMENSION S(3,3),C(3,3)
17700           RNUYX=EY*RNUXY/EX
17800           DMTR=1.0-RNUXY*RNUYX
17900           C(1,1)=EX/DMTR
18000           C(1,2)=RNUXY*EY/DMTR
18100           C(2,2)=EY/DMTR
18200           C(3,3)=GXY
18300           C(1,3)=0.0
18400           C(2,3)=0.0
18500           DO 95 I=1,3
18600           DO 95 J=1,3
18700   95      C(J,I)=C(I,J)
18800           CT=COSD(THTA)
18900           ST=SIND(THTA)
19000           CT4=CT**4
19100           ST4=ST**4
19200           CS22=SQRT(CT4*ST4)
19300           CS13=CT*(ST**3)
19400           CS31=ST*(CT**3)
19500           H1=2.0*(C(1,2)+2.0*C(3,3))
19600           H2=C(1,1)-C(1,2)-2.0*C(3,3)
```

```
19700           H3=C(1,2)-C(2,2)+2.0*C(3,3)
19800           H11=H1*CS22
19900           S(1,1)=C(1,1)*CT4+H11+C(2,2)*ST4
20000           S(1,2)=(C(1,1)+C(2,2)-4.0*C(3,3))*CS22+C(1,2)*(ST4+CT4)
20100           S(2,2)=C(1,1)*ST4+H11+C(2,2)*CT4
20200           S(1,3)=H2*CS31+H3*CS13
20300           S(2,3)=H2*CS13+H3*CS31
20400           S(3,3)=(C(1,1)+C(2,2)-2.*C(1,2)-2.*C(3,3))*CS22+C(3,3)*(ST
20500           DO 110 I=1,3
20600           DO 110 J=1,3
20700   110     S(J,I)=S(I,J)
20800           RETURN
20900           END
21000   C       ********************************************
21100           SUBROUTINE BMTRX(IEL,CORD,NODE,B,BT,AREA)
21200   C       ********************************************
21300           DIMENSION CORD(2,75),NODE(3,100),B(3,6),BT(6,3)
21400           N1=NODE(1,IEL)
21500           N2=NODE(2,IEL)
21600           N3=NODE(3,IEL)
21700           X1=CORD(1,N1)
21800           X2=CORD(1,N2)
21900           X3=CORD(1,N3)
22000           Y1=CORD(2,N1)
22100           Y2=CORD(2,N2)
22200           Y3=CORD(2,N3)
22300           AREA=0.5*  ABS(  X2*Y3-X3*Y2-X1*Y3+X3*Y1+X1*Y2-X2*Y1  )
22400           A1=X2*Y3-X3*Y2
```

```
22500            A2=X3*Y1-X1*Y3
22600            A3=X1*Y2-X2*Y1
22700            D1=Y2-Y3
22800            D2=Y3-Y1
22900            D3=Y1-Y2
23000            C1=X3-X2
23100            C2=X1-X3
23200            C3=X2-X1
23300            DO 20 I=1,3
23400            DO 20 J=1,6
23500   20       B(I,J)=0.0
23600            B(1,1)=D1
23700            B(1,3)=D2
23800            B(1,5)=D3
23900            B(2,2)=C1
24000            B(2,4)=C2
24100            B(2,6)=C3
24200            B(3,1)=C1
24300            B(3,2)=D1
24400            B(3,3)=C2
24500            B(3,4)=D2
24600            B(3,5)=C3
24700            B(3,6)=D3
24800            DO 25 I=1,3
24900            DO 25 J=1,6
25000            B(I,J)=B(I,J)/(2.0*AREA)
25100   25       BT(J,I)=B(I,J)
25200            RETURN
```

```
25300           END
25400   C       ************************************
25500           SUBROUTINE FSM(B,BT,S,AREA,AE,THCK)
25600   C       ************************************
25700           DIMENSION B(3,6),BT(6,3),S(3,3),AE(6,6),BTS(6,3)
25800           DO 100 I=1,6
25900           DO 100 J=1,3
26000           SUM=0.0
26100           DO 15 K=1,3
26200   15      SUM=SUM+BT(I,K)*S(K,J)
26300           BTS(I,J)=SUM
26400   100     CONTINUE
26500           DO 40 I=1,6
26600           DO 40 J=1,6
26700           SUM=0.0
26800           DO 30 K=1,3
26900   30      SUM=SUM+BTS(I,K)*B(K,J)
27000   40      AE(I,J)=SUM*AREA*THCK
27100           RETURN
27200           END
27300   C       ************************************
27400           SUBROUTINE ASMBLE(IEL,AE,NODE,A)
27500   C       ************************************
27600           DIMENSION AE(6,6),NODE(3,100),A(150,150)
27700           DO 45 I1=1,3
27800           DO 45 J1=1,2
27900           DO 45 I2=1,3
28000           DO 45 J2=1,2
```

```
28100           M=(I1-1)*2+J1
28200           L=(I2-1)*2+J2
28300           IG=(NODE(I1,IEL)-1)*2+J1
28400           JG=(NODE(I2,IEL)-1)*2+J2
28500           A(IG,JG)=A(IG,JG)+AE(M,L)
28600   45      CONTINUE
28700           RETURN
28800           END
28900   C       ************************************
29000           SUBROUTINE POLAR(IEL,CORD,NODE,SS)
29100   C       ************************************
29200           DIMENSION CORD(2,75),NODE(3,100),SS(3)
29300           N1=NODE(1,IEL)
29400           N2=NODE(2,IEL)
29500           N3=NODE(3,IEL)
29600           X1=CORD(1,N1)
29700           X2=CORD(1,N2)
29800           X3=CORD(1,N3)
29900           Y1=CORD(2,N1)
30000           Y2=CORD(2,N2)
30100           Y3=CORD(2,N3)
30200           X=(X1+X2+X3)/3.0    ;   Y=(Y1+Y2+Y3)/3.0
30300           R=SQRT(X*X+Y*Y)     ;   THETA=ATAN(Y/X)
30400           S2=SIN(2.0*THETA)   ;   C2=COS(2.0*THETA)
30500           ST1=(SS(1)+SS(2))/2.0  ;  ST2=(SS(1)-SS(2))/2.0  ;  ST3=SS(3)
30600           SS1=ST1+ST2*C2+ST3*S2
30700           SS2=ST1-ST2*C2-ST3*S2
30800           SS3=-ST2*S2+ST3*C2
```

```
30900           WRITE(22,1000) IEL,SS1,IEL,SS2,IEL,SS3
31000  1000     FORMAT(5X,'SGMR(',I3,')=',E12.5,5X,'SGMT(',I3,')=',E12.5,5X,
31100           1'TAORT(',I3,')=',E12.5)
31200           RETURN ; END
31300  C        ******************************************
31400           SUBROUTINE SPCL(IFRN,IFRNP1,NNSM,IEL,CORDS)
31500  C        ******************************************
31600           DIMENSION CORDS(2,75)
31700           COMMON/A1/STM(25,25)
31800           COMMON/A3/NMAX,JMAX
31900           COMMON/A6/ALP,BET,EX,EY,GXY,RNUXY
32000           COMMON/A7/NODES(12,1)
32100           COMMON/A8/THCK
32200           CALL UMTRX(IFRN,IFRNP1,NNSM,IEL,CORDS)
32300           CALL ELMTRX(IFRN,IFRNP1,NNSM,IEL,CORDS)
32400           CALL SESM(IFRNP1,NNSM)
32500           RETURN
32600           END
32700  C        **********************
32800           SUBROUTINE TRONB1(FT1)
32900  C        **********************
33000           DIMENSION T1(15,15)
33100           COMMON/A2/X1,Y1,X2,Y2
33200           COMMON/A3/NMAX,JMAX
33300           H1=X1-X2
33400           DO 8 K1=1,15
33500           DO 8 J1=1,15
33600  8        T1(K1,J1)=0.0
```

```
 33700          T1(1,1)=(F1(X1)+F1(X2))*H1/2.0
 33800          DO 2 N=1,NMAX
 33900          FR1=H1/(2.0**N)
 34000          IMAX=(2**N)-1
 34100          DO 1 I=1,IMAX,2
 34200  1       T1(N+1,1)=T1(N+1,1)+F1(FLOAT(I)*FR1+X2)
 34300  2       T1(N+1,1)=T1(N,1)/2.0+H1*T1(N+1,1)/(2.0**N)
 34400          DO 3 J=2,JMAX
 34500          NXMJP2=NMAX-J+2
 34600          FORJM1=4.0**(J-1)
 34700          DO 3 N=1,NXMJP2
 34800  3       T1(N,J)=(FORJM1*T1(N+1,J-1)-T1(N,J-1))/(FORJM1-1.0)
 34900          FT1=T1(2,JMAX)
 35000          RETURN
 35100          END
 35200  C       **************
 35300          FUNCTION F1(X)
 35400  C       **************
 35500          COMMON/A2/ X1,Y1,X2,Y2
 35600          COMMON/A3/NMAX,JMAX
 35700          COMMON/A4/T(15,15)
 35800          UL=Y1+((Y2-Y1)/(X1-X2))*(X1-X)
 35900          SLL=0.0
 36000          X3=X
 36100          CALL TROMB(UL,SLL,X3)
 36200          F1=T(2,JMAX)
 36300          RETURN
 36400          END
```

```
C       ****************************
        SUBROUTINE TROMB(UL,SLL,X3)
C       ****************************
        COMMON/A3/NMAX,JMAX
        COMMON/A4/T(15,15)
        H=UL-SLL
        DO 10 I=1,15
        DO 10 J=1,15
10      T(I,J)=0.0
        T(1,1)=(F(X3,SLL)+F(X3,UL))*H/2.0
        DO 12 N1=1,NMAX
        FR=H/2.0**N1
        IMAX1=2**N1-1
        DO 11 I1=1,IMAX1,2
11      T(N1+1,1)=T(N1+1,1)+F(X3,(FLOAT(I1)*FR+SLL))
12      T(N1+1,1)=T(N1,1)/2.0+H*T(N1+1,1)/2.0**N1
        DO 13 J1=2,JMAX
        NXMJP2=NMAX-J1+2
        FORJM1=4.0**(J1-1)
        DO 13 N1=1,NXMJP2
13      T(N1,J1)=(FORJM1*T(N1+1,J1-1)-T(N1,J1-1))/(FORJM1-1.0)
        RETURN
        END
C       ***************
        FUNCTION F(X,Y)
C       ***************
        COMMON/A5/K,L
        COMMON/A6/ALP,BET,EX,EY,GXY,RNUXY
```

```
39300           DIMENSION SGMX(40),SGMY(40),TXY(40)
39400           IF(X.EQ.0.0) GOTO 81
39500           GOTO 82
39600   81      IF(Y.EQ.0.0) Y=0.0001
39700   82      R1=SQRT((X+ALP*Y)**2+(BET*Y)**2)
39800           R2=SQRT((X-ALP*Y)**2+(BET*Y)**2)
39900           Z1=ATAN((BET*Y)/(X+ALP*Y))
40000           Z2=ATAN((-BET*Y)/(X-ALP*Y))
40100           IF(Z1.LT.0.0) Z1=3.1415926+Z1
40200           IF(Z2.GT.0.0) Z2=-3.1415926+Z2
40300           ASMBS=(ALP**2-BET**2)
40400           AMB=(ALP*BET)
40500           ADB=(ALP/BET)
40600           FAS=4.0*ALP**2
40700           REM1=K-(IFIX(FLOAT(K)/2.0)*2)
40800           IF(REM1.EQ.0.0) GOTO 112
40900           FI=(K+1)/4.0;I=FI*2;V=(FI-1.0)
41000           CPN=COSD(360*V)
41100           CZ1=COS(Z1*V);CZ2=COS(Z2*V)
41200           SZ1=SIN(Z1*V);SZ2=SIN(Z2*V)
41300           RN1=SQRT(R1**I)/R1;RN2=SQRT(R2**I)/R2
41400           RI=FI*(FI+1.0)
41500           XX1=(ASMBS*CZ1-2.0*AMB*SZ1);XX2=(2.0*ASMBS*ADB-2.0*AMB)*SZ2
41600           SGMX(K)=RI*(RN1*XX1-CPN*RN2*((ASMBS-FAS)*CZ2-XX2))
41700           SGMY(K)=RI*(CZ1*RN1-CPN*RN2*(CZ2-2.0*ADB*SZ2))
41800           XX3=(ALP*CZ1-BET*SZ1)
41900           TXY(K)=-RI*(RN1*XX3-RN2*CPN*(ALP*CZ2+SZ2*(2.0*ALP*ADB+BET)))
42000           GOTO 113
```

```
42100  112     FI=(K/4.0);I=FI*2;V=FI-1.0;CPN=COSD(360*V)
42200          CZ1=COS(Z1*V);CZ2=COS(Z2*V)
42300          SZ1=SIN(Z1*V);SZ2=SIN(Z2*V)
42400          RN1=SQRT(R1**I)/R1;RN2=SQRT(R2**I)/R2
42500          RI=FI*(FI+1.0)
42600          XX4=(SZ1*ASMBS+2.0*AMB*CZ1)
42700          SGMX(K)=RI*(RN1*XX4+CPN*RN2*(SZ2*ASMBS+2.0*AMB*CZ2))
42800          SGMY(K)=RI*(RN1*SZ1+CPN*RN2*SZ2)
42900          TXY(K)=-RI*(RN1*(BET*CZ1+ALP*SZ1)-RN2*CPN*(BET*CZ2+ALP*SZ2))
43000  113     REM2=L-(IFIX(FLOAT(L)/2.0)*2)
43100          IF(REM2.EQ.0.0) GOTO 114
43200          FI=(L+1.0)/4.0;I=FI*2;V=FI-1.0
43300          CPN=COSD(360*V);CZ1=COS(Z1*V);CZ2=COS(Z2*V)
43400          SZ1=SIN(Z1*V);SZ2=SIN(Z2*V)
43500          RN1=SQRT(R1**I)/R1
43600          RN2=SQRT(R2**I)/R2
43700          RI=FI*(FI+1.0)
43800          XXX4=(ASMBS*CZ1-2.0*AMB*SZ1);XX5=(ASMBS*2.0*ADB-2.0*AMB)*SZ2
43900          SGMX(L)=RI*(RN1*XXX4-CPN*RN2*((ASMBS-FAS)*CZ2-XX5))
44000          SGMY(L)=RI*(CZ1*RN1-CPN*RN2*(CZ2-2.0*ADB*SZ2))
44100          XX6=(ALP*CZ1-BET*SZ1)
44200          TXY(L)=-RI*(RN1*XX6-RN2*CPN*(ALP*CZ2+SZ2*(2.0*ALP*ADB+BET)))
44300          GOTO 115
44400  114     FI=L/4.0;I=FI*2;V=FI-1.0;CPN=COSD(360*V)
44500          CZ1=COS(Z1*V);CZ2=COS(Z2*V)
44600          SZ1=SIN(Z1*V);SZ2=SIN(Z2*V)
44700          RN1=SQRT(R1**I)/R1
44800          RN2=SQRT(R2**I)/R2
```

```
 44900          RI=FI*(FI+1.0)
 45000          XX7=(SZ1*ASMBS+2.0*AMB*CZ1)
 45100          SGMX(L)=RI*(RN1*XX7+CPN*RN2*(SZ2*ASMBS+2.0*AMB*CZ2))
 45200          SGMY(L)=RI*(RN1*SZ1+CPN*RN2*SZ2)
 45300          TXY(L)=-RI*(RN1*(BET*CZ1+ALP*SZ1)-RN2*CPN*(BET*CZ2+ALP*SZ2))
 45400  115     XX8=(RNUXY/EX)*(SGMX(K)*SGMY(L)+SGMX(L)*SGMY(K))
 45500          F=SGMX(K)*SGMX(L)/EX-XX8+SGMY(K)*SGMY(L)/EY+TXY(K)*TXY(L)/GXY
 45600          RETURN
 45700          END
 45800  C       ***********************************************
 45900          SUBROUTINE UMTRX(IFRN,IFRNP1,NNSM,IEL,CORDS)
 46000  C       ***********************************************
 46100          DIMENSION CORDS(2,75)
 46200          COMMON/A2/X1,Y1,X2,Y2
 46300          COMMON/A5/K,L
 46400          COMMON/A7/NODES(12,1)
 46500          COMMON/A8/THCK
 46600          COMMON/A10/U(40,40)
 46700          DO 20 K=1,IFRN
 46800          DO 20 L=1,IFRN
 46900          SUM=0.0:NNSMM1=NNSM-1
 47000          DO 5 IN=1,NNSMM1
 47100          N1=NODES(IN,1)
 47200          N2=NODES(IN+1,1)
 47300          X1=CORDS(1,N1)
 47400          Y1=CORDS(2,N1)
 47500          X2=CORDS(1,N2)
 47600          Y2=CORDS(2,N2)
```

```
47700            CALL TROMB1(FT1)
47800            SUM=SUM+FT1
47900  5         CONTINUE
48000            U(K,L)=SUM*THCK
48100  20        CONTINUE
48200            DO 113 I=IFRN+1,IFRNP1
48300            DO 113 J=IFRN+1,IFRNP1
48400  113       U(I,J)=0.0
48500            RETURN
48600            END
48700  C         ***********************************************
48800            SUBROUTINE ELMTRX(IFRN,IFRNP1,NNSM,IEL,CORDS)
48900  C         ***********************************************
49000            DIMENSION CORDS(2,75)
49100            COMMON/A6/ALP,BET,EX,EY,GXY,RNUXY
49200            COMMON/A7/NODES(12,1)
49300            COMMON/A9/EL(25,40)
49400            P1=(((ALP**2)-(BET**2))-RNUXY)/EX
49500            P2=2.0*ALP*BET/EX
49600            Q1=ALP/(EY*((ALP**2)+(BET**2)))-ALP*RNUXY/EX
49700            Q2=-BET*RNUXY/EX-BET/(EY*((ALP**2)+(BET**2)))
49800            DO 25 I=1,NNSM
49900            N1=NODES(I,1)
50000            X1=CORDS(1,N1)
50100            Y1=CORDS(2,N1)
50200            R1=SQRT((X1+ALP*Y1)**2+(BET*Y1)**2)
50300            R2=SQRT((X1-ALP*Y1)**2+(BET*Y1)**2)
50400            Z1=ATAN((BET*Y1)/(X1+ALP*Y1))
```

```
50500           Z2=ATAN((-BET*Y1)/(X1-ALP*Y1))
50600           IF(Z1.LT.0.0) Z1=3.1415926+Z1
50700           IF(Z2.GT.0.0) Z2=-3.1415926+Z2
50800           TAB=2.0*ALP/BET
50900           K=2*I-1;L=2*I
51000           EL(K,IFRNP1)=1.0
51100           EL(L,IFRNP1)=0.0
51200           DO 30 J1=1,IFRN,2
51300           FN1=(J1+1.0)/4.0;IFN1=2.0*FN1
51400           RN1=SQRT(R1**IFN1);RN2=SQRT(R2**IFN1)
51500           CPN=COSD(360*(FN1-1.0))
51600           CZ1=COS(FN1*Z1);CZ2=COS(FN1*Z2)
51700           SZ1=SIN(FN1*Z1);SZ2=SIN(FN1*Z2)
51800           FN11=FN1+1.0;AB=0.0;CB=0.0
51900           XX9=(P1*TAB+P2)
52000           AB=FN11*(RN1*(P1*CZ1-P2*SZ1)-RN2*CPN*(CZ2*(P1-TAB*P2)-SZ2*XX9))
52100           X10=(Q1*CZ1-Q2*SZ1);X11=(Q1-TAB*Q2)
52200           CB=FN11*(RN1*X10+RN2*CPN*(CZ2*X11-SZ2*(Q1*TAB+Q2)))
52300           EL(K,J1)=AB;EL(L,J1)=CB
52400   30      CONTINUE
52500           DO 40 J2=2,IFRN,2
52600           FN2=J2/4.0;IFN2=2*FN2
52700           RN1=SQRT(R1**IFN2);RN2=SQRT(R2**IFN2)
52800           CZ1=COS(FN2*Z1);CZ2=COS(FN2*Z2)
52900           SZ1=SIN(FN2*Z1);SZ2=SIN(FN2*Z2)
53000           FN21=FN2+1.0;CPN=COSD(360*(FN2-1.0))
53100           BB=FN21*(RN1*(P2*CZ1+P1*SZ1)+RN2*CPN*(P2*CZ2+P1*SZ2))
53200           DB=FN21*(RN1*(Q2*CZ1+Q1*SZ1)-RN2*CPN*(Q2*CZ2+Q1*SZ2))
```

```
53300            EL(K,J2)=BB;EL(L,J2)=DB
53400   40       CONTINUE
53500   25       CONTINUE
53600            RETURN
53700            END
53800   C        ****************************
53900            SUBROUTINE SESM(IFRNP1,NNSM)
54000   C        ****************************
54100            COMMON/A1/STM(25,25)
54200            COMMON/A9/EL(25,40)
54300            COMMON/INV/ELTELX(40,40)
54400            COMMON/A10/U(40,40)
54500            COMMON/A11/EE(40,25)
54600            DIMENSION ELT(40,25),ELTEL(40,40),ELTELT(40,40)
54700            DIMENSION ELTELS(40,40)
54800            DIMENSION EET(25,40),FETU(25,40),TEST(40,40)
54900            DOUBLE PRECISION ELTELX
55000            NNSM2=2*NNSM
55100            DO 50 I=1,NNSM2
55200            DO 50 J=1,IFRNP1
55300   50       ELT(J,I)=EL(I,J)
55400            DO 60 K=1,IFRNP1
55500            DO 65 L=1,IFRNP1
55600            SUM=0.0
55700            DO 70 J=1,NNSM2
55800   70       SUM=SUM+ELT(K,J)*EL(J,L)
55900            ELTEL(K,L)=SUM
56000   65       CONTINUE
```

```
56100   60      CONTINUE
56200   C       SCALING IS DONE WITH 10000.0
56300           DO 23 II=1,IFRNP1
56400           DO 23 JJ=1,IFRNP1
56500   23      ELTELS(II,JJ)=ELTEL(II,JJ)*1.0
56600           DO 111 IS=1,IFRNP1
56700           DO 111 JS=1,IFRNP1
56800   111     ELTELX(IS,JS)=ELTELS(IS,JS)
56900           CALL MATINV(IFRNP1,ID)
57000           DO 200 I1=1,IFRNP1
57100           DO 210 J1=1,IFRNP1
57200           SUM=0.0
57300           DO 220 I2=1,IFRNP1
57400   220     SUM=SUM+ELTELX(I1,I2)*ELTELS(I2,J1)
57500           TEST(I1,J1)=SUM
57600   210     CONTINUE
57700   200     CONTINUE
57800   C       SCALING IS DONE HERE
57900           DO 230 IH=1,IFRNP1
58000           DO 230 JH=1,IFRNP1
58100   230     ELTELI(IH,JH)=ELTELX(IH,JH)*1.0
58200           DO 75 K1=1,IFRNP1
58300           DO 80 L1=1,NNSM2
58400           SUM=0.0
58500           DO 85 J1=1,IFRNP1
58600   85      SUM=SUM+ELTELI(K1,J1)*ELT(J1,L1)
58700           EE(K1,L1)=SUM
58800   80      CONTINUE
```

```
 58900  75      CONTINUE
 59000          DO 90 I1=1,IFRNP1
 59100          DO 90 J1=1,NNSM2
 59200          EET(J1,I1)=EE(I1,J1)
 59300  90      CONTINUE
 59400          DO 95 K2=1,NNSM2
 59500          DO 100 L2=1,IFRNP1
 59600          SUM=0.0
 59700          DO 105 J2=1,IFRNP1
 59800  105     SUM=SUM+EET(K2,J2)*U(J2,L2)
 59900          EETU(K2,L2)=SUM
 60000  100     CONTINUE
 60100  95      CONTINUE
 60200          DO 110 K3=1,NNSM2
 60300          DO 115 L3=1,NNSM2
 60400          SUM=0.0
 60500          DO 120 J3=1,IFRNP1
 60600  120     SUM=SUM+EETU(K3,J3)*EE(J3,L3)
 60700          STM(K3,L3)=SUM
 60800  115     CONTINUE
 60900  110     CONTINUE
 61000          RETURN
 61100          END
 61200  C       ************************************
 61300          SUBROUTINE ASMBLS(NNSM,IEL,A,CORDS)
 61400  C       ************************************
 61500          DIMENSION A(150,150)
 61600          DIMENSION CORDS(2,75)
```

```
61700            COMMON/A1/STM(25,25)
61800            COMMON/A7/NODES(12,1)
61900            DO 45 I1=1,NNSM
62000            DO 45 J1=1,2
62100            DO 45 I2=1,NNSM
62200            DO 45 J2=1,2
62300            M=(I1-1)*2+J1;L=(I2-1)*2+J2
62400            IG=((NODES(I1,1)-1)*2+J1)
62500            JG=((NODES(I2,1)-1)*2+J2)
62600            A(IG,JG)=A(IG,JG)+STM(M,L)
62700   45       CONTINUE
62800            RETURN
62900            END
63000   C        ************************************
63100            SUBROUTINE DSMBLS(NNSM,IEL,A,CORDS)
63200   C        ************************************
63300            DIMENSION A(150,150)
63400            DIMENSION CORDS(2,75)
63500            COMMON/A1/STM(25,25)
63600            COMMON/A7/NODES(12,1)
63700            DO 313 IZ=1,75
63800            DO 313 JZ=1,75
63900   313      CORDS(IZ,JZ)=0.0
64000            DO 45 I1=1,NNSM
64100            DO 45 J1=1,2
64200            DO 45 I2=1,NNSM
64300            DO 45 J2=1,2
64400            M=(I1-1)*2+J1;L=(I2-1)*2+J2
```

```
64500           IG=((NODES(I1,1)-1)*2+J1)
64600           JG=((NODES(I2,1)-1)*2+J2)
64700           A(IG,JG)=A(IG,JG)-STM(M,L)
64800   45      CONTINUE
64900           RETURN
65000           END
65100   C       **********************************
65200           SUBROUTINE DSMBLE(IEL,AE,NODE,A)
65300   C       **********************************
65400           DIMENSION AE(6,6),NODE(3,100),A(150,150)
65500           DO 45 I1=1,3
65600           DO 45 J1=1,2
65700           DO 45 I2=1,3
65800           DO 45 J2=1,2
65900           M=(I1-1)*2+J1;L=(I2-1)*2+J2
66000           IG=((NODE(I1,IEL)-1)*2+J1)
66100           JG=((NODE(I2,IEL)-1)*2+J2)
66200           A(IG,JG)=A(IG,JG)-AE(M,L)
66300   45      CONTINUE
66400           RETURN
66500           END
66600
66700   C       ************************
66800           SUBROUTINE MATINV(M,ID)
66900   C       ************************
67000           COMMON/INV/A(40,40)
67100           DIMENSION  X(40),Y(40)
67200           DOUBLE PRECISION A,X,Y
```

```
67300           ID = 1
67400           IF( M - 1 ) 17,17,2
67500     2     A(1,1)=1.0/A(1,1)
67600           DO 12 K = 2 , M
67700                   N = K - 1
67800                   DO 11 I = 1 , N
67900                           Y(I) = 0.0
68000                           X(I) = 0.0
68100                           DO 10 J = 1 , N
68200                                   Y(I) = Y(I) + A(I,J) * A(J,K)
68300                                   X(I) = X(T) + A(K,J) * A(J,T)
68400     10                    CONTINUE
68500                           A(K,K) = A(K,K) - A(K,I) * Y(I)
68600     11            CONTINUE
68700                   IF(A(K,K)) 14 , 15 , 14
68800     14            A(K,K) = 1.0/A(K,K)
68900                   DO 12 I = 1 , N
69000                           A(K,I) = -X(I) * A(K,K)
69100                           A(I,K) = -Y(I) * A(K,K)
69200                           DO 12 J = 1 , N
69300                                   A(J,I) = A(J,I) - Y(J) * A(K,I)
69400     12    CONTINUE
69500           RETURN
69600     15    ID = 2
69700           TYPE 40, ID
69800     40    FORMAT(5X,'MATRIX IS SINGULAR AS ID IN INV =',I1)
69900     17    RETURN
70000           END
```

```
70100  C       ************************************
70200          SUBROUTINE SIF(R,NNSM,SIFAC,IFRNP1)
70300  C       ************************************
70400          DIMENSION R(150),C(25),C1(25)
70500          COMMON/A7/NODES(12,1)
70600          COMMON/A6/ALP,BET,EX,EY,GXY,RNUXY
70700          COMMON/A11/EE(40,25)
70800          M=2*NNSM
70900          DO 555 IQ=1,NNSM
71000          N1=NODES(IQ,1)
71100          K=2*N1-1
71200          L=2*N1
71300          IQ1=2*IQ-1
71400          IQ2=2*IQ
71500          C(IQ1)=R(K)
71600          C(IQ2)=R(L)
71700  555     CONTINUE
71800          DO 111 II=1,IFRNP1
71900          SUM=0.0
72000          DO 222 JJ=1,M
72100  222     SUM=SUM+EE(II,JJ)*C(JJ)
72200          C1(II)=SUM
72300  111     CONTINUE
72400          DO 126 LP=1,M
72500  126     WRITE(22,456) LP,C(LP),LP,C1(LP)
72600  456     FORMAT(5X,'C(',I2,')=',E12.4,5X,'C1(',I2,')=',F12.4)
72700  C       TYPE *, C1(1),C1(2),C1(3),C1(4),C1(5),C1(6),C1(7)
72800          SIFAC=(3.0/4.0)*SQRT(2.0*3.1415926)*2.0*(ALP/BET)*C1(1)
```

```
      RETURN
      END
C     ************************************
      SUBROUTINE STRESS(NST,CST,NNST,IFRN)
C     ************************************
      DIMENSION NST(NNST),CST(2,NNST),SGSPX(15)
      DIMENSION SGSPY(15),TSPXY(15)
      COMMON/A12/C1(25)
      COMMON/A6/ALP,BET,EX,EY,GXY,RNUXY
      ASMBS=(ALP**2-BET**2)
      AMB=ALP*BET;ADB=ALP/BET
      FAS=4.0*(ALP**2)
      DO 815 I=1,NNST
      SX=0.0;SY=0.0;TY=0.0
      X=CST(1,I);Y=CST(2,I)
      R1=SQRT((X+ALP*Y)**2+(BET*Y)**2)
      R2=SQRT((X-ALP*Y)**2+(BET*Y)**2)
      Z1=ATAN((BET*Y)/(X+ALP*Y))
      Z2=ATAN(-(BET*Y)/(X-ALP*Y))
      IF(Z1.LT.0.0) Z1=3.1415926+Z1
      IF(Z2.GT.0.0) Z2=-3.1415926+Z2
      DO 816 IF=1,IFRN
      IFS=IF-(IFIX(FLOAT(K)/2.0)*2)
      IF(IFS.EQ.0) GOTO 817
      FI=(IF+1)/4.0;II=FI*2
      V=(FI-1.0);CPN=COSD(360*V)
      CZ1=COS(Z1*V);CZ2=COS(Z2*V)
      SZ1=SIN(Z1*V);SZ2=SIN(Z2*V)
```

```
75700            RN1=SQRT(R1**II)/R1;RN2=SQRT(R2**II)/R2
75800            RI=FI*(FI+1.0)
75900            XX1=(ASMBS*CZ1-2.0*AMB*SZ1)
76000            XX2=(2.0*ASMBS*ADB-2.0*AMB)*SZ2
76100            SUM1=C1(IF)*RI*(RN1*XX1-CPN*RN2*((ASMBS-FAS)*CZ2-XX2))
76200            SUM2=C1(IF)*RI*(CZ1*RN1-CPN*RN2*(CZ2-2.0*ADB*SZ2))
76300            XX3=(ALP*CZ1-BET*SZ1)
76400            SUM3=C1(IF)*RI*(RN1*XX3-CPN*RN2*(ALP*CZ2+SZ2*(2.0*ALP*ADB+BET)
76500            GOTO 818
76600  817       FI=(IF/4.0);II=2*FI
76700            V=(FI-1.0);CPN=COSD(360*V)
76800            CZ1=COS(Z1*V);CZ2=COS(Z2*V)
76900            SZ1=SIN(Z1*V);SZ2=SIN(Z2*V)
77000            RN1=SQRT(R1**II)/R1
77100            RN2=SQRT(R2**II)/R2
77200            RI=FI*(FI+1.0)
77300            XX4=(SZ1*ASMBS+2.0*AMB*CZ1)
77400            XX5=(SZ1*ASMBS+2.0*AMB*CZ1)
77500            SUM1=C1(IF)*RI*(RN1*XX4+CPN*RN2*XX5)
77600            SUM2=C1(IF)*RI*(RN1*SZ1+CPN*RN2*SZ2)
77700            XX6=(BET*CZ1+ALP*SZ1)
77800            XX7=(BET*CZ2+ALP*SZ2)
77900            SUM3=C1(IF)*RI*(RN1*XX6-CPN*RN2*XX7)
78000  818       SX=SX+SUM1
78100            SY=SY+SUM2
78200            TY=TY+SUM3
78300  816       CONTINUE
78400            SGSPX(I)=SX
```

```
78500            SGSPY(I)=SY
78600            TSPXY(I)=TY
78700            WRITE(22,2121) I,SGSPX(I),I,SGSPY(I),I,TSPXY(I)
78800  2121      FORMAT(5X,'SGSPX(',I2,')=',E12.5,5X,'SGSPY(',I2,')=',E12.5
78900            1,5X,'TSPXY(',I2,')=',E12.5)
79000  815       CONTINUE
79100            RETURN
79200            END
```